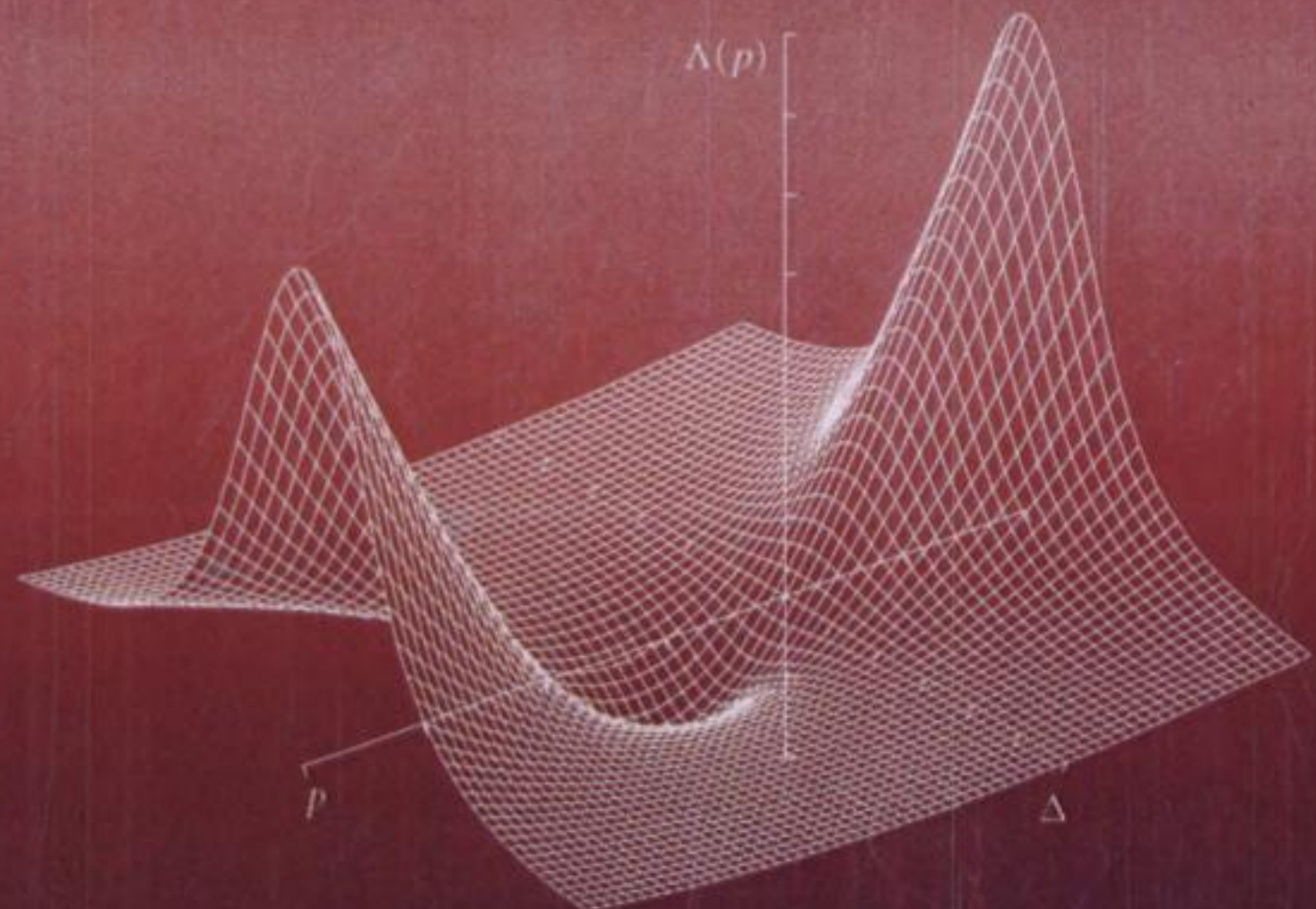


DYNAMIC STABILITY OF STRUCTURES



WEI-CHAU XIE

CAMBRIDGE

@Seismicisolation

具有版權
由
大

CAMBRIDGE UNIVERSITY PRESS
Cambridge, New York, Melbourne, Madrid, Cape Town, Singapore, São Paulo

Cambridge University Press
40 West 20th Street, New York, NY 10011-4211, USA

www.cambridge.org
Information on this title: www.cambridge.org/9780521852661

© Professor Wei-Chau Xie 2006

This publication is in copyright. Subject to statutory exception
and to the provisions of relevant collective licensing agreements,
no reproduction of any part may take place without
the written permission of Cambridge University Press.

First published 2006

Printed in the United States of America

A catalog record for this publication is available from the British Library.

Library of Congress Cataloging in Publication Data

Xie, Wei-Chau, 1964–

Dynamic stability of structures / Wei-Chau Xie.

p. cm.

Includes bibliographical references and index.

ISBN-13: 978-0-521-85266-1 (hardback)

ISBN-10: 0-521-85266-8 (hardback)

1. Structural dynamics. 2. Structural stability. I. Title.

TA654.X54 2005

624.1'71 – dc22

2005026016

ISBN-13 978-0-521-85266-1 hardback

ISBN-10 0-521-85266-8 hardback

Cambridge University Press has no responsibility for
the persistence or accuracy of URLs for external or
third-party Internet Web sites referred to in this publication
and does not guarantee that any content on such
Web sites is, or will remain, accurate or appropriate.

具有版權的資料

Contents

<i>Preface</i>	xv
1 <i>Introduction</i>	1
1.1 <i>Concept of Stability</i>	3
1.2 <i>Conservative Systems</i>	4
1.3 <i>Nonconservative Systems</i>	8
1.4 <i>Gyroscopic Systems</i>	18
1.5 <i>Motivating Examples</i>	19
1.5.1 <i>Column under Axial Load</i>	20
1.5.2 <i>Beam in Plane Motion</i>	22
1.5.3 <i>Viscoelastic Beam under Dynamic Axial Load</i>	28
1.5.4 <i>Flexural-Torsional Vibration of a Rectangular Beam</i>	33
1.5.5 <i>Vibration of a Rotating Shaft</i>	37
<i>Problems</i>	41

P A R T I

Dynamic Stability of Structures under Deterministic Loadings

2 <i>Linear Differential Equations with Periodic Coefficients</i>	45
2.1 <i>Stability of the Mathieu–Hill Equations</i>	45
2.2 <i>Effect of Damping on the Mathieu–Hill Equations</i>	53
2.3 <i>Stability of Linear Differential Equations with Periodic Coefficients</i>	55
2.4 <i>Stability of the Mathieu Equations</i>	56
2.4.1 <i>Formulation</i>	56
2.4.2 <i>Boundaries of the First Stability Region</i>	59
2.4.3 <i>Boundaries of the Second Stability Region</i>	60
2.4.4 <i>Boundaries of the Third Stability Region</i>	63
2.5 <i>Stability of the Damped Mathieu Equations</i>	64
2.5.1 <i>Periodic Solutions of Period $2T$</i>	64
2.5.2 <i>Periodic Solutions of Period T</i>	66
<i>Problems</i>	67

3 Approximate Methods	68
3.1 The Method of Averaging	68
3.1.1 Stability of the Undamped Mathieu Equations	68
3.1.2 Stability of the Damped Mathieu Equations	75
3.2 The Method of Multiple Scales	76
3.2.1 Motivating Example	76
3.2.2 Stability of the Undamped Mathieu Equations	79
3.3 Multiple Degrees-of-Freedom Non-Gyroscopic Systems	79
3.3.1 Averaged Equations of Motion	79
3.3.2 Parametric Resonances	81
3.4 Two Degrees-of-Freedom Gyroscopic Systems	91
3.4.1 Unperturbed System	92
3.4.2 Perturbed System	93
3.5 Multiple Degrees-of-Freedom Gyroscopic Systems	101
Problems	106
4 Nonlinear Systems under Periodic Excitations	108
4.1 Pendulum under Support Excitation	108
4.2 Column under Harmonic Axial Load	113
4.2.1 Steady-State Solutions	113
4.2.2 Stability of the Steady-State Solutions	116
4.2.2.1 Non-Trivial Solution	117
4.2.2.2 Trivial Solution	118
4.2.2.3 Instability Region	122
4.3 Snap-Through of a Shallow Arch	125
4.3.1 Equations of Motion	125
4.3.2 Amplitude–Load–Frequency Relation	125
4.4 Multiple Degrees-of-Freedom Systems	126
4.4.1 Equations of Motion	126
4.4.2 Resonance Conditions and Averaged Equations	129
4.4.3 Stability of the Steady-State Solutions	130
4.5 Examples	138
4.5.1 Column under Harmonic Axial Load	138
4.5.2 Snap-Through of a Shallow Arch	141
4.5.2.1 Main Resonance	141
4.5.2.2 Parametric Resonance	143
Problems	151

PART II

Dynamic Stability of Structures under Stochastic Loadings

5 Random Processes and Stochastic Differential Equations	155
5.1 Description of Random Processes	156
5.2 Processes with Orthogonal Increments	164
5.3 Wiener Process or Brownian Process	165
5.4 White Noise Process	171
5.5 Markov Processes	173
5.6 Diffusion Processes	175
5.6.1 Definition	175
5.6.2 Kolmogorov Equations	177
5.6.2.1 Backward Kolmogorov Equation	177
5.6.2.2 Forward Kolmogorov Equation (Fokker–Planck Equation)	179
5.6.2.3 Properties of the Fokker–Planck Equations	181
5.7 Stochastic Integrals	187
5.7.1 Stochastic Riemann Integrals	187
5.7.2 Riemann–Stieltjes Integrals	188
5.8 Generalized Stochastic Integral	189
5.9 The Itô Integral	192
5.10 Stochastic Differential Equations	194
5.10.1 General Theory of Stochastic Differential Equations	194
5.10.2 Ornstein–Uhlenbeck Process	196
5.10.3 Bounded Noise Process	199
5.11 Itô’s Differential Rule (Itô’s Lemma)	202
5.12 The Stratonovich Integral	204
5.13 The Stratonovich Stochastic Differential Equations	206
5.14 Approximation of a Physical Process by a Diffusion Process	209
5.15 Classification of the Boundaries of a Diffusion Process	210
5.16 The Method of Averaging	212
5.16.1 Averaging Method for Stochastic Differential Equations	212
5.16.2 Averaging Method for Integro–Differential Equations	221
5.17 Monte Carlo Simulation	222
5.17.1 Generation of Normally Distributed Random Numbers	223
5.17.2 Simulation of the Standard Wiener Process $W(t)$	224

5.17.3	Simulation of the Stochastic Differential Equations	224
5.17.3.1	Strong Approximation Schemes	225
5.17.3.2	Weak Approximation Schemes	227
5.17.4	Example – Duffing-van der Pol Equation	229
5.17.4.1	Strong Approximation Schemes	230
5.17.4.2	Weak Approximation Schemes	231
Problems		232
6	Almost-Sure Stability of Systems under Ergodic Excitations	234
6.1	Definitions	234
6.2	A.S. Asymptotic Stability of Second-Order Linear Stochastic Systems	236
6.2.1	Basic Equations	237
6.2.2	Systems with Arbitrary Ergodic Coefficients	239
6.2.3	Systems under Random Excitations with Known Probability Density Functions	241
6.2.3.1	Optimization Model	241
6.2.3.2	The Complex Method for Constrained Optimization	244
6.2.3.3	Numerical Solution for Systems with Ergodic Gaussian Coefficients	245
6.3	Stability of a Shallow Arch	247
6.3.1	Introduction	247
6.3.2	Static Case	248
6.3.3	Dynamic Case	251
6.3.3.1	Equations of Motion	251
6.3.3.2	Two-Dimensional Fokker-Planck Equation	252
6.3.3.3	Perturbation Equations	253
6.3.3.4	Sufficient Almost-Sure Asymptotic Stability Boundary	254
6.3.4	Numerical Example	255
6.3.4.1	Sufficient A.S. Stability Condition Using Schwarz's Inequality	256
6.3.4.2	Sufficient A.S. Stability Condition Using the Optimization Method	257
7	Moment Stability of Stochastic Systems	261
7.1	Moment Stability of Linear Stochastic Systems	261
7.2	Effect of Random Noise on the Stability of a Damped Mathieu Equation	263
7.2.1	Formulation: Averaged Equations	263

7.2.2	Moment Stability	265
7.3	Moment Stability of Coupled Linear Systems	268
7.3.1	Introduction	268
7.3.2	Averaged Equations	270
7.3.3	Moment Stability	272
7.3.4	Application: Flexural-Torsional Vibration of a Rectangular Beam	275
8	Lyapunov Exponents	277
8.1	Introduction	277
8.2	Simulation of Lyapunov Exponents	280
8.3	Lyapunov Exponents of Continuous Stochastic Dynamical Systems	283
8.4	Simulation of the Largest Lyapunov Exponent Using Khasminskii's Formulation	289
8.4.1	Systems under Non-White Excitations	289
8.4.2	Systems under White Noise Excitations	291
8.5	Lyapunov Exponents of Two-Dimensional Systems	292
8.5.1	Systems Exhibiting Pitchfork Bifurcation	293
8.5.1.1	Formulation of the Largest Lyapunov Exponent	293
8.5.1.2	Lyapunov Exponent of the Nilpotent System	295
8.5.1.3	Lyapunov Exponent by Asymptotic Expansion of Integrals	298
8.5.1.4	Lyapunov Exponent by Digital Simulation	299
8.5.2	Systems Exhibiting Hopf Bifurcation	301
8.5.2.1	Lyapunov Exponent by Asymptotic Expansion of Integrals	302
8.5.2.2	Lyapunov Exponent by Stochastic Averaging	305
8.5.2.3	Lyapunov Exponent by Digital Simulation	306
8.5.3	Lyapunov Exponent of a Two-Dimensional Viscoelastic System under Bounded Noise Excitation	308
8.6	Lyapunov Exponents and Stochastic Stability of Coupled Linear Systems	318
8.6.1	Formulation	318
8.6.2	Non-Singular Case	322
8.6.3	Singular Case	328
8.6.4	White Noise Excitation	330
8.6.5	Generalization to Multiple Degrees-of-Freedom Systems	331
8.6.6	Monte Carlo Simulation	332
8.6.7	Application: Flexural-Torsional Stability of a Rectangular Beam	333
8.6.7.1	Non-Follower Force Case	334

8.6.7.2	Follower Force Case	336
8.6.7.3	White Noise Excitation	336
9	Moment Lyapunov Exponents	338
9.1	Introduction	338
9.1.1	The Concept of Moment Lyapunov Exponent	338
9.1.2	<u>The Partial Differential Eigenvalue Problem for Moment Lyapunov Exponent</u>	342
9.2	Monte Carlo Simulation of the Moment Lyapunov Exponents	348
9.3	Moment Lyapunov Exponent of an Oscillator under Weak White Noise Excitation	353
9.3.1	Eigenvalue Problem for the Moment Lyapunov Exponents	354
9.3.2	Determination of the Moment Lyapunov Exponents Using a Method of Perturbation	356
9.4	<u>Moment Lyapunov Exponents of a Two-Dimensional Near-Nilpotent System</u>	359
9.4.1	Introduction	359
9.4.2	Formulation	361
9.4.3	Lyapunov Exponents	364
9.4.4	Moment Lyapunov Exponents	367
9.4.4.1	Two-Point Boundary-Value Problems	367
9.4.4.2	Numerical Solutions of Moment Lyapunov Exponents	369
9.5	Moment Lyapunov Exponents of an Oscillator under Real Noise Excitation	373
9.5.1	Formulation	373
9.5.2	Weak Noise Expansion of the Moment Lyapunov Exponent	375
9.5.2.1	Zeroth-Order Perturbation	376
9.5.2.2	Solution of $\mathcal{L}_0 T(\zeta, \varphi) = f(\zeta)g(\varphi)$	377
9.5.2.3	First-Order Perturbation	379
9.5.2.4	Second-Order Perturbation	380
9.5.2.5	Higher-Order Perturbation	381
9.5.2.6	Stability Index	383
9.5.3	Numerical Determination of Moment Lyapunov Exponents	384
9.5.4	Monte Carlo Simulation of Moment Lyapunov Exponents	387
9.6	Parametric Resonance of an Oscillator under Bounded Noise Excitation	390
9.6.1	Formulation	390
9.6.2	Weak Noise Expansions of the Moment Lyapunov Exponent Using a Method of Singular Perturbation	394
9.6.2.1	Perturbation Expansion	394



You have either reached a page that is unavailable for viewing or reached your viewing limit for this

@Seismicisolation



You have either reached a page that is unavailable for viewing or reached your viewing limit for this

@Seismicisolation

Preface

Background and Scope of the Book

Investigation of the dynamic stability of elastic systems frequently leads to the study of the dynamic behaviour of the solutions derived from a parametrized family of differential equations. Examples of such systems include slender columns and thin plates under axial loading, or buildings, bridges, and aircraft structures under wind loading.

When the loadings are dynamic (either deterministic functions or random processes), the structures are then called parametrically excited. Parametric instability or resonance is characterized by exponential growth of the response amplitudes even in the presence of damping.

As a result, parametric resonance is more dangerous than ordinary resonance, in which the loading appears as the forcing term, rather than as a parameter, in the governing equations of motion.

The nature of the problems to be solved is characterized, in general, by the nature of the loading. When the loadings are deterministic periodic functions, the resulting governing equations of motion are of the Mathieu–Hill types; whereas when the excitations are random forces, the dynamics of structures is governed by stochastic differential equations. Hence, this book is divided into two parts, i.e. Part I: dynamic stability of structures under deterministic loadings (Chapters 2–4) and Part II: dynamic stability of structures under stochastic loadings (Chapters 5–9).

It is the purpose of this book to present a systematic introduction to the theory of parametric stability of structures under both deterministic and stochastic loadings.

Chapter 1 presents a general introduction to the concept of stability, conservative systems, nonconservative systems, and gyroscopic systems. Equations of motion of several structural systems are derived. The dynamic stability of these systems is studied throughout the book.

The dynamic stability of linear differential equations with periodic coefficients, i.e. Mathieu–Hill equations and Mathieu equations, is studied in Chapter 2.

The method of averaging, developed by Bogoliubov and Mitropolski, is applied in Chapter 3 to obtain the stability regions of Mathieu equations, linear multiple degrees-of-freedom non-gyroscopic and gyroscopic systems. Subharmonic and combination resonances of these systems are investigated.

In Chapter 4, nonlinear systems under periodic excitations are studied. The effect of nonlinearity on the stability of steady-state solutions is determined. Examples of a column under axial harmonic load and snap-through of a shallow arch are used to illustrate the procedures of analysis.

The theory of random processes, stochastic calculus, stochastic differential equations, and various techniques for solving these equations, such as the method of stochastic averaging and Monte Carlo simulation schemes, are presented in Chapter 5. This Chapter lays the necessary theoretical foundation for the study of stochastic dynamic stability.

Almost-sure stability of systems under the excitation of non-white ergodic random processes is investigated in Chapter 6.

Moment stability of stochastic dynamical systems is presented in Chapter 7. Both first and second moment stability conditions of a second-order system under combined harmonic and stochastic excitation, and a coupled multiple degrees-of-freedom linear system under stochastic excitation, are determined to illustrate the approaches.

The modern theory of stochastic dynamic stability is founded on Lyapunov exponents and moment Lyapunov exponents, which are presented in Chapters 8 and 9, respectively. The concepts of both exponents are introduced and a variety of application problems are studied through the determination of these characteristic numbers using various methods and techniques. The almost-sure asymptotic stability of a stochastic dynamical system is characterized by the largest Lyapunov exponent; whereas the p th moment stability is determined by the p th moment Lyapunov exponent. Furthermore, the Lyapunov exponent and the moment Lyapunov exponent characterize how rapidly the response grows or decays sample-wise and moment-wise, respectively.

Since the largest Lyapunov exponent is equal to the derivative of the p th moment Lyapunov exponent at $p = 0$, the moment Lyapunov exponent is the ideal avenue and the ultimate characteristic number for the study of the dynamic stability of stochastic dynamical systems. Knowledge of the moment Lyapunov exponent gives the almost-sure asymptotic stability of a stochastic dynamical system through the Lyapunov exponent. If the system is almost-surely stable, the p th moment becomes unstable when p is greater than the stability index, which is the non-trivial zero of the moment Lyapunov exponent.

The book is primarily for engineering students and practitioners as the main audience. Readers with a good knowledge of advanced calculus, linear algebra, probability, differential equations, engineering mechanics, and structural dynamics, which can be acquired in a relevant undergraduate program, should be able to follow the book. Of course, a certain degree of mathematical sophistication is helpful. The book is presented in a style that can be studied by an engineer with suitable background without sacrificing mathematical rigour. For Chapters 2–4 and 6–9, the basic theory is first presented. Application problems are then formulated and solved, sometimes using more than one approach. The emphasis is on applications and various methods and techniques, both analytical and numerical, for solving engineering problems. Theory and application problems are presented as self-contained as possible. All important steps of analysis are provided to make the book suitable as a textbook and especially for self-study. This book is not intended to be a complete research monograph; a comprehensive survey of the research publications is therefore not provided.

Computer software packages for symbolic computations, such as *Maple*, are very useful in mathematical analysis. However, they cannot replace learning and thinking. It is important to develop analytical skills and proficiency through “hand” calculations, which will also help the development of insight into the problems and appreciation of the solution process. By providing *Maple* programs for some typical problems that can be solved efficiently using *Maple*, a balanced presentation is attempted so that the readers can not only run the *Maple* programs to solve the problems on hand but also learn the frequently used commands and techniques. It is advisable to use *Maple* mainly as a tool for verification and checking rather than relying on it to solve every problem and being lost often in pages of *Maple* output.

Part I of the book presents the classic theory of dynamic stability of structures under deterministic loadings. These materials are suitable for a one term (semester) graduate course. In fact, a large part of the materials of Part I and some sections of Chapters 1 and 5 are based on the lecture notes of a graduate course taught by Professor S. T. Ariaratnam at the University of Waterloo. A draft of this book was used in a one term graduate course at Waterloo, in which materials in Chapters 1 to 5, and many sections of Chapters 8 and 9 were covered.

Acknowledgements

First and foremost, my sincere appreciation goes to Professor S. T. Ariaratnam of the University of Waterloo, my graduate supervisor for both master’s and doctoral degrees and later my colleague, who led me into this exciting area and with whom I had many fruitful collaborations. I am very grateful to many people who have helped me in various ways in my professional career, including Professor N. Sri Namachchivaya of the University of Illinois at Urbana-Champaign, Professor W. Wedig of Universität Karlsruhe, Professors Y. K. Lin and I. Elishakoff of Florida Atlantic University, Professor G. I. Schuëller of the University of Innsbruck, and Professor M. D. Grigoriu of Cornell University.

My student Mr. Qinghua Huang has carefully read the book and made many helpful and critical suggestions. Students in the graduate course who used a draft of this book as the text have made many encouraging comments and constructive suggestions.

Special thanks are due to Mr. John Bennett, my mentor, teacher, and friend, for his advice and guidance. He has also painstakingly proof-read and copy-edited the book.

This book would not be possible without the unfailing love and support of my mother, who has always believed in me. I particularly thank my wife Cong-Rong and lovely daughters Victoria and Tiffany for their love, understanding, encouragement, and support.

I appreciate hearing your comments through email (xie@uwaterloo.ca) or regular correspondence.

Wei-Chau Xie

Waterloo, Ontario, Canada

具有透音時鐘
李

@Seismicisolation

C H A P T E R

Introduction

Many failures of engineering structures, under either static or dynamic loadings, have been attributed to structural instability, in which large deformations of the structures are observed. In the study of stability of structures, it is the nature of the loading that characterizes the nature of the problem to be solved. The loading may be static, deterministic, or random. In the case of static loading, an extensive amount of literature exists, e.g. [87], [60], and [83]. This book deals with stability of structures under dynamic excitations.

Problems of parametric resonance arise naturally in studies of the dynamic stability of a class of elastic systems, such as a column under compressive axial load. These systems ordinarily exhibit a bifurcational form of instability under applied static loads. The externally applied loads appear in the equations of motion in the form of coefficients or parameters. As a result, when the loadings are dynamic or time dependent, the systems are called *parametrically excited systems* and the instability is referred as *parametric instability* or *parametric resonance*. Parametric instability problems also occur in the analysis of the steady-state motions of nonlinear dynamical systems.

Motivating Example: As a motivating example, consider a person playing on a swing as shown in Figure 1.1. The person stands up at the two extreme positions and squats down at the lowest position. Setting up the equation of motion yields

$$\Sigma M_O = I(\theta) \ddot{\theta} : \quad I(\theta) \ddot{\theta} + mg L(\theta) \sin\theta = 0, \quad (1.0.1)$$

where $I(\theta)$ is the combined mass moment of inertia of the swing and the person about the pivot O , $L(\theta)$ is the location of the centre of gravity, and mg is the weight. When θ is small, equation (1.0.1) becomes

$$\ddot{\theta} + \left[mg \frac{L(\theta)}{I(\theta)} \right] \theta = 0, \quad \text{or} \quad \ddot{\theta} + \left[mg \frac{L(t)}{I(t)} \right] \theta = 0. \quad (1.0.2)$$

Equation (1.0.2) is a parametrically excited system, in which the changes of the mass moment of inertia and the location of the centre of gravity appear in the parameter of



You have either reached a page that is unavailable for viewing or reached your viewing limit for this

@Seismicisolation



You have either reached a page that is unavailable for viewing or reached your viewing limit for this

@Seismicisolation

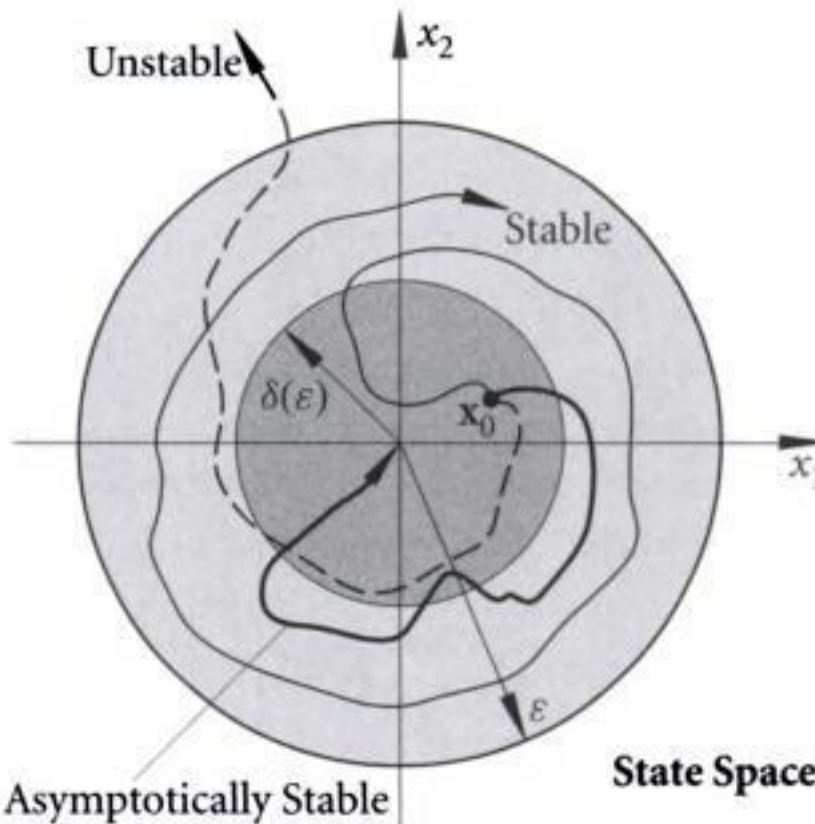


Figure 1.2 Illustration of Lyapunov stability.

However, this is not true for systems of infinite dimension, and stability must be defined with respect to a specified norm. For an elastic continuum, the following energy norms can be used:

$$\|\mathbf{u}\|^2 = \frac{1}{V} \int_V \mathbf{u} \cdot \mathbf{u} dV, \quad \|\dot{\mathbf{u}}\|^2 = \frac{1}{M} \int_V \rho \dot{\mathbf{u}} \cdot \dot{\mathbf{u}} dV,$$

where $\mathbf{u}(\mathbf{x}, t)$ is the displacement field, $\dot{\mathbf{u}}(\mathbf{x}, t)$ is the velocity field, and ρ , V , and M are the density, volume, and mass of the elastic continuum, respectively. According to Koiter, the elastic continuum is stable if, given ε and ε' , there exist $\delta(\varepsilon, \varepsilon')$ and $\delta'(\varepsilon, \varepsilon')$ such that

$$\|\mathbf{u}\| < \varepsilon \text{ and } \|\dot{\mathbf{u}}\| < \varepsilon' \text{ for all } t > 0, \quad \text{if } \|\mathbf{u}(\mathbf{x}_0, 0)\| < \delta \text{ and } \|\dot{\mathbf{u}}(\mathbf{x}_0, 0)\| < \delta'.$$

Depending on the characteristics of the structures and the loadings applied, the stability problems of structures can be classified as shown in Figure 1.3 (see, e.g. [59]).

1.2 Conservative Systems

For a conservative system, a potential energy functional $V[u(x), \mu]$ can be established, in which $u(x)$ is the displacement field and μ is the load parameter. The minimum potential energy law, which follows Lagrange's theorem, states that the system is in a state of stable equilibrium if, and only if, the value of the potential energy is a *relative* minimum. The word "relative" is used because there may be other minima nearby, separated from this minimum by small hills as illustrated in Figure 1.4.

The displacement field may be approximated as

$$u(x) = \sum_{i=1}^n q_i \phi_i(x), \tag{1.2.1}$$

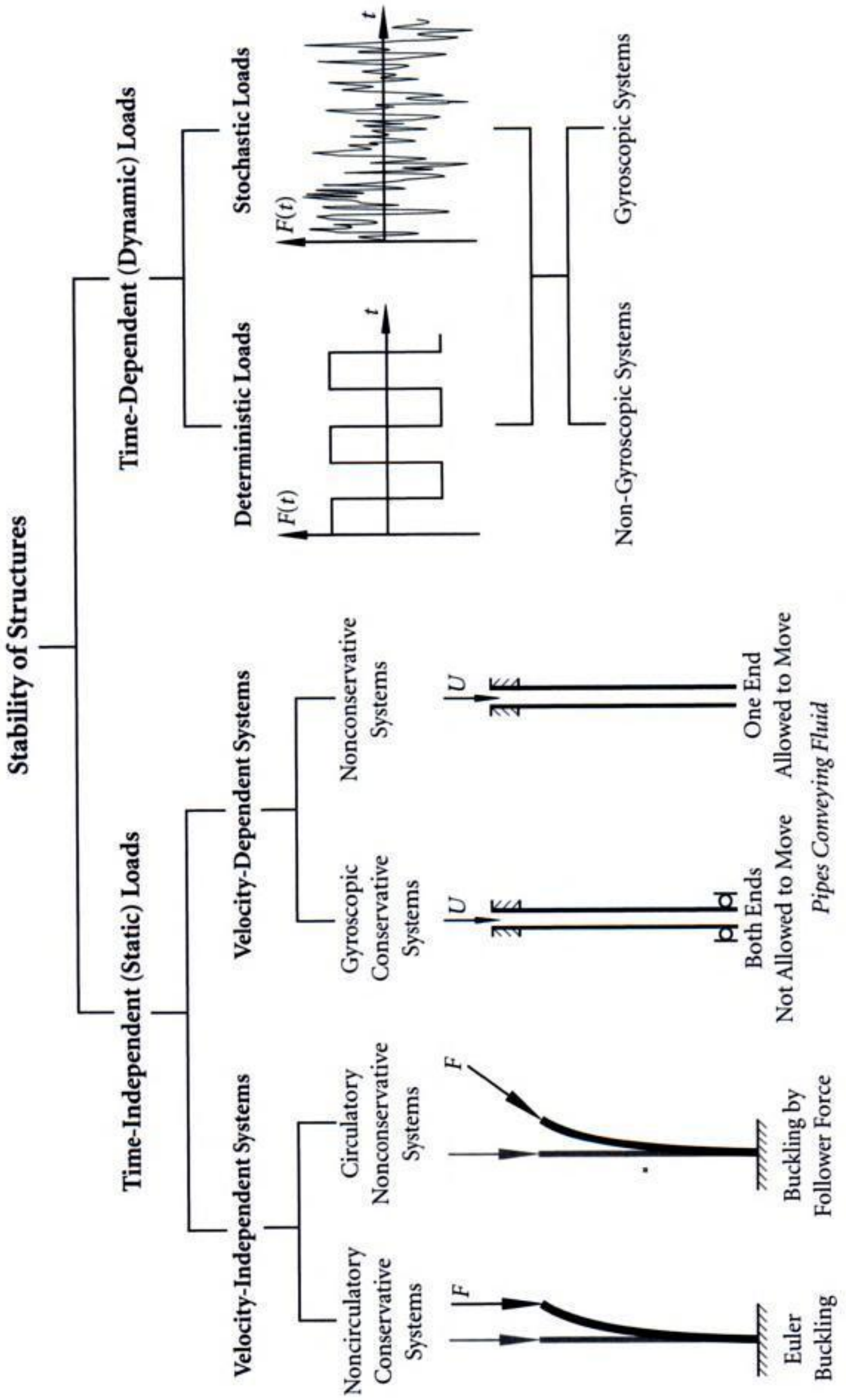


Figure 1.3 Classification of stability problems of structures.



You have either reached a page that is unavailable for viewing or reached your viewing limit for this

@Seismicisolation

Let D_i be the determinant of the i th principal minor of matrix \mathbf{H}_0 , defined as

$$D_i = \begin{vmatrix} \frac{\partial^2 V}{\partial q_1^2} & \frac{\partial^2 V}{\partial q_1 \partial q_2} & \cdots & \frac{\partial^2 V}{\partial q_1 \partial q_i} \\ \frac{\partial^2 V}{\partial q_2 \partial q_1} & \frac{\partial^2 V}{\partial q_2^2} & \cdots & \frac{\partial^2 V}{\partial q_2 \partial q_i} \\ \vdots & \vdots & \cdots & \vdots \\ \frac{\partial^2 V}{\partial q_i \partial q_1} & \frac{\partial^2 V}{\partial q_i \partial q_2} & \cdots & \frac{\partial^2 V}{\partial q_i^2} \end{vmatrix}_{\mathbf{q}=\mathbf{q}_0}, \quad i = 1, 2, \dots, n. \quad (1.2.4a)$$

If all determinants D_i are positive, i.e.

$$D_i > 0, \quad i = 1, 2, \dots, n, \quad (1.2.4b)$$

matrix $\mathbf{H}_0(\mathbf{q}_0)$ is positive definite, and hence the equilibrium \mathbf{q}_0 is stable.

Special Case. $n=1$

In this case, the stability conditions (1.2.4b) are reduced to

$$\frac{d^2 V}{dq^2} > 0, \quad (1.2.5)$$

where $q = q_1$ and the derivative is evaluated at $q = q_0 = q_{10}$.

Special Case. $n=2$

In this case, the stability conditions (1.2.4b) become

$$\frac{\partial^2 V}{\partial q_1^2} > 0, \quad \frac{\partial^2 V}{\partial q_1^2} \frac{\partial^2 V}{\partial q_2^2} - \left(\frac{\partial^2 V}{\partial q_1 \partial q_2} \right)^2 > 0, \quad (1.2.6)$$

where the derivatives are evaluated at $q_1 = q_{10}$ and $q_2 = q_{20}$.

Example 1.2.1: Study the stability of a rod of length l under a compressive load P . The rod is supported at A by a hinge and a rotational spring of stiffness κ . This is a simplified model of the Euler buckling of a cantilever under an axial compressive load.

Solution: Impose a small rotation $q = \theta$ on the structure as shown in Figure 1.5. The potential energy of the system is

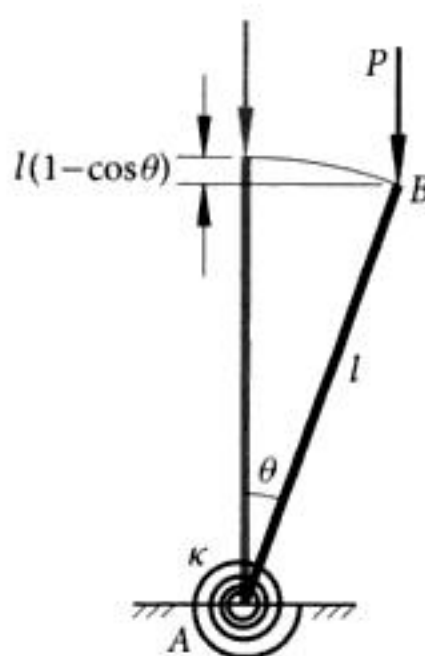
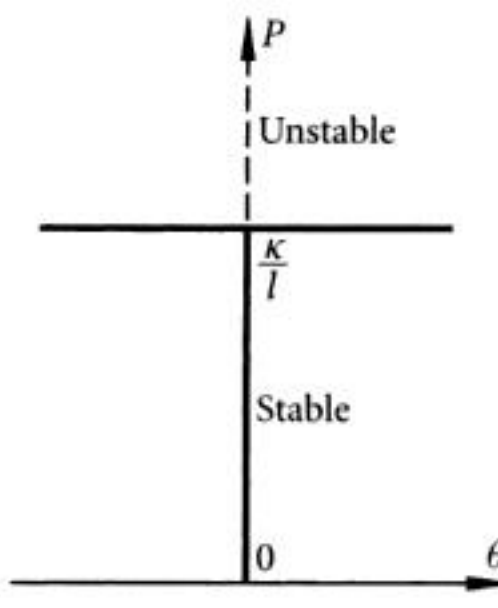
$$V(\theta) = \frac{1}{2}\kappa\theta^2 - Pl(1 - \cos\theta). \quad (1.2.7)$$

For small amplitudes of rotation θ , the Taylor series of $\cos\theta = 1 - \frac{1}{2}\theta^2 + O(\theta^4)$ can be used and equation (1.2.7) becomes

$$V(\theta) = \frac{1}{2}\theta^2(\kappa - Pl). \quad (1.2.8)$$

For equilibrium, it is required that

$$\frac{dV}{d\theta} = \theta(\kappa - Pl) = 0. \quad (1.2.9)$$

**Figure 1.5** A rod under compressive load.**Figure 1.6** Load-rotation ($P-\theta$) curve.

Equation (1.2.9) has two solutions. When $P \neq \kappa/l$, the angle of rotation θ is always 0, which is the non-buckled configuration. When $P = \kappa/l$, θ can be any nonzero values, corresponding to the buckled configuration. The stability of the non-buckled configuration $\theta = 0$ is determined by the second-order derivative

$$\frac{d^2V}{d\theta^2} = \kappa - Pl. \quad (1.2.10)$$

- When $P < \kappa/l$, $d^2V/d\theta^2 > 0$, which means that the potential energy is minimum at $\theta = 0$ and the non-buckled configuration $\theta = 0$ is stable.
- When $P = \kappa/l$, $d^2V/d\theta^2 = 0$. The equilibrium position $\theta = 0$ is critical and buckling occurs.
- When $P > \kappa/l$, $d^2V/d\theta^2 < 0$, implying that the non-buckled configuration is unstable.

The load-rotation ($P-\theta$) curve is shown in Figure 1.6. ■

1.3 Nonconservative Systems

A force is *conservative* if the work W done along the displacement of its point of application depends solely on the initial and final positions of this point. A force not satisfying this condition is *nonconservative*. A system is conservative if all forces acting on this system are conservative, otherwise it is nonconservative. Some examples of nonconservative systems include an elastic cantilever under follower force, a panel or air-foil in supersonic flow, and a pipe conveying fluid as shown in Figure 1.7. Stability of nonconservative systems is studied in [27], [59], and [60].

Example 1.3.1: As an example of a nonconservative system, study the stability of the structure shown in Figure 1.8 under a follower force P . Light rigid bars AB of length l_1 and BC of length l_2 are connected at B by a hinge and a torsional spring of stiffness κ_2 . Bar AB is supported at A by a hinge and a torsional spring of stiffness κ_1 . Two

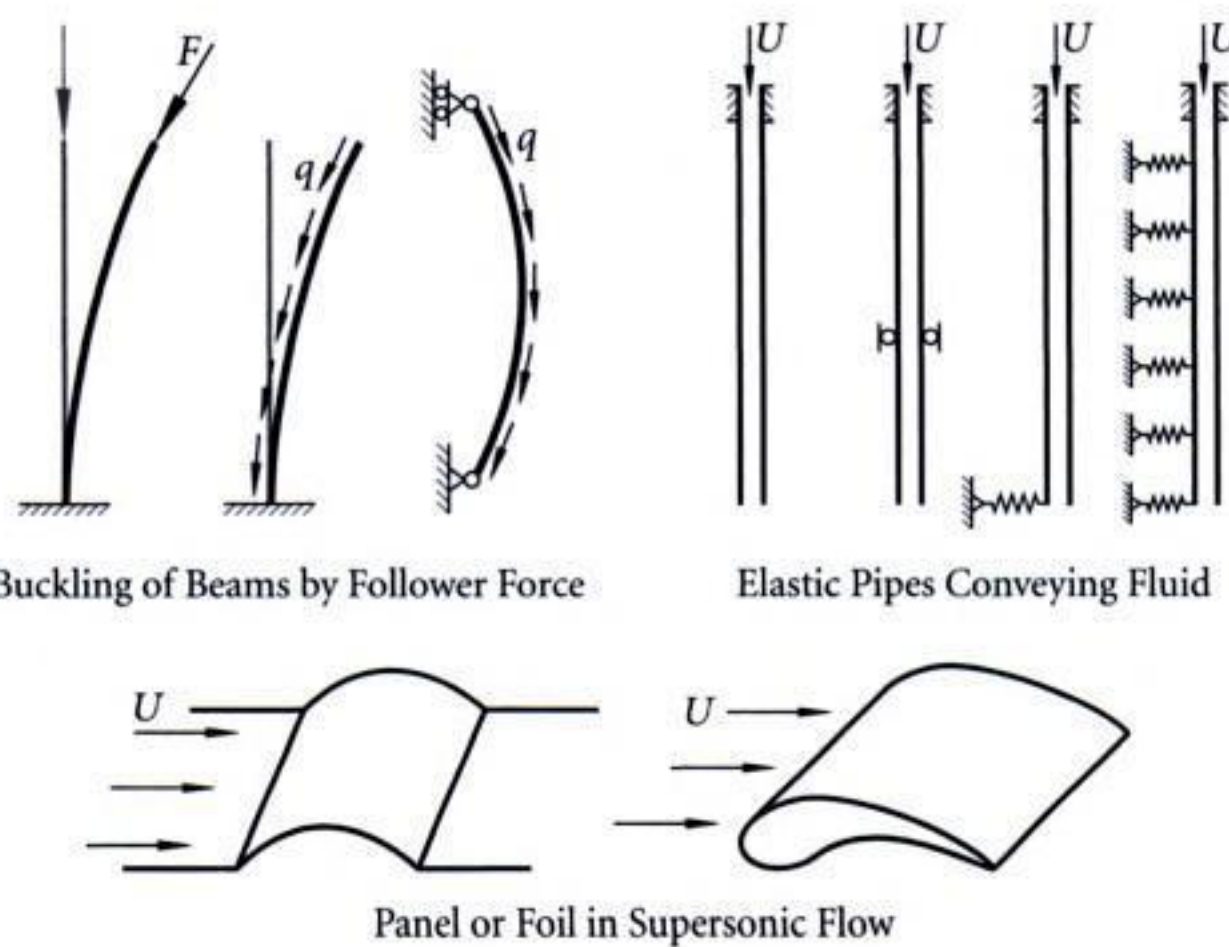


Figure 1.7 Examples of nonconservative systems.

point masses m_1 and m_2 are lumped at B and C , respectively. A force P , which always follows the direction of CB , is applied at C .

Solution: Consider the dynamic equilibrium of bar BC . From d'Alembert's principle, one obtains, by summing up the moments about point B ,

$$m_2 l_2 \ddot{q}_2 + \kappa_2(\theta_2 - \theta_1) = 0, \quad \theta_1 = \frac{q_1}{l_1}, \quad \theta_2 = \frac{q_2 - q_1}{l_2}. \quad (1.3.1)$$

Similarly, consider the dynamic equilibrium of the entire structure. Summing up the moments about point A yields

$$m_1 l_1 \ddot{q}_1 + m_2(l_1 + l_2) \ddot{q}_2 + \kappa_1 \theta_1 + P l_1 (\theta_2 - \theta_1) = 0. \quad (1.3.2)$$

Seeking a solution of the form $\{q_1(t), q_2(t)\} = \{\hat{q}_1, \hat{q}_2\} e^{\lambda t}$ and substituting into equations (1.3.1) and (1.3.2) result in a system of two linear algebraic equations:

$$\begin{aligned} -\kappa_2 \left(\frac{1}{l_1} + \frac{1}{l_2} \right) \hat{q}_1 + \left(m_2 l_2 \lambda^2 + \frac{\kappa_2}{l_2} \right) \hat{q}_2 &= 0, \\ \left[m_1 l_1 \lambda^2 + \frac{\kappa_1}{l_1} - P \left(1 + \frac{l_1}{l_2} \right) \right] \hat{q}_1 + \left[m_2 (l_1 + l_2) \lambda^2 + P \frac{l_1}{l_2} \right] \hat{q}_2 &= 0. \end{aligned} \quad (1.3.3)$$

To have nonzero solutions for \hat{q}_1 and \hat{q}_2 , the determinant of the coefficient matrix of equations (1.3.3) must be zero, i.e.

$$\begin{vmatrix} -\kappa_2 \left(\frac{1}{l_1} + \frac{1}{l_2} \right) & m_2 l_2 \lambda^2 + \frac{\kappa_2}{l_2} \\ m_1 l_1 \lambda^2 + \frac{\kappa_1}{l_1} - P \left(1 + \frac{l_1}{l_2} \right) & m_2 (l_1 + l_2) \lambda^2 + P \frac{l_1}{l_2} \end{vmatrix} = 0,$$



You have either reached a page that is unavailable for viewing or reached your viewing limit for this

@Seismicisolation

Some numerical results of P_{cr} can be easily obtained from equation (1.3.7):

$$\kappa_1 = \kappa_2 = 1, \quad m_1 = m_2 = 1, \quad l_1 = l_2 = 1, \quad P_{\text{cr}} = 2.0,$$

$$\kappa_1 = 2, \quad \kappa_2 = 4, \quad m_1 = 8, \quad m_2 = 1, \quad l_1 = l_2 = 1, \quad P_{\text{cr}} = 17.0. \quad \blacksquare$$

In general, the equations of motion of a nonconservative system are of the form

$$\mathbf{M}\ddot{\mathbf{x}} + \mathbf{D}\dot{\mathbf{x}} + \mathbf{K}\mathbf{x} + \mu \mathbf{B}\mathbf{x} = \mathbf{0}, \quad (1.3.8)$$

where \mathbf{M} , \mathbf{D} , \mathbf{K} , and \mathbf{B} are the mass, damping, elastic stiffness, and geometric stiffness matrices of dimension $n \times n$, respectively, and μ is the load parameter. Matrices \mathbf{M} and \mathbf{K} are symmetric, i.e. $\mathbf{M}^T = \mathbf{M}$ and $\mathbf{K}^T = \mathbf{K}$. For nonconservative systems, $\mathbf{B}^T \neq \mathbf{B}$.

To study system (1.3.8), the method of modal analysis is applied. First consider the undamped free vibration given by

$$\mathbf{M}\ddot{\mathbf{x}} + \mathbf{K}\mathbf{x} = \mathbf{0}. \quad (1.3.9)$$

Seeking a solution of the form $\mathbf{x}(t) = \hat{\mathbf{x}} e^{i\omega t}$ and substituting into equation (1.3.9) yield

$$(\mathbf{K} - \omega^2 \mathbf{M}) \hat{\mathbf{x}} = \mathbf{0}. \quad (1.3.10)$$

To have non-trivial solutions, it is necessary that the determinant of the coefficient matrix be zero, i.e. $\det(\mathbf{K} - \omega^2 \mathbf{M}) = 0$, from which one obtains n eigenvalues ω_{i0} , $i = 1, 2, \dots, n$. Corresponding to each eigenvalue ω_{i0} , an eigenvector $\hat{\mathbf{x}}_i$ can be obtained from equation (1.3.10). The modal matrix $\Phi = [\hat{\mathbf{x}}_1, \hat{\mathbf{x}}_2, \dots, \hat{\mathbf{x}}_n]$, formed from the eigenvectors, possesses the properties:

$$\Phi^T \mathbf{M} \Phi = \text{diag}\{m_1, m_2, \dots, m_n\}, \quad \Phi^T \mathbf{K} \Phi = \text{diag}\{m_1 \omega_{10}^2, m_2 \omega_{20}^2, \dots, m_n \omega_{n0}^2\}.$$

Applying the transformation $\mathbf{x} = \Phi \mathbf{q}$ to equations (1.3.8) and multiplying Φ^T from the left yield

$$\Phi^T \mathbf{M} \Phi \ddot{\mathbf{q}} + \Phi^T \mathbf{D} \Phi \dot{\mathbf{q}} + \Phi^T \mathbf{K} \Phi \mathbf{q} + \mu \Phi^T \mathbf{B} \Phi \mathbf{q} = \mathbf{0}. \quad (1.3.11)$$

Note that a general damping matrix cannot be diagonalized by the modal matrix Φ , and the modal damping is usually taken in practice to simplify the analysis. Equation (1.3.11) becomes

$$\ddot{\mathbf{q}} + \mathbf{d} \dot{\mathbf{q}} + \omega_0^2 \mathbf{q} + \mu \mathbf{b} \mathbf{q} = \mathbf{0}, \quad (1.3.12a)$$

or

$$\ddot{q}_i + d_i \dot{q}_i + \omega_{i0}^2 q_i + \mu \sum_{j=1}^n b_{ij} q_j = 0, \quad i = 1, 2, \dots, n, \quad (1.3.12b)$$

where \mathbf{b} is a full matrix,

$$\omega_0^2 = \text{diag}\{\omega_{10}^2, \omega_{20}^2, \dots, \omega_{n0}^2\}, \quad \mathbf{d} = \text{diag}\{d_1, d_2, \dots, d_n\},$$

in which d_i is the damping coefficient for the i th normal mode.

Seeking a solution of the form $\mathbf{q}(t) = \hat{\mathbf{q}} e^{\lambda t}$ and substituting into equation (1.3.12a) result in

$$(\lambda^2 \mathbf{I} + \lambda \mathbf{d} + \omega_0^2 + \mu \mathbf{b}) \hat{\mathbf{q}} = \mathbf{0}.$$

In order to have non-trivial solutions, the determinant of the coefficient matrix must be zero, i.e.

$$\det(\lambda^2 \mathbf{I} + \lambda \mathbf{d} + \omega_0^2 + \mu \mathbf{b}) = 0, \quad (1.3.13)$$

which leads to a polynomial equation of degree $2n$ in λ . The roots of equation (1.3.13) are in general complex numbers of the form $\lambda(\mu) = \alpha(\mu) \pm i\omega(\mu)$.

Depending on the changes of the eigenvalues $\lambda(\mu)$ as the load parameter μ is increased, different types of instability of the structures can occur. For simplicity of illustration, consider the undamped case when $\mathbf{d} = \mathbf{0}$.

Case I. Divergence

As shown in Figure 1.9, when the load parameter $\mu = 0$, the eigenvalues are purely imaginary, i.e. $\alpha_i(0) = \text{Re}[\lambda_i(0)] = 0$, $\omega_i(0) = \text{Im}[\lambda_i(0)] \neq 0$. The solutions of equation (1.3.13) are oscillatory in the form

$$q_i(t) = \hat{q}_i (A_i \sin \omega_i t + B_i \cos \omega_i t).$$

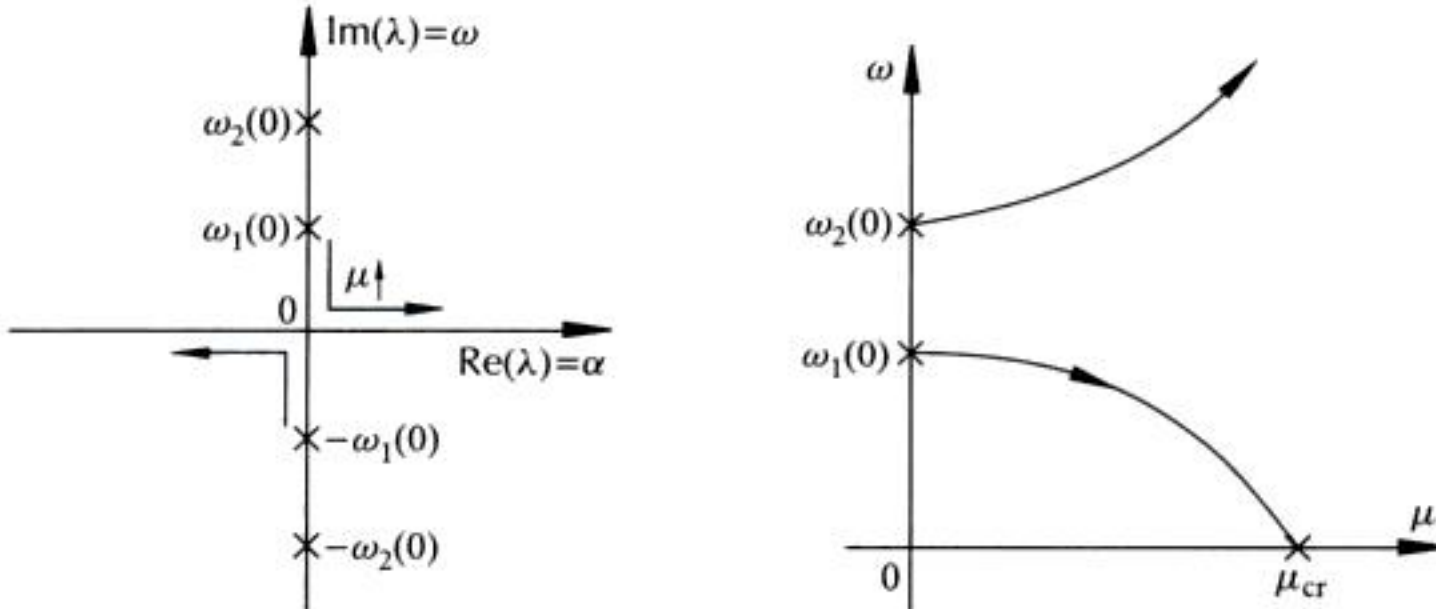


Figure 1.9 Changes of eigenvalues with the load parameter.

Suppose one of the frequencies, say $\omega_1(\mu)$, decreases and passes through zero as μ increases. For $\mu < \mu_{cr}$, $\alpha_1(\mu) = 0$ and $\omega_1(\mu) \neq 0$; at $\mu = \mu_{cr}$, $\alpha_1(0) = \omega_1(0) = 0$; when $\mu > \mu_{cr}$, $\alpha_1(\mu) > 0$ and $\omega_1(\mu) = 0$. The structure is buckled and the instability is known as *divergence* (buckling) or *pitchfork bifurcation*. The response of the system from this critical mode is non-oscillatory and grows exponentially in the form (Figure 1.10)

$$q_1(t) = \hat{q}_1 e^{\alpha_1 t}.$$

Case II. Coupled-Mode Flutter

Similar to Case I, when the load parameter $\mu = 0$, the eigenvalues are purely imaginary. If the two adjacent frequencies, say $\omega_1(\mu)$ and $\omega_2(\mu)$, coalesce when μ increases as



You have either reached a page that is unavailable for viewing or reached your viewing limit for this

@Seismicisolation

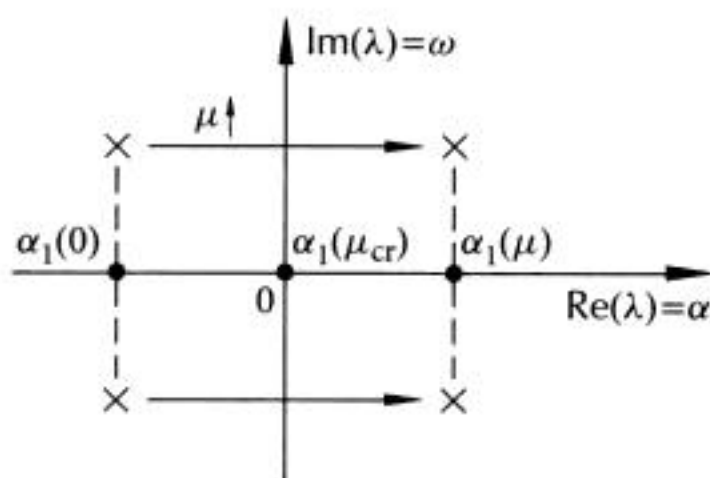


Figure 1.13 Changes of eigenvalues.

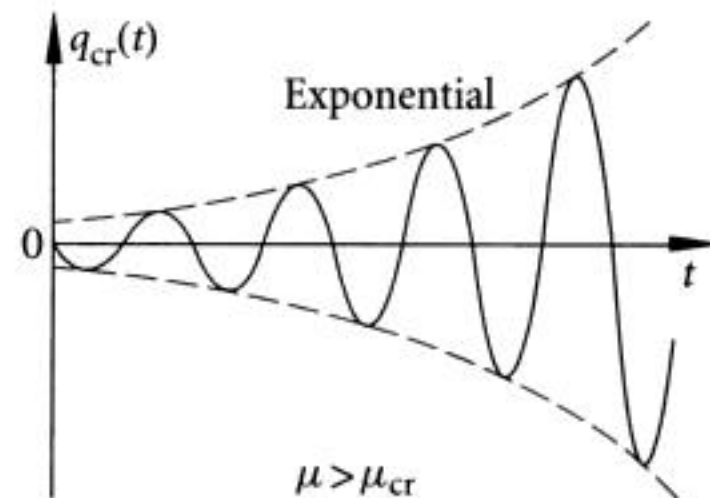


Figure 1.14 Single-mode flutter.

Example 1.3.2: Consider again the nonconservative system described in Example 1.3.1. Suppose that masses m_1 and m_2 are connected to dashpot dampers of damping coefficients d_1 and d_2 , respectively, as shown in Figure 1.15. Study the stability of the damped system to illustrate the possible destabilizing effect of damping in a nonconservative system.

Solution: Following the same procedure as in Example 1.3.1, it is easy to derive the equations of motion by including the damping forces as

$$m_2 l_2 \ddot{q}_2 + \kappa_2 (\theta_2 - \theta_1) + d_2 l_2 \dot{q}_2 = 0,$$

$$m_1 l_1 \ddot{q}_1 + m_2 (l_1 + l_2) \ddot{q}_2 + \kappa_1 \theta_1 + P l_1 (\theta_2 - \theta_1) + d_1 l_1 \dot{q}_1 + d_2 (l_1 + l_2) \dot{q}_2 = 0,$$

where $\theta_1 = q_1/l_1$, $\theta_2 = (q_2 - q_1)/l_2$.

Seeking a solution of the form $\{q_1(t), q_2(t)\} = \{\hat{q}_1, \hat{q}_2\} e^{\lambda t}$ leads to

$$-\kappa_2 \left(\frac{1}{l_1} + \frac{1}{l_2} \right) \hat{q}_1 + \left(m_2 l_2 \lambda^2 + d_2 l_2 \lambda + \frac{\kappa_2}{l_2} \right) \hat{q}_2 = 0,$$

$$\left[m_1 l_1 \lambda^2 + d_1 l_1 \lambda + \frac{\kappa_1}{l_1} - P \left(1 + \frac{l_1}{l_2} \right) \right] \hat{q}_1 + \left[(l_1 + l_2) (m_2 \lambda^2 + d_2 \lambda) + P \frac{l_1}{l_2} \right] \hat{q}_2 = 0.$$

To have nonzero solutions, the determinant of the coefficient matrix of these equations must be zero. After expanding the determinant, one obtains a polynomial equation of degree four

$$\lambda^4 + a_3 \lambda^3 + a_2 \lambda^2 + a_1 \lambda + a_0 = 0, \quad (1.3.14)$$

where

$$a_0 = \frac{k_1 k_2}{m_1 m_2 l_1^2 l_2^2},$$

$$a_1 = \frac{1}{m_1 m_2} \left[\frac{\kappa_2}{l_2} \left(\frac{2d_2}{l_1} + \frac{d_1 + d_2}{l_2} \right) + \frac{d_2}{l_1^2} (\kappa_1 + \kappa_2) - P d_2 \left(\frac{1}{l_1} + \frac{1}{l_2} \right) \right],$$

$$a_2 = \frac{k_1}{m_1 l_1^2} + \frac{k_2}{m_2 l_2^2} + \frac{k_2}{m_1} \left(\frac{1}{l_1} + \frac{1}{l_2} \right)^2 - \frac{P}{m_1} \left(\frac{1}{l_1} + \frac{1}{l_2} \right) + \frac{d_1 d_2}{m_1 m_2}, \quad a_3 = \frac{d_1}{m_1} + \frac{d_2}{m_2}.$$

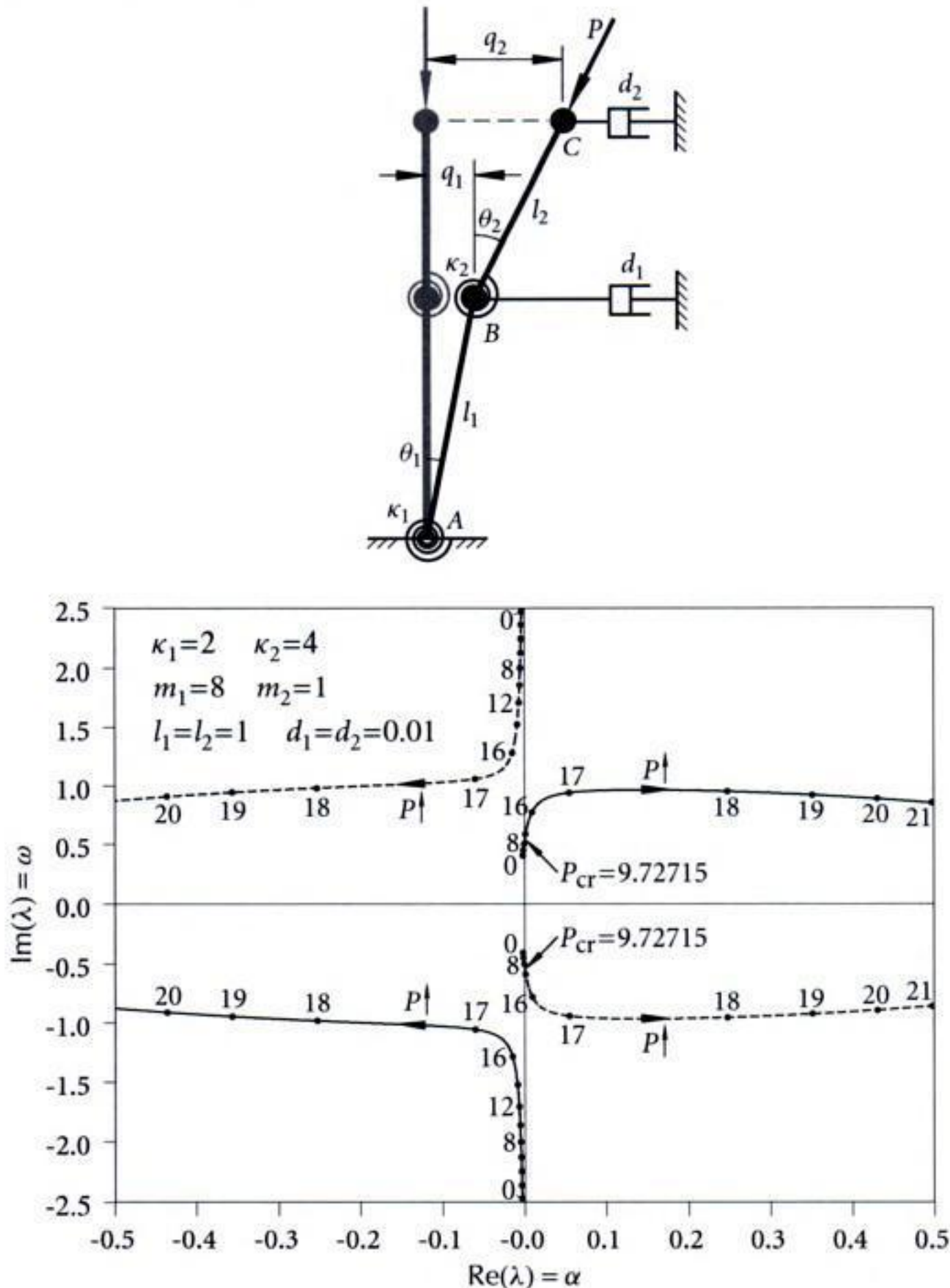


Figure 1.15 Damped nonconservative system.

For a given value of P , equation (1.3.14) can be solved to obtain the four roots of λ . The changes of the roots λ as P increases are shown in Figure 1.15 for the case $\kappa_1=2$, $\kappa_2=4$, $m_1=8$, $m_2=1$, $l_1=l_2=1$, $d_1=d_2=0.01$. When $P=0$, there are two pairs of complex roots all with negative real parts. When P is increased, one pair of the complex roots cross the imaginary axis, leading to a positive real part. The resultant instability is the single-mode flutter. At the point of crossing, this pair of complex roots become purely imaginary and the critical value of P is $P_{\text{cr}}=9.72715$.

For comparison, the changes of the roots λ as P increases are plotted in Figure 1.16 for the undamped system ($d_1=d_2=0$). When $P < P_{\text{cr}}=17.0$, there are two pairs of purely imaginary roots. These two pairs of purely imaginary roots coalesce at

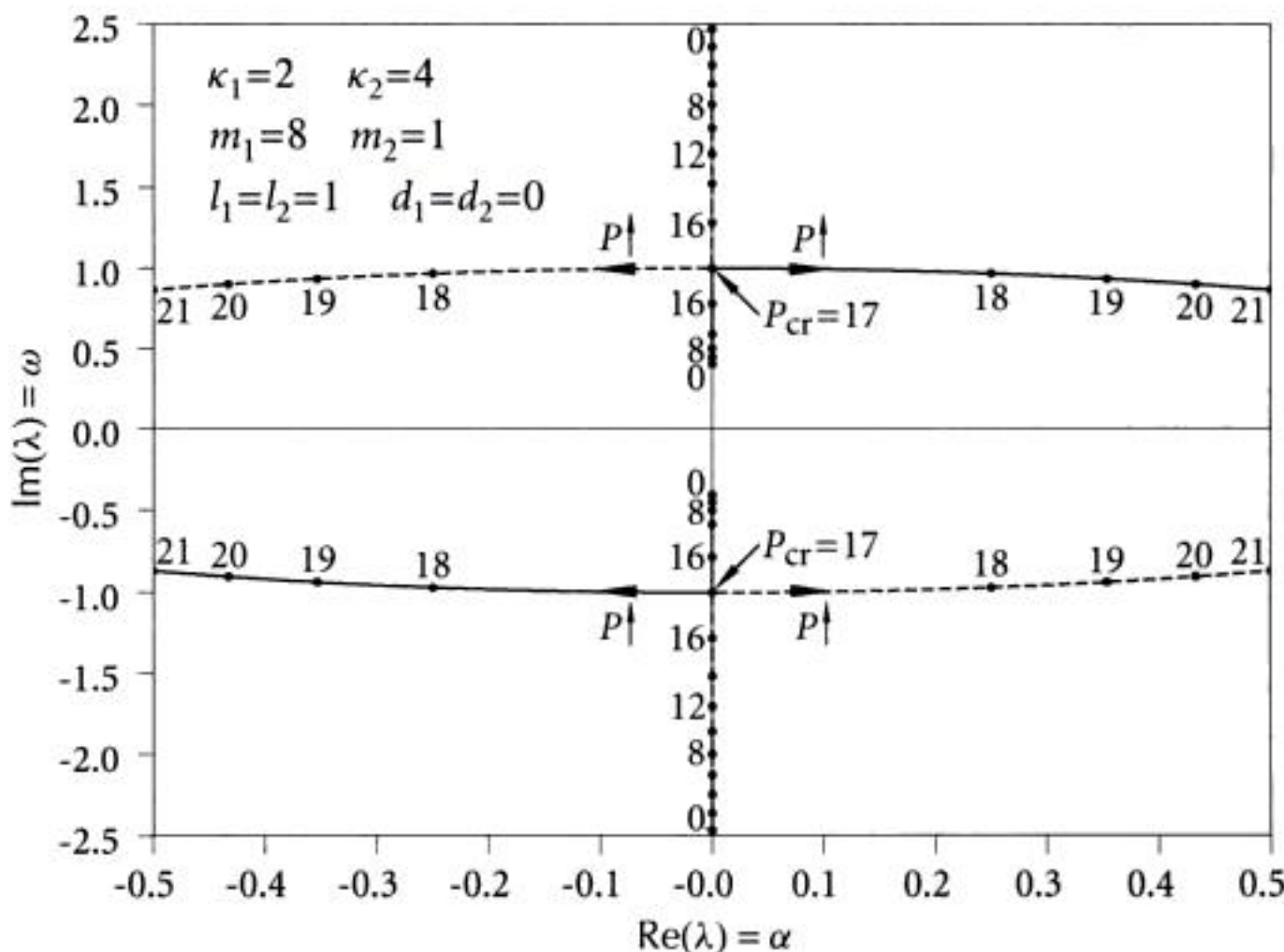


Figure 1.16 Changes of eigenvalues for undamped nonconservative system.

$P = P_{\text{cr}} = 17.0$ and then branch off for $P > P_{\text{cr}}$, resulting in one pair of complex roots with a positive real part and another pair with a negative real part.

The critical value $P_{\text{cr}} = 9.72715$ for the damped case is smaller than that of the undamped case, $P_{\text{cr}} = 17.0$, indicating that the damping has a destabilizing effect.

However, for this nonconservative system, damping is not always destabilizing for all combinations of parameters. For example, for the damped case $\kappa_1 = \kappa_2 = 1$, $m_1 = m_2 = 1$, $l_1 = l_2 = 1$, $d_1 = d_2 = 0.01$, the critical value $P_{\text{cr}} = 2.00005$ as compared to $P_{\text{cr}} = 2.0$ for the undamped case. ■

It is noted that, for conservative systems, it is a safe practice to neglect small damping in analysis and design. This is not the case for nonconservative systems; even a small damping may lead to a significant drop in the load that a structure is able to carry.

Effect of Constraints

Example 1.3.3: Suppose an additional constraint is imposed to mass m_2 of the nonconservative system in Example 1.3.1 to prevent it from moving in the horizontal direction. Study the effect of this additional constraint on the stability of the structure.

Solution: The structure degenerates to a single degree-of-freedom system, the motion of which can be described by the generalized coordinate q_1 as shown in Figure 1.17. Consider the equilibrium of bar BC. Summing up the moments about point B gives

$$R_C l_2 + \kappa_2(\theta_1 + \theta_2) = 0,$$

which leads to $R_C = -\kappa_2(\theta_1 + \theta_2)/l_2$, where $\theta_1 = q_1/l_1$, $\theta_2 = q_1/l_2$.



You have either reached a page that is unavailable for viewing or reached your viewing limit for this

@Seismicisolation



You have either reached a page that is unavailable for viewing or reached your viewing limit for this

@Seismicisolation



You have either reached a page that is unavailable for viewing or reached your viewing limit for this

@Seismicisolation



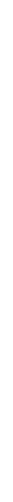
You have either reached a page that is unavailable for viewing or reached your viewing limit for this

@Seismicisolation



You have either reached a page that is unavailable for viewing or reached your viewing limit for this

@Seismicisolation



You have either reached a page that is unavailable for viewing or reached your viewing limit for this

@Seismicisolation



You have either reached a page that is unavailable for viewing or reached your viewing limit for this

@Seismicisolation



You have either reached a page that is unavailable for viewing or reached your viewing limit for this

@Seismicisolation



You have either reached a page that is unavailable for viewing or reached your viewing limit for this

@Seismicisolation



You have either reached a page that is unavailable for viewing or reached your viewing limit for this

@Seismicisolation



You have either reached a page that is unavailable for viewing or reached your viewing limit for this

@Seismicisolation



You have either reached a page that is unavailable for viewing or reached your viewing limit for this

@Seismicisolation



You have either reached a page that is unavailable for viewing or reached your viewing limit for this

@Seismicisolation



You have either reached a page that is unavailable for viewing or reached your viewing limit for this

@Seismicisolation



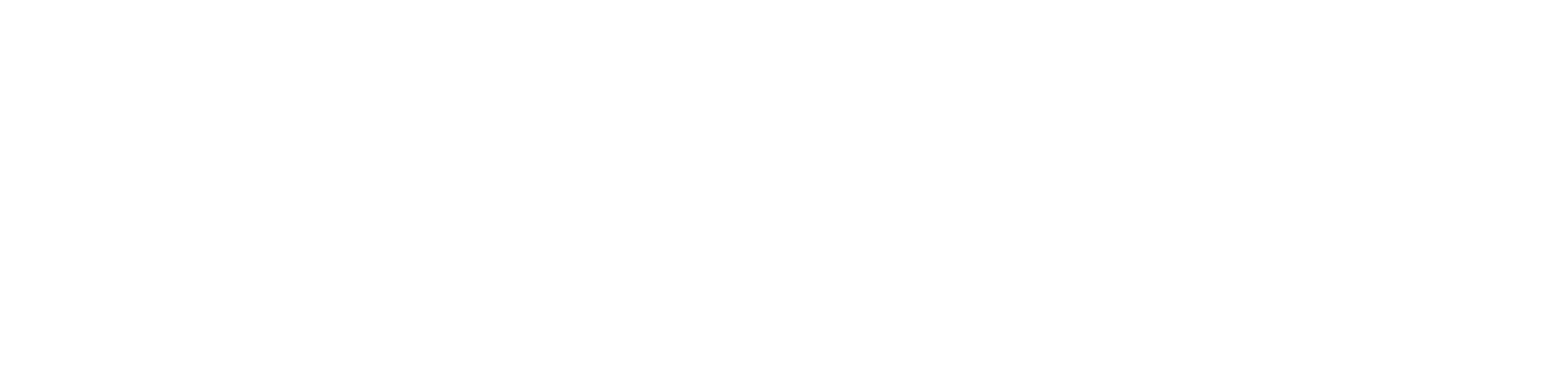
You have either reached a page that is unavailable for viewing or reached your viewing limit for this

@Seismicisolation



You have either reached a page that is unavailable for viewing or reached your viewing limit for this

@Seismicisolation



You have either reached a page that is unavailable for viewing or reached your viewing limit for this

@Seismicisolation



You have either reached a page that is unavailable for viewing or reached your viewing limit for this

@Seismicisolation



You have either reached a page that is unavailable for viewing or reached your viewing limit for this

@Seismicisolation



You have either reached a page that is unavailable for viewing or reached your viewing limit for this

@Seismicisolation



You have either reached a page that is unavailable for viewing or reached your viewing limit for this

@Seismicisolation



You have either reached a page that is unavailable for viewing or reached your viewing limit for this

@Seismicisolation



You have either reached a page that is unavailable for viewing or reached your viewing limit for this

@Seismicisolation

(1.5.53),

$$\zeta = Z e^{-i\Omega t}, \quad \bar{\zeta} = \bar{Z} e^{i\Omega t}, \quad \dot{\zeta} = (\dot{Z} - i\Omega Z) e^{-i\Omega t}, \quad \ddot{\zeta} = (\ddot{Z} - i2\Omega \dot{Z} - \Omega^2 Z) e^{-i\Omega t}.$$

After substitution of these equations into (1.5.60b), the equations of motion in the non-rotating complex plane become

$$m[(\ddot{Z} - i2\Omega \dot{Z} - \Omega^2 Z) + i2\Omega(\dot{Z} - i\Omega Z) - \Omega^2 Z] + D_i(\dot{Z} - i\Omega Z) + \frac{\partial^2}{\partial z^2} \left(EI^+ \frac{\partial^2 Z}{\partial z^2} + EI^- \frac{\partial^2 \bar{Z}}{\partial z^2} e^{i2\Omega t} \right) + P \frac{\partial^2 Z}{\partial z^2} = 0. \quad (1.5.61)$$

Including the external damping term with coefficient D_e , one finds that equation (1.5.61) becomes

$$m[(\ddot{Z} - i2\Omega \dot{Z} - \Omega^2 Z) + i2\Omega(\dot{Z} - i\Omega Z) - \Omega^2 Z] + D_i(\dot{Z} - i\Omega Z) + D_e \dot{Z} + \frac{\partial^2}{\partial z^2} \left(EI^+ \frac{\partial^2 Z}{\partial z^2} + EI^- \frac{\partial^2 \bar{Z}}{\partial z^2} e^{i2\Omega t} \right) + P \frac{\partial^2 Z}{\partial z^2} = 0. \quad (1.5.62)$$

Upon transformation of equation (1.5.62) into the rotating coordinates, the complex equation becomes

$$m(\ddot{\zeta} + i2\Omega \dot{\zeta} - \Omega^2 \zeta) + (D_i + D_e)\dot{\zeta} + iD_e\Omega \zeta + \frac{\partial^2}{\partial z^2} \left(EI^+ \frac{\partial^2 \zeta}{\partial z^2} + EI^- \frac{\partial^2 \bar{\zeta}}{\partial z^2} \right) + P \frac{\partial^2 \zeta}{\partial z^2} = 0.$$

Separating the complex equation into real and imaginary parts, one obtains the equations of motion in the rotating coordinate system as

$$m(\ddot{\xi} - 2\Omega \dot{\eta} - \Omega^2 \xi) + (D_i + D_e)\dot{\xi} - D_e\Omega \eta + \frac{\partial^2}{\partial z^2} \left(EI_\eta \frac{\partial^2 \xi}{\partial z^2} \right) + P \frac{\partial^2 \xi}{\partial z^2} = 0, \quad (1.5.63)$$

$$m(\ddot{\eta} + 2\Omega \dot{\xi} - \Omega^2 \eta) + (D_i + D_e)\dot{\eta} + D_e\Omega \xi + \frac{\partial^2}{\partial z^2} \left(EI_\xi \frac{\partial^2 \eta}{\partial z^2} \right) + P \frac{\partial^2 \eta}{\partial z^2} = 0.$$

For small bearings, the shaft may be modelled as simply supported and the boundary conditions are

$$\text{at } z=0 \text{ and } z=L : \quad \xi = \frac{\partial^2 \xi}{\partial z^2} = \eta = \frac{\partial^2 \eta}{\partial z^2} = 0.$$

Consider the fundamental mode of the form

$$\xi(z, t) = q_1(t) \sin \frac{\pi z}{L}, \quad \eta(z, t) = q_2(t) \sin \frac{\pi z}{L}, \quad (1.5.64)$$

which satisfies the boundary conditions. Substituting equations (1.5.64) into (1.5.63) results in

$$\ddot{q}_1 + \left(\frac{D_i}{m} + \frac{D_e}{m} \right) \dot{q}_1 - 2\Omega \dot{q}_2 + \left\{ \frac{\pi^2}{mL^2} [\bar{P}_1 - P(t)] - \Omega^2 \right\} q_1 - \frac{D_e}{m} \Omega q_2 = 0, \quad (1.5.65)$$

$$\ddot{q}_2 + \left(\frac{D_i}{m} + \frac{D_e}{m} \right) \dot{q}_2 + 2\Omega \dot{q}_1 + \left\{ \frac{\pi^2}{mL^2} [\bar{P}_2 - P(t)] - \Omega^2 \right\} q_2 + \frac{D_e}{m} \Omega q_1 = 0,$$

where $\bar{P}_1 = EI_\eta (\pi/L)^2$ and $\bar{P}_2 = EI_\xi (\pi/L)^2$ are the Euler buckling loads of a simply supported beam about the η - and ξ -axes, respectively.

With the use of the following notations,

$$2\beta_i = \frac{D_i}{m}, \quad 2\beta_e = \frac{D_e}{m}, \quad \bar{\omega}_{1,2}^2 = \frac{\pi^2}{mL^2} \bar{P}_{1,2}, \quad p(t) = \frac{\pi^2}{mL^2} P(t),$$

equations (1.5.65) may be written as

$$\ddot{q}_1 + 2(\beta_i + \beta_e) \dot{q}_1 - 2\Omega \dot{q}_2 + [\bar{\omega}_1^2 - \Omega^2 - p(t)] q_1 - 2\beta_e \Omega q_2 = 0, \quad (1.5.66a)$$

$$\ddot{q}_2 + 2(\beta_i + \beta_e) \dot{q}_2 + 2\Omega \dot{q}_1 + [\bar{\omega}_2^2 - \Omega^2 - p(t)] q_2 + 2\beta_e \Omega q_1 = 0,$$

or in the matrix form

$$\ddot{\mathbf{q}} + 2(\beta_i + \beta_e) \dot{\mathbf{q}} + 2\Omega \begin{bmatrix} 0 & -1 \\ 1 & 0 \end{bmatrix} \dot{\mathbf{q}} + \begin{bmatrix} \bar{\omega}_1^2 - \Omega^2 & -2\beta_e \Omega \\ 2\beta_e \Omega & \bar{\omega}_2^2 - \Omega^2 \end{bmatrix} \mathbf{q} - p(t) \mathbf{q} = 0, \quad (1.5.66b)$$

where $\mathbf{q} = \{q_1, q_2\}^T$ and the third term is the gyroscopic term, which arises from the Coriolis forces. This is a gyroscopic system under parametric excitations.

Problems

- 1.1** Study the stability of the structure shown in Figure 1.28 under a force P applied at end C . Light rigid bars AB of length l_1 and BC of length l_2 are connected at B by a hinge and a torsional spring of stiffness κ_2 . Bar AB is supported at A by a hinge and a torsional spring of stiffness κ_1 .

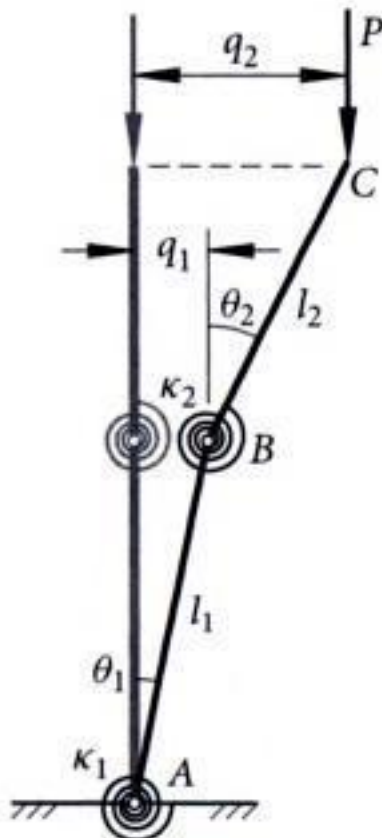


Figure 1.28

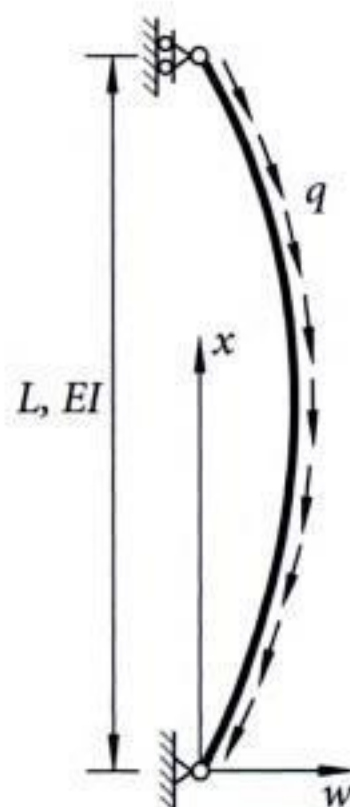


Figure 1.29

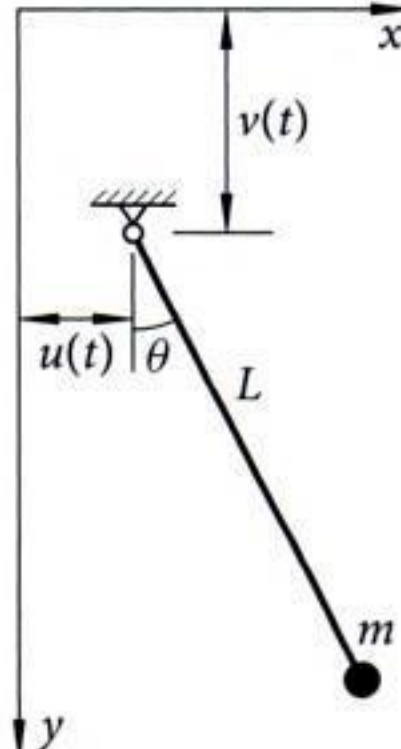


Figure 1.30

- 1.2** Consider the simply supported beam under the uniformly distributed follower force q as shown in Figure 1.29.

1.2.1. Show that the governing equation of equilibrium is given by

$$\frac{d^4 u}{d\xi^4} + \lambda(1-\zeta) \frac{d^2 u}{d\xi^2} = 0,$$

where

$$u = \frac{w}{L}, \quad \zeta = \frac{x}{L}, \quad \lambda = \frac{qL}{EI}.$$

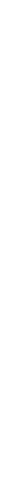
1.2.2. Applying the transformation

$$\xi = \frac{2}{3} [\lambda(1-\zeta)^3]^{1/2}, \quad v\xi^{1/3} = \frac{d^2 u}{d\xi^2},$$

transform this equation to a Bessel's equation and determine the exact solution of the divergence load q_{cr} .

1.3 Derive the equation of motion of a pendulum with a moving support which moves horizontally and vertically with prescribed motions $u(t)$ and $v(t)$, respectively, as shown in Figure 1.30. The generalized coordinate is θ .

1.4 For the beam in plane motion considered in Section 1.5.2, derive the equation of motion for Case (i) with initial imperfection $\bar{v}(x) = q_0 \sin(\pi x/L)$.



You have either reached a page that is unavailable for viewing or reached your viewing limit for this

@Seismicisolation



You have either reached a page that is unavailable for viewing or reached your viewing limit for this

@Seismicisolation



You have either reached a page that is unavailable for viewing or reached your viewing limit for this

@Seismicisolation



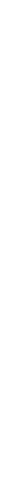
You have either reached a page that is unavailable for viewing or reached your viewing limit for this

@Seismicisolation



You have either reached a page that is unavailable for viewing or reached your viewing limit for this

@Seismicisolation



You have either reached a page that is unavailable for viewing or reached your viewing limit for this

@Seismicisolation



You have either reached a page that is unavailable for viewing or reached your viewing limit for this

@Seismicisolation



You have either reached a page that is unavailable for viewing or reached your viewing limit for this

@Seismicisolation



You have either reached a page that is unavailable for viewing or reached your viewing limit for this

@Seismicisolation



You have either reached a page that is unavailable for viewing or reached your viewing limit for this

@Seismicisolation



You have either reached a page that is unavailable for viewing or reached your viewing limit for this

@Seismicisolation



You have either reached a page that is unavailable for viewing or reached your viewing limit for this

@Seismicisolation



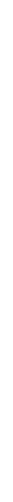
You have either reached a page that is unavailable for viewing or reached your viewing limit for this

@Seismicisolation



You have either reached a page that is unavailable for viewing or reached your viewing limit for this

@Seismicisolation



You have either reached a page that is unavailable for viewing or reached your viewing limit for this

@Seismicisolation



You have either reached a page that is unavailable for viewing or reached your viewing limit for this

@Seismicisolation



You have either reached a page that is unavailable for viewing or reached your viewing limit for this

@Seismicisolation



You have either reached a page that is unavailable for viewing or reached your viewing limit for this

@Seismicisolation



You have either reached a page that is unavailable for viewing or reached your viewing limit for this

@Seismicisolation



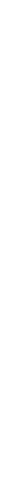
You have either reached a page that is unavailable for viewing or reached your viewing limit for this

@Seismicisolation



You have either reached a page that is unavailable for viewing or reached your viewing limit for this

@Seismicisolation



You have either reached a page that is unavailable for viewing or reached your viewing limit for this

@Seismicisolation



You have either reached a page that is unavailable for viewing or reached your viewing limit for this

@Seismicisolation

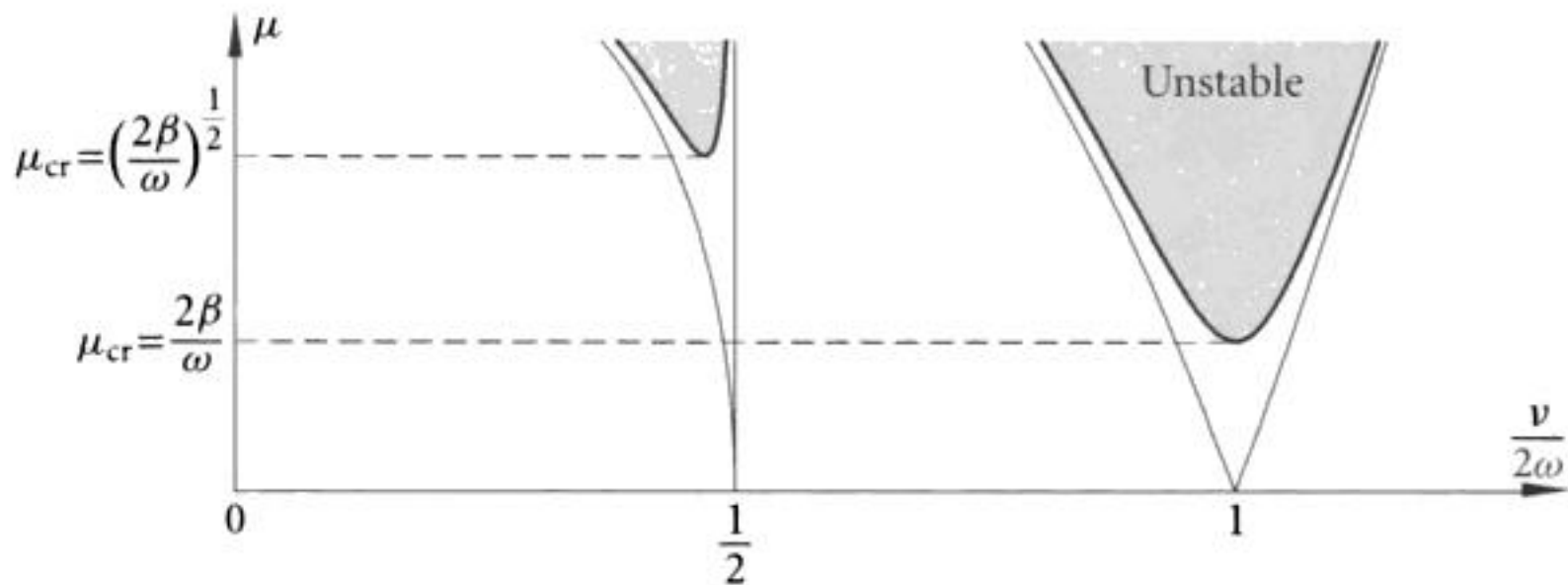


Figure 2.8 The first and second stability boundaries.

2.5.2 Periodic Solutions of Period T

Substituting the periodic solution of period T given by equation (2.4.6) into (2.5.1) and equating the coefficients of various harmonics $\sin(kvt/2)$ and $\cos(kvt/2)$ to zero lead to

$$1 : \quad b_0 - \mu b_2 = 0,$$

$$\cos vt : \quad (4\beta r/\omega)a_2 - 2\mu b_0 + (1-4r^2)b_2 - \mu b_4 = 0,$$

$$\sin(kvt/2), k=2, 4, \dots : \quad -\mu a_{k+2} + (1-k^2r^2)a_k - \mu a_{k-2} - (2k\beta r/\omega)b_k = 0,$$

$$\cos(kvt/2), k=4, 6, \dots : \quad (2k\beta r/\omega)a_k - \mu b_{k-2} + (1-k^2r^2)b_k - \mu b_{k+2} = 0,$$

where $r = v/(2\omega)$ and $a_0 = 0$.

This is a system of homogeneous linear algebraic equations for the coefficients $a_2, a_4, \dots, b_0, b_2, b_4, \dots$. For non-trivial solutions, setting the determinant of the coefficient matrix of the vector $\{ \dots, a_4, a_2, b_0, b_2, b_4, \dots \}^T$ to zero yields

$$\Delta_T = \begin{vmatrix} \dots & 1-16r^2 & -\mu & 0 & 0 & -8\beta r/\omega & 0 & \dots \\ \dots & -\mu & 1-4r^2 & 0 & -4\beta r/\omega & 0 & 0 & \dots \\ \dots & 0 & 0 & 1 & -\mu & 0 & 0 & \dots \\ \dots & 0 & 4\beta r/\omega & -2\mu & 1-4r^2 & -\mu & 0 & \dots \\ \dots & 8\beta r/\omega & 0 & 0 & -\mu & 1-16r^2 & -\mu & \dots \end{vmatrix} = 0. \quad (2.5.4)$$

Boundaries of the Second Stability Region

For the first-order approximation, the 3×3 submatrix corresponding to the coefficients $\{a_2, b_0, b_2\}^T$ in equation (2.5.4) yields

$$\begin{vmatrix} 1-4r^2 & 0 & -4\beta r/\omega \\ 0 & 1 & -\mu \\ 4\beta r/\omega & -2\mu & 1-4r^2 \end{vmatrix} = 0,$$

which leads to, after expanding the determinant,

$$(1-4r^2)^2 - 2\mu^2(1-4r^2) + (4\beta r/\omega)^2 = 0.$$

This may be regarded as a quadratic equation in $(1-4r^2)$; solving for the r in it yields

$$\begin{aligned} \frac{\nu}{2\omega} = r &= \frac{1}{2} \sqrt{1 - \mu^2 \pm \sqrt{\mu^4 - \left(\frac{4\beta r}{\omega}\right)^2}} \\ &\approx \frac{1}{2} \sqrt{1 - \mu^2 \pm \sqrt{\mu^4 - \left(\frac{2\beta}{\omega}\right)^2}}, \end{aligned} \quad (2.5.5)$$

in which the stability boundary $r = \frac{1}{2}$ for $\mu \rightarrow 0$ is substituted. The stability boundaries are shown in Figure 2.8.

From equation (2.5.5), the minimal value of the amplitude of forcing for instability $\mu_{cr} = (2\beta/\omega)^{1/2}$ is obtained. In general, the minimal value of μ for the k th instability region is

$$\mu_{k,cr} = O\left[(2\beta/\omega)^{1/k}\right]. \quad (2.5.6)$$

• In this Chapter, exact analytical formulations are presented for the determination of the stability regions or the stability boundaries of the Mathieu–Hill equations, the Mathieu equations, and linear differential equations with periodic coefficients. In Chapter 3, approximate methods, especially the method of averaging, are introduced to tackle problems of linear systems under harmonic excitations.

Problems

- 2.1 For Example 2.1.1, determine the stability boundaries for the cases of $h=1$ and $h>1$. Plot the results for the first four stability regions.
- 2.2 Determine the first-order and second-order approximations of the fourth stability boundaries near $\nu/(2\omega)=\frac{1}{4}$ for the undamped Mathieu equation (2.4.1).
- 2.3 Determine the first-order and second-order approximations of the fifth stability boundaries near $\nu/(2\omega)=\frac{1}{5}$ for the undamped Mathieu equation (2.4.1).
- 2.4 For the damped Mathieu equation (2.5.1), determine the first-order approximation of the third stability boundaries near $\nu/(2\omega)=\frac{1}{3}$. Plot the result in comparison with the stability boundaries with $\beta=0$.

C H A P T E R

3

Approximate Methods

3.1 The Method of Averaging

In this Section, the method of averaging, developed by Bogoliubov and Mitropolski [26], is applied to study the first stability regions of the undamped and damped Mathieu equations. The method of averaging is introduced through these examples.

3.1.1 Stability of the Undamped Mathieu Equations

Consider the undamped Mathieu equation

$$\ddot{q}(t) + \omega^2(1 - 2\varepsilon\mu \cos vt)q(t) = 0, \quad (3.1.1)$$

for small amplitude of parametric excitation with $0 < \varepsilon \ll 1$ being a small parameter. Apply the time scaling $\tau = vt$ and denote differentiation with respect to τ using a prime, i.e. $(\cdot)' = d(\cdot)/d\tau$. Equation (3.1.1) becomes

$$q''(\tau) + \frac{\omega^2}{v^2}(1 - 2\varepsilon\mu \cos \tau)q(\tau) = 0. \quad (3.1.2)$$

Let the parametric excitation frequency v vary around a reference frequency ω_0 , i.e. $v = \omega_0(1 - \varepsilon\Delta)$, where Δ is the detuning parameter. Equation (3.1.2) can be written as

$$q''(\tau) + \frac{\omega^2}{\omega_0^2(1 - \varepsilon\Delta)^2}(1 - 2\varepsilon\mu \cos \tau)q(\tau) = 0.$$

Denoting $\kappa = \omega/\omega_0$, and because $(1 - \varepsilon\Delta)^{-2} \approx 1 + 2\varepsilon\Delta$, one obtains, after dropping terms of orders higher than $\mathcal{O}(\varepsilon)$,

$$q''(\tau) + \kappa^2 q(\tau) = -2\varepsilon\kappa^2(\Delta - \mu \cos \tau)q(\tau). \quad (3.1.3)$$

The complementary solution of equation (3.1.3) when setting the right side to zero is given by

$$q_C(\tau) = a \cos \Phi(\tau), \quad q'_C(\tau) = -a\kappa \sin \Phi(\tau), \quad \Phi(\tau) = \kappa\tau + \varphi, \quad (3.1.4)$$



You have either reached a page that is unavailable for viewing or reached your viewing limit for this

@Seismicisolation



You have either reached a page that is unavailable for viewing or reached your viewing limit for this

@Seismicisolation



You have either reached a page that is unavailable for viewing or reached your viewing limit for this

@Seismicisolation



You have either reached a page that is unavailable for viewing or reached your viewing limit for this

@Seismicisolation



You have either reached a page that is unavailable for viewing or reached your viewing limit for this

@Seismicisolation



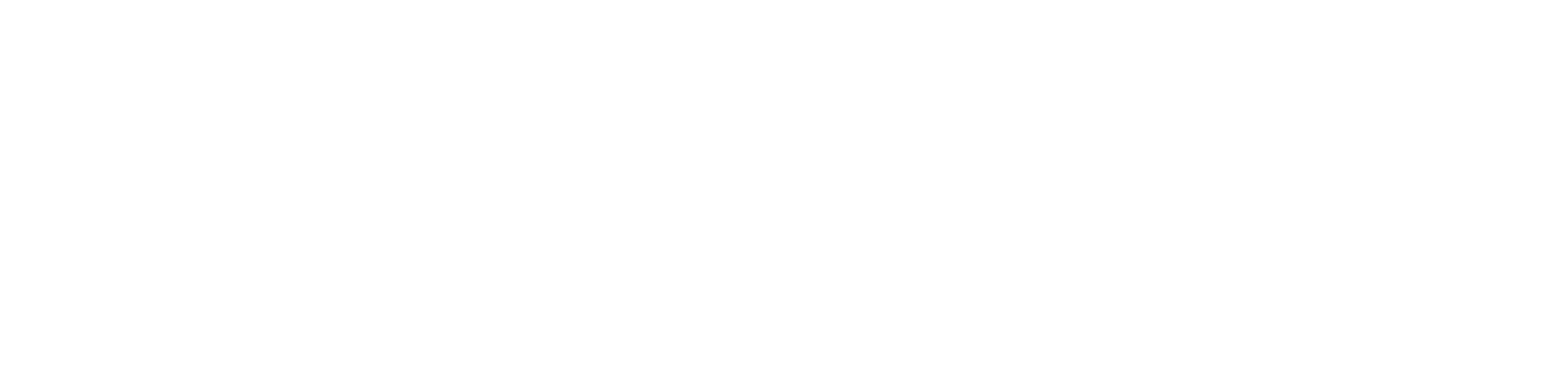
You have either reached a page that is unavailable for viewing or reached your viewing limit for this

@Seismicisolation



You have either reached a page that is unavailable for viewing or reached your viewing limit for this

@Seismicisolation



You have either reached a page that is unavailable for viewing or reached your viewing limit for this

@Seismicisolation



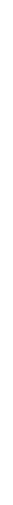
You have either reached a page that is unavailable for viewing or reached your viewing limit for this

@Seismicisolation



You have either reached a page that is unavailable for viewing or reached your viewing limit for this

@Seismicisolation



You have either reached a page that is unavailable for viewing or reached your viewing limit for this

@Seismicisolation



You have either reached a page that is unavailable for viewing or reached your viewing limit for this

@Seismicisolation



You have either reached a page that is unavailable for viewing or reached your viewing limit for this

@Seismicisolation



You have either reached a page that is unavailable for viewing or reached your viewing limit for this

@Seismicisolation



You have either reached a page that is unavailable for viewing or reached your viewing limit for this

@Seismicisolation



You have either reached a page that is unavailable for viewing or reached your viewing limit for this

@Seismicisolation



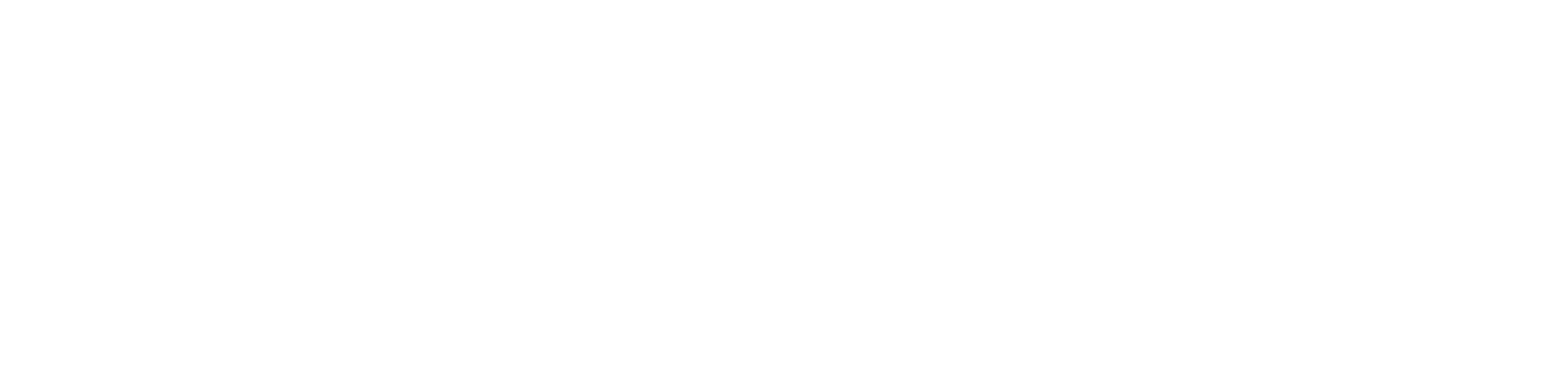
You have either reached a page that is unavailable for viewing or reached your viewing limit for this

@Seismicisolation



You have either reached a page that is unavailable for viewing or reached your viewing limit for this

@Seismicisolation



You have either reached a page that is unavailable for viewing or reached your viewing limit for this

@Seismicisolation

Since $\kappa_r \kappa_s > 0$, inequality (3.3.26) yields

$$\begin{aligned} [(\kappa_r \zeta_r + \kappa_s \zeta_s)(\kappa_s \mp \kappa_r)(\zeta_r \mp \zeta_s) - \kappa_r \kappa_s (\zeta_r \mp \zeta_s)^2 \pm (\kappa_r \zeta_r + \kappa_s \zeta_s)^2] \Delta^2 \\ > (\kappa_r \zeta_r + \kappa_s \zeta_s)^2 (\pm \frac{1}{4} \mu^2 p_{rs} p_{sr} - \zeta_r \zeta_s), \end{aligned}$$

or

$$(\kappa_r \pm \kappa_s)^2 \zeta_r \zeta_s \Delta^2 > (\kappa_r \zeta_r + \kappa_s \zeta_s)^2 (\pm \frac{1}{4} \mu^2 p_{rs} p_{sr} - \zeta_r \zeta_s).$$

Since $|\kappa_r \pm \kappa_s| = 1$, the stability region is given by

$$\Delta^2 > \frac{(\kappa_r \zeta_r + \kappa_s \zeta_s)^2}{\zeta_r \zeta_s} (\pm \frac{1}{4} \mu^2 p_{rs} p_{sr} - \zeta_r \zeta_s). \quad (3.3.27)$$

- When $p_{rs} p_{sr} < 0$, (3.3.27) is always true for $\kappa_r + \kappa_s = 1$ or there is no instability for $v \approx \omega_r + \omega_s$.
- When $p_{rs} p_{sr} > 0$, (3.3.27) is always true for $|\kappa_r - \kappa_s| = 1$ or there is no instability for $v \approx |\omega_r - \omega_s|$.

Since $\kappa_r = \omega_r / \omega_0$, $\kappa_s = \omega_s / \omega_0$, $\varepsilon \Delta = 1 - v / \omega_0$, the instability region is, from (3.3.27),

$$\left| 1 - \frac{v}{\omega_0} \right| < \frac{\varepsilon}{\omega_0} \left(\omega_r \sqrt{\frac{\zeta_r}{\zeta_s}} + \omega_s \sqrt{\frac{\zeta_s}{\zeta_r}} \right) \sqrt{\frac{1}{4} \mu^2 |p_{rs} p_{sr}| - \zeta_r \zeta_s}, \quad \omega_0 = |\omega_r \pm \omega_s|. \quad (3.3.28)$$

The minimal value for instability is $\mu_{cr} |p_{rs} p_{sr}|^{1/2} = 2(\zeta_r \zeta_s)^{1/2}$. The instability regions of both of the undamped case (3.3.23) and damped case (3.3.28) are plotted in Figure 3.5.

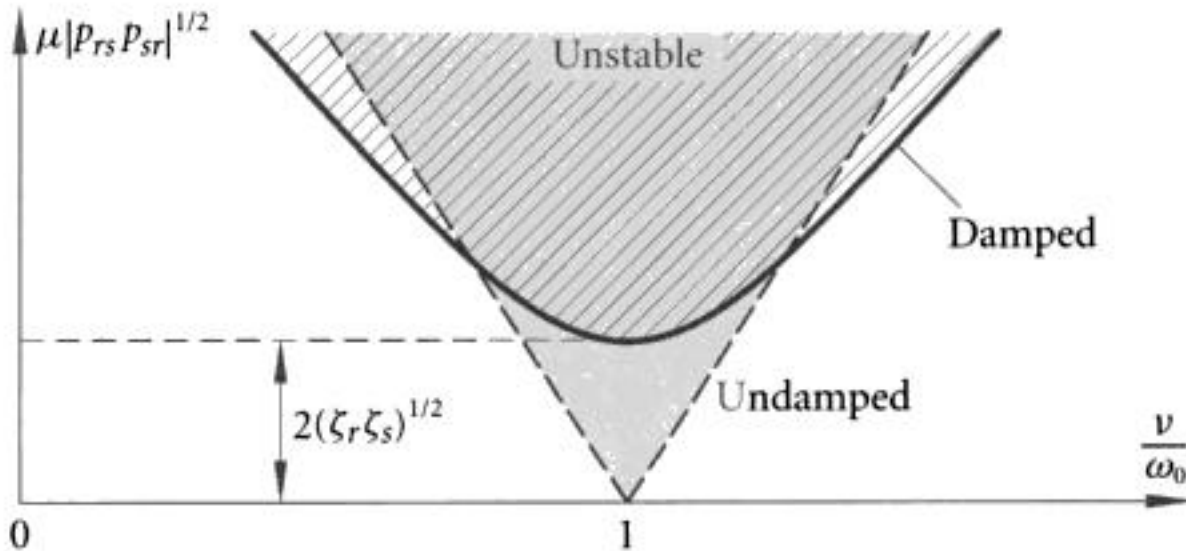


Figure 3.5 Instability regions for combination resonance $\omega_0 = |\omega_r \pm \omega_s|$.

Denoting

$$\frac{\beta_r}{\beta_s} = \frac{\omega_r \zeta_r}{\omega_s \zeta_s} = \gamma^2,$$

and making $\zeta_r, \zeta_s \rightarrow 0$, one may write (3.3.28) as

$$\left| 1 - \frac{v}{\omega_0} \right| < \varepsilon \frac{\mu}{2\omega_0} \left(\gamma + \frac{1}{\gamma} \right) \sqrt{\omega_r \omega_s |p_{rs} p_{sr}|}, \quad \omega_0 = |\omega_r \pm \omega_s|. \quad (3.3.29)$$

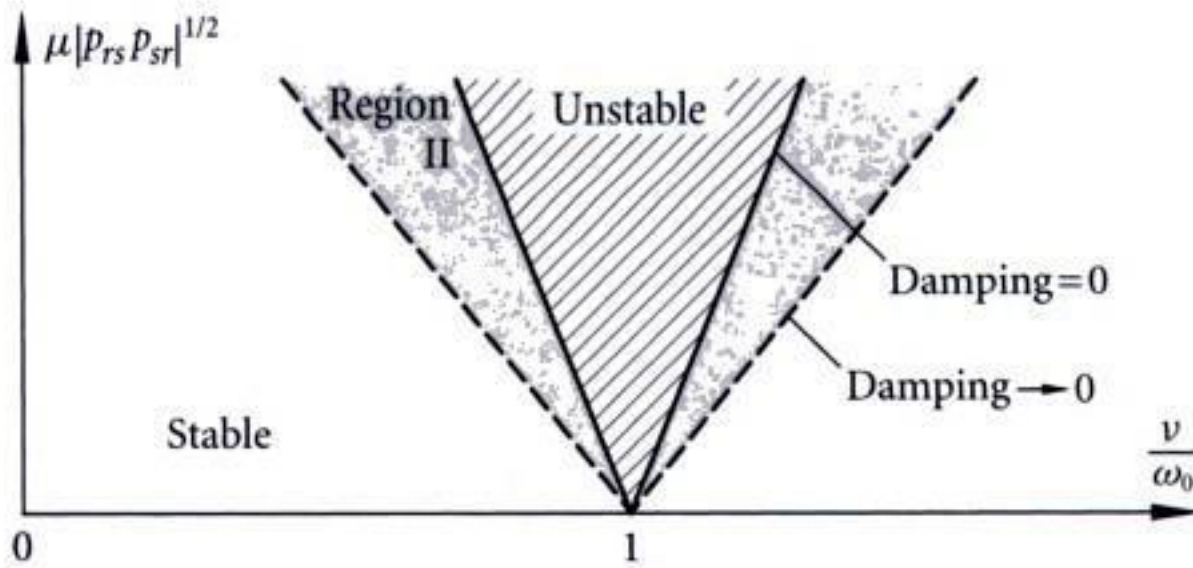


Figure 3.6 Instability regions for combination resonance $\omega_0 = |\omega_r \pm \omega_s|$.

When $\gamma = 1$, the result (3.3.23) for the undamped case is recovered. Since $\gamma + 1/\gamma \geq 2$, it is found that the region of instability is widened, as shown in Figure 3.6. By taking the ratio γ arbitrarily small or large, the region of instability can be made arbitrarily wide. However, it can be shown, by solving for the exponent ρ , that the growth of the response in Region II is extremely small; hence this region is described as *quasi-stable*.

Example 3.3.1: Suppose the equations of motion of a two degrees-of-freedom system are of the form

$$\begin{aligned}\ddot{q}_1 + \omega_1^2 q_1 + 2\varepsilon\mu \cos vt (p_{11} q_1 + p_{12} q_2) &= 0, \\ \ddot{q}_2 + \omega_1^2 q_2 + q_1 + 2\varepsilon\mu \cos vt (p_{11} q_1 + p_{12} q_2) &= 0.\end{aligned}\quad (3.3.30)$$

Investigate the stability of the system for $v \approx 2\omega_1$.

Solution: Taking $q_1 = \varepsilon^\alpha u_1$, $q_2 = u_2$, one finds that the equations of motion (3.3.30) become

$$\begin{aligned}\ddot{u}_1 + \omega_1^2 u_1 + 2\varepsilon\mu \cos vt (p_{11} u_1 + \varepsilon^{-\alpha} p_{12} u_2) &= 0, \\ \ddot{u}_2 + \omega_1^2 u_2 + \varepsilon^\alpha u_1 + 2\varepsilon\mu \cos vt (\varepsilon^\alpha p_{21} u_1 + p_{22} u_2) &= 0.\end{aligned}\quad (3.3.31)$$

Applying the time scaling $\tau = vt$, $v = \omega_0(1 - \varepsilon^\beta \Delta)$, where ω_0 is a reference frequency and Δ is the detuning parameter, and denoting $(\cdot)' = d(\cdot)/d\tau$, one obtains equations (3.3.31) as, after dropping terms of order $\mathcal{O}(\varepsilon^\beta)$ in the series expansion,

$$\begin{aligned}u_1'' + \kappa_1^2 u_1 &= -2\varepsilon^\beta \kappa_1^2 \Delta u_1 - 2\mu \cos \tau (\varepsilon f_{11} u_1 + \varepsilon^{1-\alpha} f_{12} u_2), \\ u_2'' + \kappa_1^2 u_2 &= -2\varepsilon^\beta \kappa_1^2 \Delta u_2 - \varepsilon^\alpha u_1 / \omega_0^2 - 2\mu \cos \tau (\varepsilon^{1+\alpha} f_{21} u_1 + \varepsilon f_{22} u_2),\end{aligned}\quad (3.3.32)$$

where $\kappa_1 = \omega_1 / \omega_0$, $f_{ij} = p_{ij} / \omega_0^2$, for $i, j = 1, 2$.

To determine the effect of the parametric resonance and the repeated modal frequencies, at least one coupling term must be kept. Hence, it is reasonable to take $\alpha = \beta = \frac{1}{2}$. If terms of order $\mathcal{O}(\varepsilon^{1/2})$ are dropped, equations (3.3.32) are reduced to

$$\begin{aligned}u_1'' + \kappa_1^2 u_1 &= -2\varepsilon^{1/2} (\kappa_1^2 \Delta u_1 + \mu f_{12} u_2 \cos \tau), \\ u_2'' + \kappa_1^2 u_2 &= -\varepsilon^{1/2} (2\kappa_1^2 \Delta u_2 + u_1 / \omega_0^2).\end{aligned}\quad (3.3.33)$$

Transforming (u_i, u'_i) to (a_i, φ_i) , $i=1, 2$, through

$$u_i(\tau) = a_i(\tau) \cos \Phi_i(\tau), \quad u'_i(\tau) = -a_i(\tau) \kappa_1 \sin \Phi_i(\tau), \quad \Phi_i(\tau) = \kappa_1 \tau + \varphi_i(\tau),$$

results in

$$\begin{aligned} a'_1 \cos \Phi_1 - a_1 \varphi'_1 \sin \Phi_1 &= 0, \\ a'_1 \sin \Phi_1 + a_1 \varphi'_1 \cos \Phi_1 &= 2\epsilon^{1/2} (\kappa_1 \Delta a_1 \cos \Phi_1 + \mu f_{12} a_2 \cos \tau \cos \Phi_2 / \kappa_1), \\ a'_2 \cos \Phi_2 - a_2 \varphi'_2 \sin \Phi_2 &= 0, \\ a'_2 \sin \Phi_2 + a_2 \varphi'_2 \cos \Phi_2 &= \epsilon^{1/2} [2\kappa_1 \Delta a_2 \cos \Phi_2 + a_1 \cos \Phi_1 / (\omega_0^2 \kappa_1)]. \end{aligned} \quad (3.3.34)$$

Solving equations (3.3.34) for a'_1, φ'_1, a'_2 and φ'_2 yields

$$\begin{aligned} a'_1 &= 2\epsilon^{1/2} (\kappa_1 \Delta a_1 \sin \Phi_1 \cos \Phi_1 + \mu f_{12} a_2 \cos \tau \sin \Phi_1 \cos \Phi_2 / \kappa_1), \\ a_1 \varphi'_1 &= 2\epsilon^{1/2} (\kappa_1 \Delta a_1 \cos^2 \Phi_1 + \mu f_{12} a_2 \cos \tau \cos \Phi_1 \cos \Phi_2 / \kappa_1), \\ a'_2 &= \epsilon^{1/2} [2\kappa_1 \Delta a_2 \sin \Phi_2 \cos \Phi_2 + a_1 \cos \Phi_1 \sin \Phi_2 / (\omega_0^2 \kappa_1)], \\ a_2 \varphi'_2 &= \epsilon^{1/2} [2\kappa_1 \Delta a_2 \cos^2 \Phi_2 + a_1 \cos \Phi_1 \cos \Phi_2 / (\omega_0^2 \kappa_1)]. \end{aligned} \quad (3.3.35)$$

For approximate solutions, apply the method of averaging to approximate $a_1, \varphi_1, a_2, \varphi_2$ by their averaged values $\bar{a}_1, \bar{\varphi}_1, \bar{a}_2, \bar{\varphi}_2$, respectively. The averaged equations are, for $\kappa_1 = \frac{1}{2}$ or $\nu \approx 2\omega_1$,

$$\begin{aligned} \bar{a}'_1 &= A \bar{a}_2 \sin(\bar{\varphi}_1 + \bar{\varphi}_2), & \bar{a}_1 \bar{\varphi}'_1 &= \kappa_1 \hat{\Delta} \bar{a}_1 + A \bar{a}_2 \cos(\bar{\varphi}_1 + \bar{\varphi}_2), \\ \bar{a}'_2 &= -B \bar{a}_1 \sin(\bar{\varphi}_1 - \bar{\varphi}_2), & \bar{a}_2 \bar{\varphi}'_2 &= \kappa_1 \hat{\Delta} \bar{a}_2 + B \bar{a}_1 \cos(\bar{\varphi}_1 - \bar{\varphi}_2), \end{aligned} \quad (3.3.36)$$

where $\hat{\Delta} = \epsilon^{1/2} \Delta$, $A = \epsilon^{1/2} \mu f_{12} / (2\kappa_1)$, $B = \epsilon^{1/2} / (2\omega_0^2 \kappa_1)$. To solve equations (3.3.36), convert to rectangular coordinates using

$$x_1 = \bar{a}_1 \cos \bar{\varphi}_1, \quad y_1 = \bar{a}_1 \sin \bar{\varphi}_1, \quad x_2 = \bar{a}_2 \cos \bar{\varphi}_2, \quad y_2 = \bar{a}_2 \sin \bar{\varphi}_2.$$

The averaged equations in the rectangular coordinates become

$$\begin{aligned} x'_1 &= -\kappa_1 \hat{\Delta} y_1 + A y_2, & y'_1 &= \kappa_1 \hat{\Delta} x_1 + A x_2, \\ x'_2 &= -B y_1 - \kappa_1 \hat{\Delta} y_2, & y'_2 &= B x_1 + \kappa_1 \hat{\Delta} x_2, \end{aligned} \quad (3.3.37)$$

which are a set of first-order linear ordinary differential equations with constant coefficients. The solutions of equations (3.3.37) are of the form $C e^{\rho \tau}$, in which the characteristic numbers ρ are the roots of

$$\begin{vmatrix} \rho & 0 & \kappa_1 \hat{\Delta} & -A \\ 0 & \rho & B & \kappa_1 \hat{\Delta} \\ -\kappa_1 \hat{\Delta} & -A & \rho & 0 \\ -B & -\kappa_1 \hat{\Delta} & 0 & \rho \end{vmatrix} = 0,$$



You have either reached a page that is unavailable for viewing or reached your viewing limit for this

@Seismicisolation



You have either reached a page that is unavailable for viewing or reached your viewing limit for this

@Seismicisolation



You have either reached a page that is unavailable for viewing or reached your viewing limit for this

@Seismicisolation



You have either reached a page that is unavailable for viewing or reached your viewing limit for this

@Seismicisolation



You have either reached a page that is unavailable for viewing or reached your viewing limit for this

@Seismicisolation



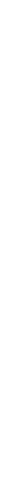
You have either reached a page that is unavailable for viewing or reached your viewing limit for this

@Seismicisolation



You have either reached a page that is unavailable for viewing or reached your viewing limit for this

@Seismicisolation



You have either reached a page that is unavailable for viewing or reached your viewing limit for this

@Seismicisolation



You have either reached a page that is unavailable for viewing or reached your viewing limit for this

@Seismicisolation



You have either reached a page that is unavailable for viewing or reached your viewing limit for this

@Seismicisolation



You have either reached a page that is unavailable for viewing or reached your viewing limit for this

@Seismicisolation



You have either reached a page that is unavailable for viewing or reached your viewing limit for this

@Seismicisolation



You have either reached a page that is unavailable for viewing or reached your viewing limit for this

@Seismicisolation



You have either reached a page that is unavailable for viewing or reached your viewing limit for this

@Seismicisolation



You have either reached a page that is unavailable for viewing or reached your viewing limit for this

@Seismicisolation

where

$$\begin{aligned} f_r(\mathbf{a}, \varphi, t) &= \sum_{s=1}^n (\bar{D}_{rs}^1 Q_s + \bar{D}_{rs}^2 P_s), & g_r(\mathbf{a}, \varphi, t) &= \sum_{s=1}^n (\bar{S}_{rs}^1 Q_s + \bar{S}_{rs}^2 P_s), \\ l_r(\mathbf{a}, \varphi, t) &= \sum_{s=1}^n (\bar{D}_{rs}^3 Q_s + \bar{D}_{rs}^4 P_s), & m_r(\mathbf{a}, \varphi, t) &= \sum_{s=1}^n (\bar{S}_{rs}^3 Q_s + \bar{S}_{rs}^4 P_s). \end{aligned}$$

Solving equations (3.5.34) for \dot{a}_r and $a_r \dot{\varphi}_r$ results in the equations of motion in the standard form, for $r = 1, 2, \dots, n$,

$$\begin{aligned} \dot{a}_r(t) &= \varepsilon [F_r(\mathbf{a}, \varphi, t) + f(t) G_r(\mathbf{a}, \varphi, t)], \\ a_r(t) \dot{\varphi}_r(t) &= \varepsilon [L_r(\mathbf{a}, \varphi, t) + f(t) M_r(\mathbf{a}, \varphi, t)], \end{aligned} \quad (3.5.35)$$

where

$$\begin{aligned} F_r(\mathbf{a}, \varphi, t) &= -f_r(\mathbf{a}, \varphi, t) \cos \Phi_r + l_r(\mathbf{a}, \varphi, t) \sin \Phi_r, \\ G_r(\mathbf{a}, \varphi, t) &= -g_r(\mathbf{a}, \varphi, t) \cos \Phi_r + m_r(\mathbf{a}, \varphi, t) \sin \Phi_r, \\ L_r(\mathbf{a}, \varphi, t) &= +f_r(\mathbf{a}, \varphi, t) \sin \Phi_r + l_r(\mathbf{a}, \varphi, t) \cos \Phi_r, \\ M_r(\mathbf{a}, \varphi, t) &= +g_r(\mathbf{a}, \varphi, t) \sin \Phi_r + m_r(\mathbf{a}, \varphi, t) \cos \Phi_r. \end{aligned}$$

Approximate methods, such as the method of averaging, can then be applied to equations (3.5.35) to investigate the stability behaviour of the system.

- In this Chapter, approximate methods, such as the method of averaging and the method of multiple scales, are introduced for the determination of stability regions of linear systems under harmonic excitations. The method of averaging is very powerful, yet simple to apply, for obtaining first-order approximations of the stability regions. In Chapter 4, the effect of nonlinearity on the stability behaviour of dynamical systems is studied.

Problems

3.1 Investigate the stability regions for the equations of motion of the flexural-torsional vibration of a rectangular beam under both non-follower and follower dynamic load $P(t) = P_0 \cos \nu t$, which are derived in Section 1.5.4 and are given by equations (1.5.52).

3.2 For the damped case of Case III, Combination Resonance, studied in Section 3.3, show that, by solving for ρ , the growth of the response in Region II shown in Figure 3.6 is extremely small and hence this region is described as quasi-stable.

3.3 Referring to Example 3.3.1, consider the equations of motion of a three degrees-of-freedom system of the form

$$\ddot{q}_1 + \omega_1^2 q_1 + 2\varepsilon\mu \cos \nu t (p_{11} q_1 + p_{12} q_2 + p_{13} q_3) = 0,$$

$$\ddot{q}_2 + \omega_1^2 q_2 + q_1 + 2\varepsilon\mu \cos \nu t (p_{21} q_1 + p_{22} q_2 + p_{23} q_3) = 0,$$
$$\ddot{q}_3 + \omega_3^2 q_3 + 2\varepsilon\mu \cos \nu t (p_{31} q_1 + p_{32} q_2 + p_{33} q_3) = 0.$$

Investigate the stability of the system for $\nu \approx \omega_1 + \omega_3$.

3.4 For the two-dimensional gyroscopic system considered in Section 3.4, study the case $|\kappa_1 - \kappa_2| = 1$, i.e. $\omega_0 = |\omega_1 - \omega_2|$ or $\nu \approx |\omega_1 - \omega_2|$. Proceeding as in Case IV, show that there is no instability when $\Omega < \bar{\omega}_1$, and when $\Omega > \bar{\omega}_2$ the region of instability is given by (3.4.21).

3.5 Show that if \mathbf{H} is a sign-definite matrix, then the eigenvalues of (3.5.11) are purely imaginary and occur in conjugate pairs, i.e. $\lambda_r = \pm i\omega_r$.

3.6 Using the orthogonality conditions (3.5.24), show that $\mathbf{T} = [\mathbf{X} \ \mathbf{Y}]$ is a symplectic matrix, i.e. equation (3.5.25) is satisfied.

C H A P T E R

4

Nonlinear Systems under Periodic Excitations

In Chapters 2 and 3, dynamic stability of linear systems under periodic excitations has been studied. In this Chapter, the effect of nonlinearity on the dynamic stability behaviour of these systems is investigated.

4.1 Pendulum under Support Excitation

As a motivating example, consider the dynamic behaviour of a pendulum under a prescribed vertical support excitation $y(t)$. The length of the pendulum is l and the mass is m . The motion of the pendulum is described by angle θ as shown in Figure 4.1.

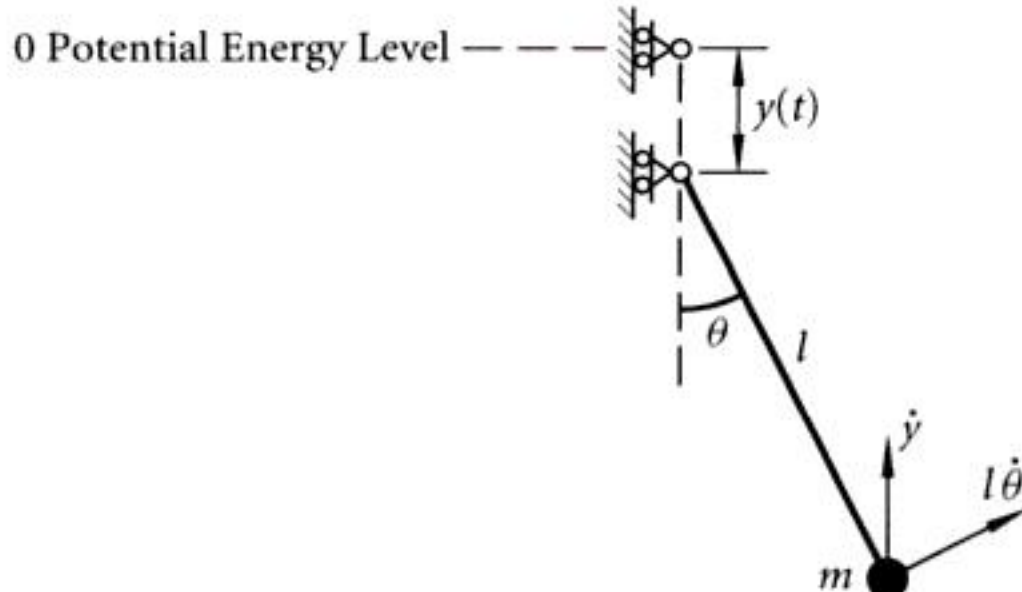


Figure 4.1 Pendulum under vertical support excitation.

Equations of Motion

The kinetic energy of the system is

$$T = \frac{1}{2}m[(l\dot{\theta}\cos\theta)^2 + (\dot{y} + l\dot{\theta}\sin\theta)^2],$$



You have either reached a page that is unavailable for viewing or reached your viewing limit for this

@Seismicisolation



You have either reached a page that is unavailable for viewing or reached your viewing limit for this

@Seismicisolation



You have either reached a page that is unavailable for viewing or reached your viewing limit for this

@Seismicisolation



You have either reached a page that is unavailable for viewing or reached your viewing limit for this

@Seismicisolation



You have either reached a page that is unavailable for viewing or reached your viewing limit for this

@Seismicisolation



You have either reached a page that is unavailable for viewing or reached your viewing limit for this

@Seismicisolation



You have either reached a page that is unavailable for viewing or reached your viewing limit for this

@Seismicisolation



You have either reached a page that is unavailable for viewing or reached your viewing limit for this

@Seismicisolation



You have either reached a page that is unavailable for viewing or reached your viewing limit for this

@Seismicisolation



You have either reached a page that is unavailable for viewing or reached your viewing limit for this

@Seismicisolation



You have either reached a page that is unavailable for viewing or reached your viewing limit for this

@Seismicisolation



You have either reached a page that is unavailable for viewing or reached your viewing limit for this

@Seismicisolation



You have either reached a page that is unavailable for viewing or reached your viewing limit for this

@Seismicisolation



You have either reached a page that is unavailable for viewing or reached your viewing limit for this

@Seismicisolation



You have either reached a page that is unavailable for viewing or reached your viewing limit for this

@Seismicisolation



You have either reached a page that is unavailable for viewing or reached your viewing limit for this

@Seismicisolation



You have either reached a page that is unavailable for viewing or reached your viewing limit for this

@Seismicisolation



You have either reached a page that is unavailable for viewing or reached your viewing limit for this

@Seismicisolation



You have either reached a page that is unavailable for viewing or reached your viewing limit for this

@Seismicisolation



You have either reached a page that is unavailable for viewing or reached your viewing limit for this

@Seismicisolation



You have either reached a page that is unavailable for viewing or reached your viewing limit for this

@Seismicisolation



You have either reached a page that is unavailable for viewing or reached your viewing limit for this

@Seismicisolation



You have either reached a page that is unavailable for viewing or reached your viewing limit for this

@Seismicisolation



You have either reached a page that is unavailable for viewing or reached your viewing limit for this

@Seismicisolation



You have either reached a page that is unavailable for viewing or reached your viewing limit for this

@Seismicisolation



You have either reached a page that is unavailable for viewing or reached your viewing limit for this

@Seismicisolation



You have either reached a page that is unavailable for viewing or reached your viewing limit for this

@Seismicisolation



You have either reached a page that is unavailable for viewing or reached your viewing limit for this

@Seismicisolation



You have either reached a page that is unavailable for viewing or reached your viewing limit for this

@Seismicisolation



You have either reached a page that is unavailable for viewing or reached your viewing limit for this

@Seismicisolation



You have either reached a page that is unavailable for viewing or reached your viewing limit for this

@Seismicisolation



You have either reached a page that is unavailable for viewing or reached your viewing limit for this

@Seismicisolation



You have either reached a page that is unavailable for viewing or reached your viewing limit for this

@Seismicisolation



You have either reached a page that is unavailable for viewing or reached your viewing limit for this

@Seismicisolation



You have either reached a page that is unavailable for viewing or reached your viewing limit for this

@Seismicisolation



You have either reached a page that is unavailable for viewing or reached your viewing limit for this

@Seismicisolation

and c_0 given by equation (4.5.16) becomes

$$c_0 = \frac{3}{32\omega_0^2} C_{1111} \tilde{a}_1^4 = \frac{3}{128\omega_1^2} C_{1111} \tilde{a}_1^4.$$

Since $k_1=2$, $k_2=0$, $\kappa_1=\omega_1/\omega_0=\frac{1}{2}$, the amplitude-frequency relationship given by equation (4.4.14) is

$$\begin{aligned} \frac{\nu}{\omega_0} &= 1 + \varepsilon \frac{k_1}{\tilde{a}_{10}\kappa_1} \left(\frac{\partial c_0}{\partial \tilde{a}_{10}} \pm \mu \frac{\partial b_2}{\partial \tilde{a}_{10}} \right) \\ &= 1 + \varepsilon \frac{2}{\tilde{a}_{10} \cdot \frac{1}{2}} \left(\frac{3}{32\omega_1^2} C_{1111} \tilde{a}_{10}^3 \pm \mu \frac{\varepsilon}{24\omega_1^4} C_{111} \tilde{a}_{10} \right), \end{aligned}$$

or, since $\omega_0=2\omega_1$,

$$\frac{\nu}{2\omega_1} = 1 + \frac{3\varepsilon}{8\omega_1^2} C_{1111} \tilde{a}_{10}^2 \pm \mu \frac{\varepsilon^2}{6\omega_1^4} C_{111}, \quad (4.5.17)$$

which is similar to that of a column under axial harmonic load, equation (4.5.3).

Case II. $\omega_0=2\omega_2$, Subharmonic Resonance of Order 2

This case is similar to Case I. The system behaves as a single degree-of-freedom system with the response of the system being $\tilde{a}_1=0$ and $\tilde{a}_2 \neq 0$. The resonance coefficient is

$$\tilde{B}_{22} = \frac{8\varepsilon q_0}{\nu^2 - \omega_1^2} \frac{EA}{4m} \left(\frac{\pi}{L} \right)^4,$$

and, with $\omega_0=2\omega_2$ and $\nu \approx 2\omega_2$,

$$\begin{aligned} b = b_{02} &= \frac{1}{8\omega_0^2} \tilde{B}_{22} \tilde{a}_2^2 = \frac{\varepsilon q_0}{4\omega_2^2 (4\omega_2^2 - \omega_1^2)} \frac{EA}{4m} \left(\frac{\pi}{L} \right)^4 \tilde{a}_2^2 = \frac{\varepsilon}{48\omega_2^2 (4\omega_2^2 - \omega_1^2)} C_{122} \tilde{a}_2^2, \\ c_0 &= \frac{3}{32\omega_0^2} C_{2222} \tilde{a}_2^4 = \frac{3}{128\omega_2^2} C_{2222} \tilde{a}_2^4. \end{aligned}$$

From (4.4.14), since $k_1=0$, $k_2=2$, $\kappa_2=\frac{1}{2}$, the amplitude-frequency relation is

$$\begin{aligned} \frac{\nu}{\omega_0} &= 1 + \varepsilon \frac{k_2}{\kappa_2 \tilde{a}_{20}} \left(\frac{\partial c_0}{\partial \tilde{a}_{20}} \pm \mu \frac{\partial b_{02}}{\partial \tilde{a}_{20}} \right) \\ &= 1 + \varepsilon \frac{2}{\frac{1}{2} \cdot \tilde{a}_{20}} \left[\frac{3}{32\omega_2^2} C_{2222} \tilde{a}_{20}^3 \pm \mu \frac{\varepsilon}{24\omega_2^2 (4\omega_2^2 - \omega_1^2)} C_{122} \tilde{a}_{20} \right], \end{aligned}$$

or, since $\omega_0=2\omega_2$,

$$\frac{\nu}{2\omega_2} = 1 + \frac{3\varepsilon}{8\omega_2^2} C_{2222} \tilde{a}_{20}^2 \pm \mu \frac{\varepsilon^2}{6\omega_2^2 (4\omega_2^2 - \omega_1^2)} C_{122}. \quad (4.5.18)$$

Case III. $\omega_0 = \omega_1 + 2\omega_2$, Combination Resonance of Order 3

The resonance coefficient is \tilde{B}_{122} . From equation (4.4.28d),

$$b_{12} = \frac{1}{24\omega_0^2} \tilde{B}_{122} \tilde{a}_1 \tilde{a}_2^2 = \frac{1}{24\omega_0^2} \frac{3\varepsilon}{2(\nu^2 - \omega_1^2)} C_{1122} \tilde{a}_1 \tilde{a}_2^2, \quad (4.5.19)$$

and c_0 is given by equation (4.5.16).

Since $k_1 = 1$, $k_2 = 2$, $\kappa_1 = \omega_1/\omega_0$, $\kappa_2 = \omega_2/\omega_0$, the amplitude-frequency relation given by equation (4.4.14) is

$$\begin{aligned} \frac{\nu}{\omega_0} &= 1 + \varepsilon \left[\frac{k_1}{\kappa_1 \tilde{a}_{10}} \left(\frac{\partial c_0}{\partial \tilde{a}_{10}} \pm \mu \frac{\partial b_{12}}{\partial \tilde{a}_{10}} \right) + \frac{k_2}{\kappa_2 \tilde{a}_{20}} \left(\frac{\partial c_0}{\partial \tilde{a}_{20}} \pm \mu \frac{\partial b_{12}}{\partial \tilde{a}_{20}} \right) \right] \\ &= 1 + \varepsilon \left[\frac{1}{16\omega_0 \omega_1 \tilde{a}_{10}} \left(6C_{1111} \tilde{a}_{10}^3 + 2C_{1122} \tilde{a}_{10} \tilde{a}_{20}^2 \pm \frac{\varepsilon \mu}{\omega_0^2 - \omega_1^2} C_{1122} \tilde{a}_{20}^2 \right) \right. \\ &\quad \left. + \frac{2}{16\omega_0 \omega_2 \tilde{a}_{20}} \left(6C_{2222} \tilde{a}_{20}^3 + 2C_{1122} \tilde{a}_{10}^2 \tilde{a}_{20} \pm \frac{2\varepsilon \mu}{\omega_0^2 - \omega_1^2} C_{1122} \tilde{a}_{10} \tilde{a}_{20} \right) \right]. \quad (4.5.20) \end{aligned}$$

Suppose that the system has equal damping coefficients β_1 and β_2 , both of which tend to zero; hence $2\zeta_1\omega_1 = 2\zeta_2\omega_2$. From equation (4.4.10b), one obtains

$$\frac{\tilde{a}_{20}^2}{\tilde{a}_{10}^2} = \frac{k_2 \omega_1}{k_1 \omega_2} = \frac{2\omega_1}{\omega_2}. \quad (4.5.21)$$

Hence, equation (4.5.20) becomes

$$\frac{\nu}{\omega_0} = 1 + \frac{\varepsilon}{8\omega_0 \omega_1} \left[3C_{1111} + 12 \left(\frac{\omega_1}{\omega_2} \right)^2 C_{2222} + 4 \left(\frac{\omega_1}{\omega_2} \right) C_{1122} \right] \tilde{a}_{10}^2 \pm \frac{\varepsilon^2 \cdot 3\mu C_{1122} \tilde{a}_{10}}{8\omega_0 \omega_2 (\omega_0^2 - \omega_1^2)}, \quad (4.5.20')$$

where $\omega_0 = \omega_1 + 2\omega_2$.

A typical plot of the amplitude-frequency relation (4.5.20') is shown in Figure 4.13. Now the stability of the steady-state solution must be examined.

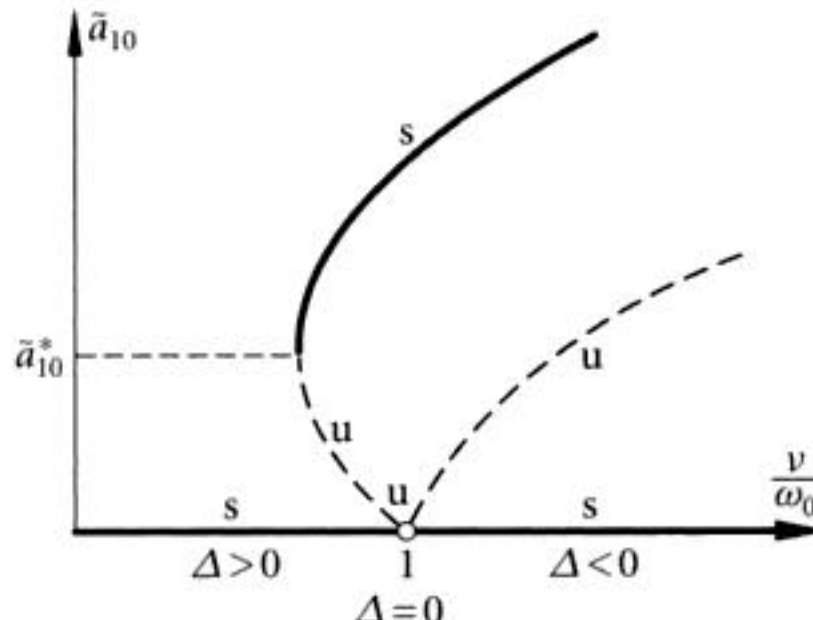


Figure 4.13 Amplitude-frequency relation.

Stability of the Steady-State Solutions

From equations (4.4.15b) and (4.4.17), the two first integrals of the equations of motion are, since $k_1 = 1$ and $k_2 = 2$,

$$\kappa_1 \tilde{a}_1^2 - \frac{1}{4} \kappa_2 \tilde{a}_2^2 = 2C_1, \quad (4.5.22a)$$

$$\frac{1}{4} \Delta \kappa_2 \tilde{a}_2^2 + (c_0 + \mu b_{12} \cos \varphi) = C_2, \quad \varphi = \varphi_1 + 2\varphi_2, \quad (4.5.22b)$$

in which the constant on the right side of equation (4.5.22a) is written as $2C_1$ for the simplicity of expressions later in the analysis.

Introduce the auxiliary variable as in equation (4.4.18)

$$p = \frac{\kappa_2}{4} \tilde{a}_2^2, \quad \text{or} \quad \tilde{a}_2^2 = \frac{4}{\kappa_2} p. \quad (4.5.23a)$$

From equations (4.5.22a) and (4.5.23a), one obtains

$$\tilde{a}_1^2 = \frac{2}{\kappa_1} (C_1 + p). \quad (4.5.23b)$$

Equation (4.4.22) becomes

$$f(p) = \mu^2 b_{12}^2 - [C_2 - (p\Delta + c_0)]^2, \quad (4.5.24a)$$

and differentiation with respect to p yields

$$f'(p) = 2\mu^2 b_{12} \frac{db_{12}}{dp} + 2[C_2 - (p\Delta + c_0)] \left(\Delta + \frac{dc_0}{dp} \right). \quad (4.5.24b)$$

The steady-state solutions $p = p_0$ are given by the common roots of $f(p) = f'(p) = 0$. Thus, for $p = p_0$, equation (4.5.24a) leads to

$$C_2 - (p\Delta + c_0) = \pm \mu b_{12}, \quad (4.5.25)$$

and substituting into equation (4.5.24b) results in

$$\mu^2 b_{12} \frac{db_{12}}{dp} \pm \mu b_{12} \left(\Delta + \frac{dc_0}{dp} \right) = 0,$$

or

$$b_{12} \left[\Delta + \frac{d}{dp} (c_0 \pm \mu b_{12}) \right] = 0,$$

the solution of which are

$$b_{12} = 0, \quad (4.5.26a)$$

$$\Delta + \frac{d}{dp} (c_0 \pm \mu b_{12}) = 0. \quad (4.5.26b)$$

Equation (4.5.26b) corresponds to the amplitude-frequency relation obtained in equation (4.5.20').



You have either reached a page that is unavailable for viewing or reached your viewing limit for this

@Seismicisolation



You have either reached a page that is unavailable for viewing or reached your viewing limit for this

@Seismicisolation



You have either reached a page that is unavailable for viewing or reached your viewing limit for this

@Seismicisolation



You have either reached a page that is unavailable for viewing or reached your viewing limit for this

@Seismicisolation



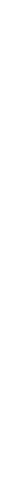
You have either reached a page that is unavailable for viewing or reached your viewing limit for this

@Seismicisolation



You have either reached a page that is unavailable for viewing or reached your viewing limit for this

@Seismicisolation



You have either reached a page that is unavailable for viewing or reached your viewing limit for this

@Seismicisolation



You have either reached a page that is unavailable for viewing or reached your viewing limit for this

@Seismicisolation



You have either reached a page that is unavailable for viewing or reached your viewing limit for this

@Seismicisolation



You have either reached a page that is unavailable for viewing or reached your viewing limit for this

@Seismicisolation



You have either reached a page that is unavailable for viewing or reached your viewing limit for this

@Seismicisolation



You have either reached a page that is unavailable for viewing or reached your viewing limit for this

@Seismicisolation



You have either reached a page that is unavailable for viewing or reached your viewing limit for this

@Seismicisolation



You have either reached a page that is unavailable for viewing or reached your viewing limit for this

@Seismicisolation

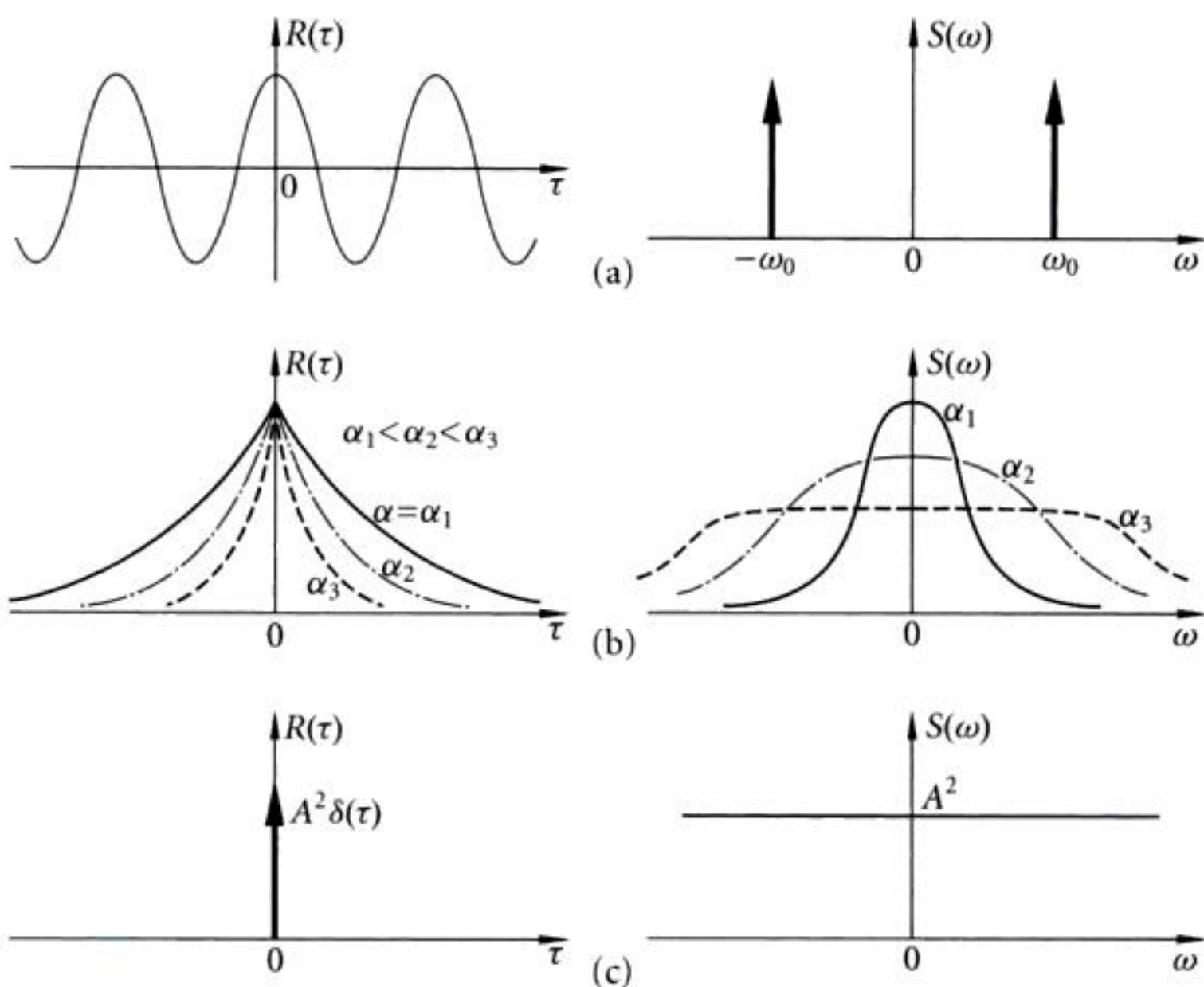


Figure 5.4 Autocorrelation functions and corresponding power spectral density functions.

$$S(\omega) = A^2 \int_{-\infty}^{+\infty} e^{-i\omega\tau} \cos \omega_0 \tau d\tau = \pi A^2 [\delta(\omega + \omega_0) + \delta(\omega - \omega_0)],$$

where $\delta(\cdot)$ denotes the Dirac delta function. Thus all the power is concentrated at the frequencies $\omega = \pm \omega_0$ as shown in Figure 5.4(a).

2. Exponential autocorrelation function as shown in Figure 5.4(b):

$$R(\tau) = A^2 e^{-\alpha|\tau|}, \quad S(\omega) = \frac{2\alpha A^2}{\alpha^2 + \omega^2}.$$

3. *White noise* process:

$$R(\tau) = A^2 \delta(\tau), \quad S(\omega) = A^2. \quad (5.1.16)$$

For this random process the spectral density function is constant over all frequencies as shown in Figure 5.4(c). The process is clearly not physically realizable since its total average power is infinite. However, it is a convenient mathematical abstraction for a process whose spectral density function remains practically constant over a wide band of frequency.

Ergodic Random Processes

The averages discussed so far have all been ensemble averages. The practical evaluation of such averages can be a challenging task since a very large number of sample functions

are required. On the other hand, the time average over a particular record defined by equation (5.1.8) can be easily computed. It is then most desirable to know under what conditions the two types of average are equal. A random process whose averages possess this property is said to be *ergodic*. In essence, ergodicity means that any particular sample function used to calculate the time averages can be expected to be typical of the whole ensemble. That is, for an ergodic random process, one has

$$\begin{aligned} E[X(t)] &= \lim_{T \rightarrow \infty} \frac{1}{T} \int_{-T}^T X^{(k)}(t) dt, \\ R(\tau) = E[X(t)X(t+\tau)] &= \lim_{T \rightarrow \infty} \frac{1}{T} \int_{-T}^T X^{(k)}(t)X^{(k)}(t+\tau) dt, \end{aligned} \quad (5.1.17)$$

where $X^{(k)}(t)$ is a typical record. Since time averages are independent of time, it is obvious that stationarity is a necessary condition for ergodicity. Many practical random processes are often assumed to be ergodic.

Gaussian Processes

An important random process is the *Gaussian process*, the probability density functions of which are given by

$$p_1(x, t) = \frac{1}{\sqrt{2\pi} \sigma(t)} \exp\left\{-\frac{[x-m(t)]^2}{2\sigma^2(t)}\right\}, \quad (5.1.18)$$

$$\begin{aligned} p_2(x_1, t_1; x_2, t_2) &= \frac{1}{2\pi \sigma_1 \sigma_2 \sqrt{1-\rho^2}} \\ &\times \exp\left\{-\frac{1}{2(1-\rho^2)} \left[\frac{(x_1-m_1)^2}{\sigma_1^2} - 2\rho \frac{(x_1-m_1)(x_2-m_2)}{\sigma_1 \sigma_2} + \frac{(x_2-m_2)^2}{\sigma_2^2} \right] \right\}, \end{aligned} \quad (5.1.19)$$

where

$$\begin{aligned} m(t) &= E[X(t)], \quad \sigma^2(t) = E[\{X(t)-m(t)\}^2], \quad \rho(t_1, t_2) = \frac{K(t_1, t_2)}{\sigma_1 \sigma_2}, \\ m_1 &= m(t_1), \quad m_2 = m(t_2), \quad \sigma_1 = \sigma(t_1), \quad \sigma_2 = \sigma(t_2), \end{aligned}$$

and generally, for $n=1, 2, \dots$,

$$p_n(x_1, t_1; \dots; x_n, t_n) = \frac{1}{(2\pi)^{n/2} |\Lambda|^{1/2}} \exp\left[-\frac{1}{2|\Lambda|} \sum_{i=1}^n \sum_{j=1}^n \lambda_{ij}(x_i-m_i)(x_j-m_j)\right], \quad (5.1.20a)$$

where Λ is the covariance matrix with elements

$$\Lambda_{ij} = E[\{X(t_i)-m(t_i)\} \{X(t_j)-m(t_j)\}],$$

and λ_{ij} is the cofactor of the element Λ_{ij} in Λ . In the matrix form, one has

$$p_n(\mathbf{x}, \mathbf{t}) = \frac{1}{(2\pi)^{n/2} |\Lambda|^{1/2}} \exp\left[-\frac{1}{2} (\mathbf{x}-\mathbf{m})^T \Lambda^{-1} (\mathbf{x}-\mathbf{m})\right]. \quad (5.1.20b)$$

Thus, a Gaussian random process is completely characterized by its mean $m(t)$ and covariance function $K(t_1, t_2)$. Many physical processes, which result from the superimposition of a large number of random factors, are often considered to be Gaussian. This assumption is a consequence of a result known as the *Central Limit Theorem*, which states that, under very general conditions, a random variable which occurs as the sum of many smaller independent random variables, each of which is almost negligible in itself, is approximately Gaussian, whatever the distributions of the component variables are.

5.2 Processes with Orthogonal Increments

Two random variables X and Y are said to be *orthogonal*, denoted as $X \perp Y$, if $E[XY] = 0$. Random variables X, Y are independent if $P\{XY\} = P\{X\}P\{Y\}$, which leads to $E[XY] = E[X]E[Y]$. For two normally distributed random variables X and Y , if they are uncorrelated, i.e. the coefficient of correlation $\rho_{XY} = 0$, then they are independent.

Consider a real (or complex) valued random process $X(t)$, $0 \leq t < \infty$, and for all time instances s and t , $E[|X(t) - X(s)|^2] < \infty$. For $s_1 < t_1 \leq s_2 < t_2$, if

$$E[\{X(t_1) - X(s_1)\} \{X(t_2) - X(s_2)\}] = E[X(t_1) - X(s_1)] E[X(t_2) - X(s_2)],$$

then the process $X(t)$ is said to have *uncorrelated increments*. If

$$E[\{X(t_1) - X(s_1)\} \{X(t_2) - X(s_2)\}] = 0,$$

then $X(t)$ is said to have *orthogonal increments*, i.e. $\{X(t_1) - X(s_1)\} \perp \{X(t_2) - X(s_2)\}$.

The random process $X(t)$ is said to have *independent increments* if for all $n \geq 2$ and $0 = t_0 < t_1 < t_2 < \dots < t_n$, the n random variables $\{X(t_k) - X(t_{k-1})\}$, $1 \leq k \leq n$, are independent.

If a random process $X(t)$ is Gaussian with zero mean, i.e. $E[X(t)] = 0$, and has uncorrelated or orthogonal increments, then $X(t)$ has independent increments.

Let $F(t) = E[|X(t) - X(0)|^2]$, where $X(t)$ is a random process with orthogonal increments. Since

$$X(t) - X(0) = X(t) - X(s) + X(s) - X(0), \quad 0 < s \leq t,$$

and $\{X(t) - X(s)\} \perp \{X(s) - X(0)\}$, then

$$\begin{aligned} F(t) &= E[|X(t) - X(s)|^2] + E[|X(s) - X(0)|^2] \\ &= E[|X(t) - X(s)|^2] + F(s), \end{aligned} \tag{5.2.1}$$

which implies that $F(t) \geq F(s)$, for $t \geq s$. Therefore, the random process $F(t)$ is monotonically nondecreasing. Equation (5.2.1) can be written in the short-hand notation $E[|dX|^2] = dF$.



You have either reached a page that is unavailable for viewing or reached your viewing limit for this

@Seismicisolation



You have either reached a page that is unavailable for viewing or reached your viewing limit for this

@Seismicisolation



You have either reached a page that is unavailable for viewing or reached your viewing limit for this

@Seismicisolation



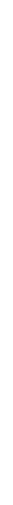
You have either reached a page that is unavailable for viewing or reached your viewing limit for this

@Seismicisolation



You have either reached a page that is unavailable for viewing or reached your viewing limit for this

@Seismicisolation



You have either reached a page that is unavailable for viewing or reached your viewing limit for this

@Seismicisolation



You have either reached a page that is unavailable for viewing or reached your viewing limit for this

@Seismicisolation



You have either reached a page that is unavailable for viewing or reached your viewing limit for this

@Seismicisolation



You have either reached a page that is unavailable for viewing or reached your viewing limit for this

@Seismicisolation



You have either reached a page that is unavailable for viewing or reached your viewing limit for this

@Seismicisolation



You have either reached a page that is unavailable for viewing or reached your viewing limit for this

@Seismicisolation



You have either reached a page that is unavailable for viewing or reached your viewing limit for this

@Seismicisolation



You have either reached a page that is unavailable for viewing or reached your viewing limit for this

@Seismicisolation



You have either reached a page that is unavailable for viewing or reached your viewing limit for this

@Seismicisolation



You have either reached a page that is unavailable for viewing or reached your viewing limit for this

@Seismicisolation



You have either reached a page that is unavailable for viewing or reached your viewing limit for this

@Seismicisolation



You have either reached a page that is unavailable for viewing or reached your viewing limit for this

@Seismicisolation



You have either reached a page that is unavailable for viewing or reached your viewing limit for this

@Seismicisolation



You have either reached a page that is unavailable for viewing or reached your viewing limit for this

@Seismicisolation



You have either reached a page that is unavailable for viewing or reached your viewing limit for this

@Seismicisolation

The boundary conditions for the Fokker–Planck equation (5.6.19) are as follows:

• $-\infty < \xi < +\infty$

By conservation of probability, one has

$$G(-\infty, t) = G(+\infty, t) = 0, \quad p_X(-\infty, t) = p_X(+\infty, t) = 0.$$

• $c \leq \xi \leq d$

In order not to have an accumulation of probability mass, one must have

$$G(c, t) = G(d, t) = 0.$$

In the case of an n -dimensional vector diffusion process $\mathbf{X}(t)$, the n -dimensional vector probability current is $\mathbf{G} = \{G_1, G_2, \dots, G_n\}^T$ with the j th component given by

$$G_j(\xi, t) = a_j(\xi, t) p_{\mathbf{X}}(\xi, t) - \frac{1}{2} \sum_{k=1}^n \frac{\partial [b_{jk}(\xi, t) p_{\mathbf{X}}(\xi, t)]}{\partial \xi_k}.$$

(vi) Stationary Solution of the Fokker–Planck Equation

If $a_j(\xi, t)$ and $b_{jk}(\xi, t)$ do not contain t , then $q(\xi, t | \xi_0, t_0)$ depends only on $\xi - \xi_0$ and the time difference $t - t_0$. As $t - t_0 \rightarrow \infty$, $q(\xi, t | \xi_0, t_0) \rightarrow p_{\text{st}}(\xi)$, which is independent of t and the initial condition (ξ_0, t_0) , and is called a *stationary solution*.

Then, from equation (5.6.16b), $p_{\text{st}}(\xi)$ satisfies

$$\begin{aligned} 0 &= - \sum_{j=1}^n \frac{\partial [a_j(\xi) p_{\text{st}}(\xi)]}{\partial \xi_j} + \frac{1}{2} \sum_{j=1}^n \sum_{k=1}^n \frac{\partial^2 [b_{jk}(\xi) p_{\text{st}}(\xi)]}{\partial \xi_j \partial \xi_k} \\ &= - \operatorname{div} \mathbf{G}(\xi, t), \end{aligned} \tag{5.6.21}$$

where

$$G_j(\xi, t) = a_j(\xi) p_{\text{st}}(\xi) - \frac{1}{2} \sum_{k=1}^n \frac{\partial [b_{jk}(\xi) p_{\text{st}}(\xi)]}{\partial \xi_k}.$$

Special Case. One-Dimensional Diffusion Process

In the special case of one-dimensional diffusion process, equation (5.6.21) reduces to

$$\frac{dG}{d\xi} = 0 \implies G(\xi) = \text{Constant},$$

where

$$G(\xi) = a(\xi) p_{\text{st}}(\xi) - \frac{1}{2} \frac{d[b(\xi) p_{\text{st}}(\xi)]}{d\xi},$$

which is of the form

$$\frac{dp_{\text{st}}(\xi)}{d\xi} + P(\xi) p_{\text{st}}(\xi) = Q(\xi),$$

where

$$P(\xi) = \frac{1}{b(\xi)} \frac{db(\xi)}{d\xi} - 2 \frac{a(\xi)}{b(\xi)}, \quad Q(\xi) = -\frac{2G}{b(\xi)}.$$

This is a first-order linear ordinary differential equation with the solution given by

$$p_{st}(\xi) = e^{-\int P(\xi)d\xi} \left[\int Q(\xi)e^{\int P(\xi)d\xi} d\xi + C_0 \right],$$

which can be written as

$$p_{st}(\xi) = \exp \left\{ - \int_{\xi_1}^{\xi} P(x) dx \right\} \cdot \left[\int_{\xi_0}^{\xi} Q(x) \exp \left\{ \int_{\xi_1}^x P(y) dy \right\} dx + C_0 \right],$$

where ξ_0 and ξ_1 are suitable constants and C_0 is a constant to be determined.

Note that

$$\exp \left\{ \int_{\xi_1}^{\xi} P(x) dx \right\} = \exp \left\{ \int_{\xi_1}^{\xi} d[\log b(x)] - 2 \int_{\xi_1}^{\xi} \frac{a(x)}{b(x)} dx \right\} = \frac{b(\xi)}{b(\xi_1)} U(\xi),$$

where

$$U(\xi) = \exp \left\{ -2 \int_{\xi_1}^{\xi} \frac{a(x)}{b(x)} dx \right\}.$$

Hence, the stationary solution of the Fokker-Planck equation is given by

$$p_{st}(\xi) = \frac{b(\xi_1)}{b(\xi)U(\xi)} \left[\int_{\xi_0}^{\xi} -\frac{2G}{b(x)} \frac{b(x)U(x)}{b(\xi_1)} dx + C_0 \right].$$

This equation can be expressed in two forms as follows:

$$p_{st}(\xi) = \frac{C}{b(\xi)U(\xi)} - \frac{2G}{b(\xi)U(\xi)} \int_{\xi_0}^{\xi} U(x) dx, \quad (5.6.22a)$$

or, if the constant C_0 is absorbed in ξ_0 ,

$$p_{st}(\xi) = \frac{C}{b(\xi)U(\xi)} \int_{\xi_0}^{\xi} U(x) dx, \quad (5.6.22b)$$

in which ξ_0 is a suitable constant and C is determined by the normalizing condition

$$\int_{-\infty}^{+\infty} p_{st}(\xi) d\xi = 1.$$

- If the diffusion process $\xi(t)$ is defined on the entire real axis, i.e. $-\infty < \xi < +\infty$, one must have $G(\pm\infty) = 0$, and hence $G(\xi) = 0$.
- On the other hand, if $\xi(t)$ is defined in the interval $[\alpha, \beta]$ and there is no cumulation of probability mass at the boundary points α and β , then $G(\alpha) = G(\beta) = 0$ and hence $G(\xi) = 0$.

The solution of the Fokker-Planck equation is then reduced to, from equation (5.6.22a),

$$p_{st}(\xi) = \frac{C}{b(\xi)U(\xi)}. \quad (5.6.23)$$

5.7 Stochastic Integrals

5.7.1 Stochastic Riemann Integrals

Let

$$Y = \int_a^b f(t) X(t) dt, \quad (5.7.1)$$

where $f(t)$ is a *deterministic function*, and $X(t)$ is a random process. Then Y is a random variable.

Divide the interval $[a, b]$ into $(n-1)$ segments with $t_1 = a < t_2 < \dots < t_{n-1} < t_n = b$, $\Delta t_j = t_{j+1} - t_j$. Define

$$Y_n = \sum_{j=1}^{n-1} f(\tau_j) X(\tau_j) \Delta t_j, \quad t_j \leq \tau_j \leq t_{j+1}. \quad (5.7.2)$$

If the random process $X(t)$ has zero mean, i.e. $E[X(t)] = 0$, then $E[Y_n] = 0$.

Pass the limit as $n \rightarrow \infty$ and $\max \Delta t_j \rightarrow 0$. Since $\{Y_n\}$ is a sequence of random variables, Y_n approaches a limit Y in mean square (m.s.) if

$$E[(Y - Y_n)^2] \rightarrow 0, \quad \text{as } n \rightarrow \infty \text{ and } \max \Delta t_j \rightarrow 0, \quad (5.7.3)$$

and it is denoted as $Y = \lim_{n \rightarrow \infty} Y_n$, in which l.i.m. stands for “limit in the mean.”

By the mean square convergence criterion, the limit Y exists if

$$\lim_{m, n \rightarrow \infty} E[Y_n Y_m]$$

exists and is equal to $E[Y^2]$, in which

$$\begin{aligned} E[Y_n Y_m] &= \sum_{j=1}^{n-1} \sum_{k=1}^{m-1} f(\tau_j) f(s_k) E[X(\tau_j) X(s_k)] \Delta t_j \Delta s_k \\ &= \sum_{j=1}^{n-1} \sum_{k=1}^{m-1} f(\tau_j) f(s_k) R_{XX}(\tau_j, s_k) \Delta t_j \Delta s_k \\ &\rightarrow \int_a^b \int_a^b f(t) f(s) R_{XX}(t, s) dt ds, \end{aligned} \quad (5.7.4)$$

as $n, m \rightarrow \infty$ and $\max \Delta t_j, \max \Delta s_j \rightarrow 0$, provided the double integral exists.

Sufficient conditions for the existence of the double integral in equation (5.7.4) are that $f(t)$ is bounded with a finite number of discontinuities in $[a, b]$ and $R_{XX}(t, s)$ is continuous on the diagonal line $t = s$, for $a \leq t \leq b$. The second condition is due to the fact that $R(t, s)$ is continuous for all t, s in $[a, b]$ if it is continuous on the line $t = s$. Thus, one has

$$E\left[\int_a^b (\cdot) dt\right] = \int_a^b E[(\cdot)] dt,$$



You have either reached a page that is unavailable for viewing or reached your viewing limit for this

@Seismicisolation



You have either reached a page that is unavailable for viewing or reached your viewing limit for this

@Seismicisolation



You have either reached a page that is unavailable for viewing or reached your viewing limit for this

@Seismicisolation



You have either reached a page that is unavailable for viewing or reached your viewing limit for this

@Seismicisolation



You have either reached a page that is unavailable for viewing or reached your viewing limit for this

@Seismicisolation



You have either reached a page that is unavailable for viewing or reached your viewing limit for this

@Seismicisolation



You have either reached a page that is unavailable for viewing or reached your viewing limit for this

@Seismicisolation



You have either reached a page that is unavailable for viewing or reached your viewing limit for this

@Seismicisolation



You have either reached a page that is unavailable for viewing or reached your viewing limit for this

@Seismicisolation



You have either reached a page that is unavailable for viewing or reached your viewing limit for this

@Seismicisolation



You have either reached a page that is unavailable for viewing or reached your viewing limit for this

@Seismicisolation



You have either reached a page that is unavailable for viewing or reached your viewing limit for this

@Seismicisolation



You have either reached a page that is unavailable for viewing or reached your viewing limit for this

@Seismicisolation



You have either reached a page that is unavailable for viewing or reached your viewing limit for this

@Seismicisolation



You have either reached a page that is unavailable for viewing or reached your viewing limit for this

@Seismicisolation



You have either reached a page that is unavailable for viewing or reached your viewing limit for this

@Seismicisolation



You have either reached a page that is unavailable for viewing or reached your viewing limit for this

@Seismicisolation



You have either reached a page that is unavailable for viewing or reached your viewing limit for this

@Seismicisolation



You have either reached a page that is unavailable for viewing or reached your viewing limit for this

@Seismicisolation



You have either reached a page that is unavailable for viewing or reached your viewing limit for this

@Seismicisolation



You have either reached a page that is unavailable for viewing or reached your viewing limit for this

@Seismicisolation



You have either reached a page that is unavailable for viewing or reached your viewing limit for this

@Seismicisolation



You have either reached a page that is unavailable for viewing or reached your viewing limit for this

@Seismicisolation



You have either reached a page that is unavailable for viewing or reached your viewing limit for this

@Seismicisolation



You have either reached a page that is unavailable for viewing or reached your viewing limit for this

@Seismicisolation

lems involving the effects of noise on electronic relays and vacuum-tube oscillators. A rigorous mathematical foundation was later laid by Khasminskii [50] and [49]. The stochastic averaging method is an extension to random differential equations of the well-known Bogoliubov–Mitropolski [26] techniques for nonlinear ordinary differential equations containing a small parameter (see Chapter 3).

Consider the equation

$$\dot{X}(t) = \varepsilon F(X, t, \xi(t), \varepsilon), \quad (5.16.1)$$

where $0 < \varepsilon \ll 1$ is a small parameter, $\xi(t)$ is a zero mean, stationary, stochastic process, and

$$F(X, t, \xi(t), \varepsilon) = F^{(0)}(X, t, \xi(t)) + \varepsilon F^{(1)}(X, t) + o(\varepsilon),$$

in which $F^{(0)}$ and $F^{(1)}$ are smooth functions of their arguments which, together with their first- and second-order derivatives, are bounded.

Let $\mathcal{M}_t(\cdot)$ denote the averaging operator defined by

$$\mathcal{M}_t(\cdot) = \lim_{T \rightarrow \infty} \frac{1}{T} \int_0^T (\cdot) dt,$$

where the integration is performed over an *explicitly appearing* time parameter t in the integrand.

Suppose the following assumptions hold:

1. The following limits exist uniformly in x and t :

$$\begin{aligned} m(\bar{X}) &= \mathcal{M}_t \left\{ F^{(1)} + \int_{-\infty}^0 E \left[\frac{\partial F^{(0)}}{\partial X} F_\tau^{(0)} \right] d\tau \right\}, \\ \sigma^2(\bar{X}) &= \mathcal{M}_t \left\{ \int_{-\infty}^{+\infty} E[F^{(0)} F_\tau^{(0)}] d\tau \right\}, \end{aligned} \quad (5.16.2)$$

where $F_\tau^{(0)} = F^{(0)}(X, t + \tau, \xi(t + \tau))$.

2. The correlation function $R(\tau) = E[\xi(t)\xi(t + \tau)]$ of the stochastic process $\xi(t)$ decays sufficiently fast to zero as τ increases, i.e. $\xi(t)$ has a small correlation time τ_c as compared to the relaxation time τ_r of the system. The correlation time τ_c characterizes the size of the time interval over which significant correlation extends between values of the process $\xi(t)$, while the relaxation time τ_r measures approximately the time scale over which a significant change of the amplitude of the response process may be observed.

Then, over a time interval of order $1/\varepsilon^2$, $X(t)$ can be approximated uniformly by a Markov diffusion process $\bar{X}(t)$ having drift coefficient $\varepsilon^2 m(\bar{X})$ and diffusion coefficient $\varepsilon^2 \sigma^2(\bar{X})$, i.e. $\bar{X}(t)$ satisfies the Itô stochastic differential equation

$$d\bar{X}(t) = \varepsilon^2 m(\bar{X}) dt + \varepsilon \sigma(\bar{X}) dW(t). \quad (5.16.3)$$



You have either reached a page that is unavailable for viewing or reached your viewing limit for this

@Seismicisolation



You have either reached a page that is unavailable for viewing or reached your viewing limit for this

@Seismicisolation



You have either reached a page that is unavailable for viewing or reached your viewing limit for this

@Seismicisolation



You have either reached a page that is unavailable for viewing or reached your viewing limit for this

@Seismicisolation



You have either reached a page that is unavailable for viewing or reached your viewing limit for this

@Seismicisolation



You have either reached a page that is unavailable for viewing or reached your viewing limit for this

@Seismicisolation



You have either reached a page that is unavailable for viewing or reached your viewing limit for this

@Seismicisolation



You have either reached a page that is unavailable for viewing or reached your viewing limit for this

@Seismicisolation



You have either reached a page that is unavailable for viewing or reached your viewing limit for this

@Seismicisolation



You have either reached a page that is unavailable for viewing or reached your viewing limit for this

@Seismicisolation



You have either reached a page that is unavailable for viewing or reached your viewing limit for this

@Seismicisolation



You have either reached a page that is unavailable for viewing or reached your viewing limit for this

@Seismicisolation



You have either reached a page that is unavailable for viewing or reached your viewing limit for this

@Seismicisolation



You have either reached a page that is unavailable for viewing or reached your viewing limit for this

@Seismicisolation



You have either reached a page that is unavailable for viewing or reached your viewing limit for this

@Seismicisolation



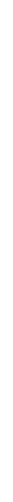
You have either reached a page that is unavailable for viewing or reached your viewing limit for this

@Seismicisolation



You have either reached a page that is unavailable for viewing or reached your viewing limit for this

@Seismicisolation



You have either reached a page that is unavailable for viewing or reached your viewing limit for this

@Seismicisolation



You have either reached a page that is unavailable for viewing or reached your viewing limit for this

@Seismicisolation



You have either reached a page that is unavailable for viewing or reached your viewing limit for this

@Seismicisolation



You have either reached a page that is unavailable for viewing or reached your viewing limit for this

@Seismicisolation

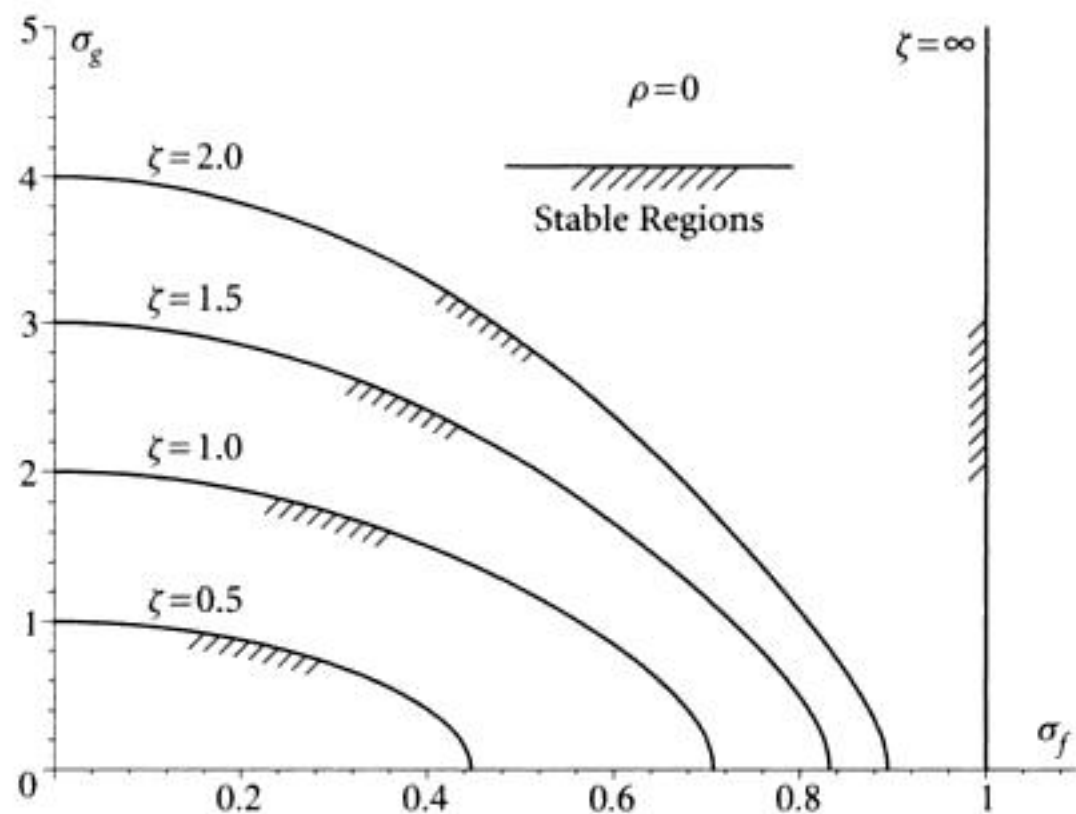


Figure 6.1 Regions of almost-sure asymptotic stability, $\rho = 0$.

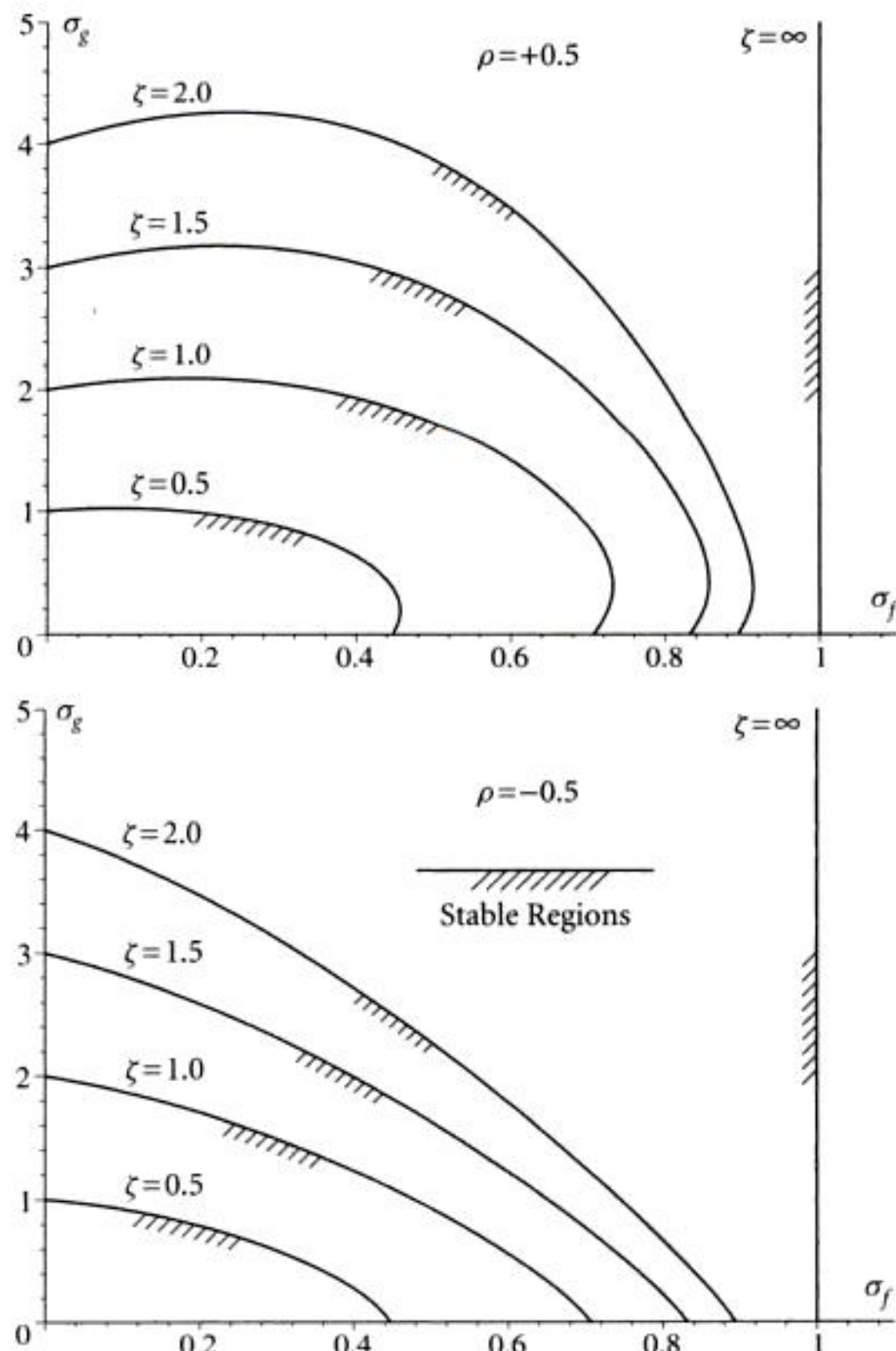


Figure 6.2 Regions of almost-sure asymptotic stability, $\rho = \pm 0.5$.



You have either reached a page that is unavailable for viewing or reached your viewing limit for this

@Seismicisolation

4. If a point repeats in giving the lowest function value on consecutive trials, it is moved one-half the distance to the centroid of the remaining points.
5. The new point is checked against the constraints and is adjusted as Step 2 if the constraints are violated, and Step 3 is then repeated.
6. Convergence is assumed when the objective function value at each point is within ϵ for m consecutive iterations.

This method is a sequential search technique, which has been proven to be effective in solving problems with nonlinear objective functions subject to nonlinear inequality constraints. No derivatives are required. The procedure attempts to find the global maximum because the initial set of points is randomly scattered throughout the feasible region.

6.2.3.3 Numerical Solution for Systems with Ergodic Gaussian Coefficients

Assume that $f(t)$ and $g(t)$ are jointly distributed Gaussian random processes with joint probability density function of the form

$$p(f, g) = \frac{1}{2\pi\sigma_f\sigma_g\sqrt{1-\rho^2}} \exp\left\{-\frac{1}{1-\rho^2}\left(\frac{f^2}{2\sigma_f^2} + \frac{g^2}{2\sigma_g^2} - \frac{\rho fg}{\sigma_f\sigma_g}\right)\right\}, \quad (6.2.26)$$

so that for any integrable function $F(f, g)$ the expected value is given by equation (6.2.24).

Changing to new variables defined by

$$\xi = \frac{f}{\sigma_f\sqrt{2(1-\rho^2)}}, \quad \eta = \frac{g}{\sigma_g\sqrt{2(1-\rho^2)}},$$

equation (6.2.24) becomes

$$\frac{\pi}{\sqrt{1-\rho^2}} E[F(f, g)] = \int_{-\infty}^{+\infty} e^{-\xi^2} d\xi \int_{-\infty}^{+\infty} F(\sigma_f, \sigma_g, \rho, \xi, \eta) e^{2\rho\xi\eta - \eta^2} d\eta. \quad (6.2.27)$$

The right side of equation (6.2.27) can be calculated numerically using, e.g. the double Gauss-Hermite integration formula. Therefore, the sufficient asymptotic stability condition (6.2.10) becomes

$$\frac{-2\pi\xi}{\sqrt{1-\rho^2}} + \int_{-\infty}^{+\infty} e^{-\xi^2} d\xi \int_{-\infty}^{+\infty} \lambda(\sigma_f, \sigma_g, \rho, \xi, \eta) e^{2\rho\xi\eta - \eta^2} d\eta < -\epsilon, \quad \epsilon > 0. \quad (6.2.28)$$

One can then construct the optimization model that may be solved by the complex method, for a given value of σ_f :

$$\text{Maximize: } V = X_1^2 = \sigma_g^2,$$



You have either reached a page that is unavailable for viewing or reached your viewing limit for this

@Seismicisolation



You have either reached a page that is unavailable for viewing or reached your viewing limit for this

@Seismicisolation



You have either reached a page that is unavailable for viewing or reached your viewing limit for this

@Seismicisolation



You have either reached a page that is unavailable for viewing or reached your viewing limit for this

@Seismicisolation



You have either reached a page that is unavailable for viewing or reached your viewing limit for this

@Seismicisolation



You have either reached a page that is unavailable for viewing or reached your viewing limit for this

@Seismicisolation



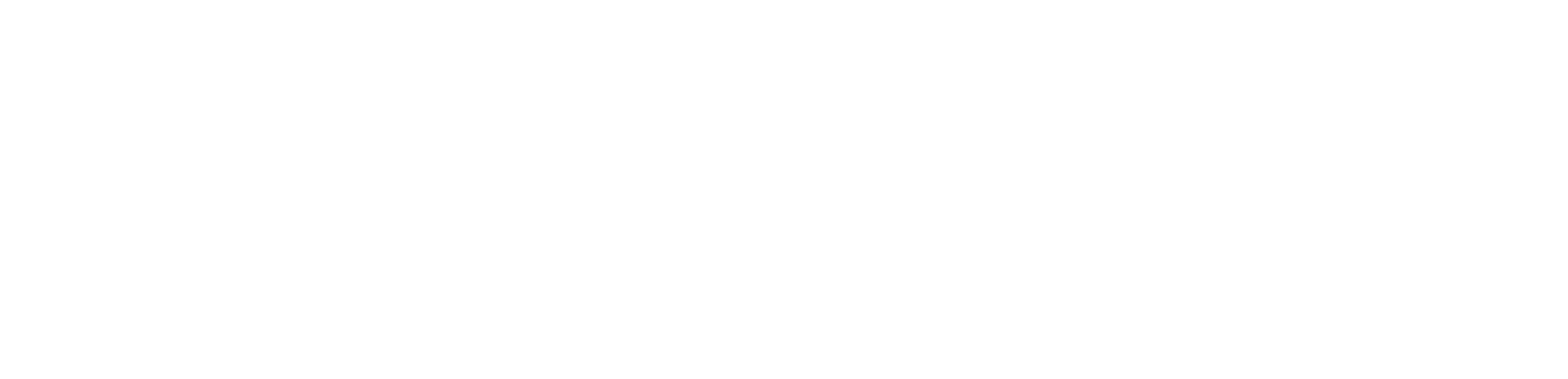
You have either reached a page that is unavailable for viewing or reached your viewing limit for this

@Seismicisolation



You have either reached a page that is unavailable for viewing or reached your viewing limit for this

@Seismicisolation



You have either reached a page that is unavailable for viewing or reached your viewing limit for this

@Seismicisolation



You have either reached a page that is unavailable for viewing or reached your viewing limit for this

@Seismicisolation

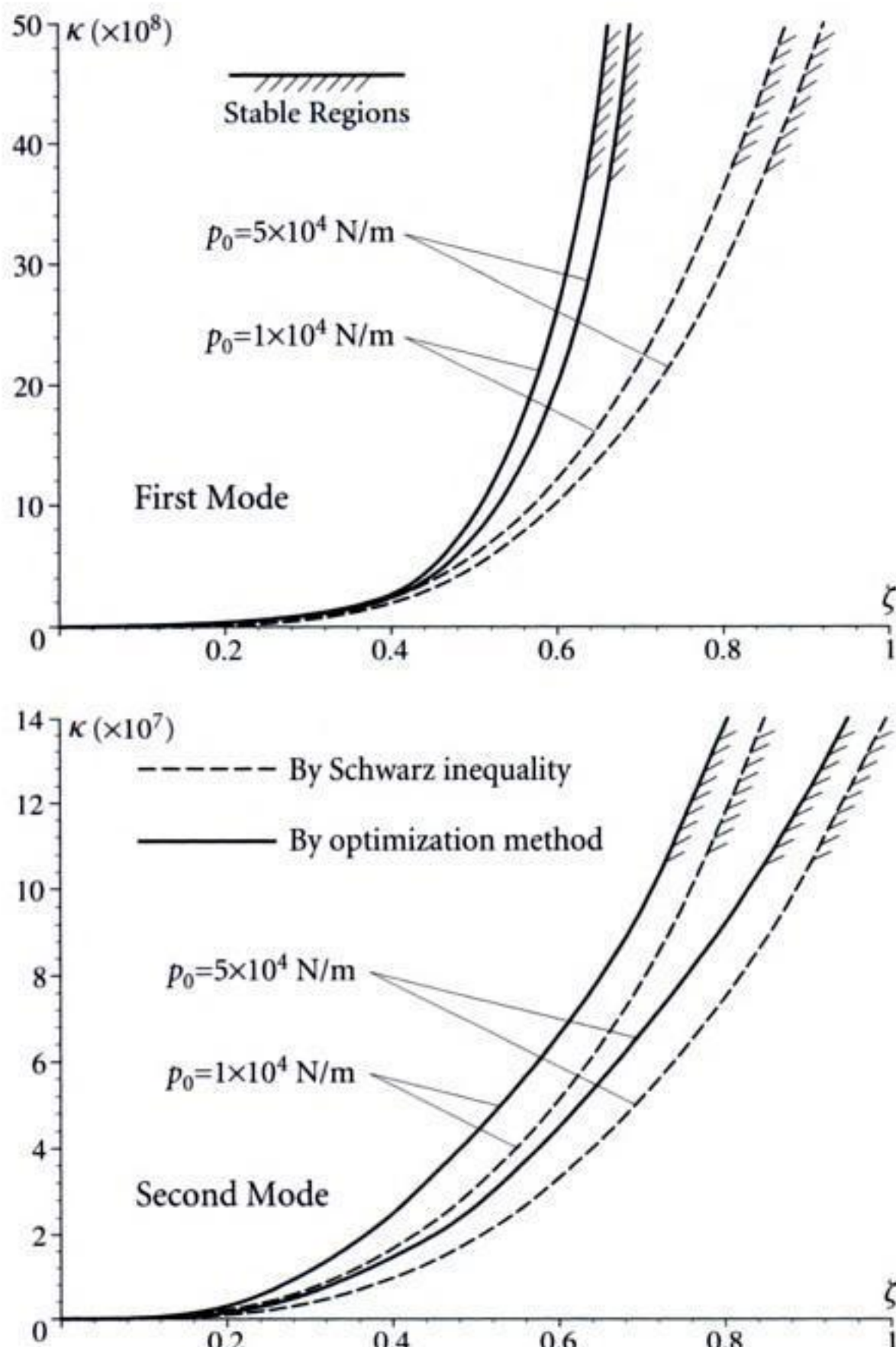


Figure 6.11 Regions of almost-sure asymptotic stability, $q_0 = 0.07$ m.

method, but also to decide the constraints of the optimization model. For example, $\underline{\kappa} = \kappa_0$, where κ_0 is the result found by using Schwarz's inequality. The range of α_1 is also decided by this result and δ is a positive small quantity.

The optimization model can be solved numerically; the results are shown in Figures 6.10 and 6.11. The stability regions obtained are found to be considerably larger than those found by using Schwarz's inequality (6.3.31), which, however, is easier to apply.

Discussions

For the sinusoidal arch considered in this Section, sufficient a.s. asymptotic stability regions for both the vibrating mode and the resting modes are obtained by using Schwarz's inequality and the optimization method. The following conclusions may be drawn:



You have either reached a page that is unavailable for viewing or reached your viewing limit for this

@Seismicisolation



You have either reached a page that is unavailable for viewing or reached your viewing limit for this

@Seismicisolation



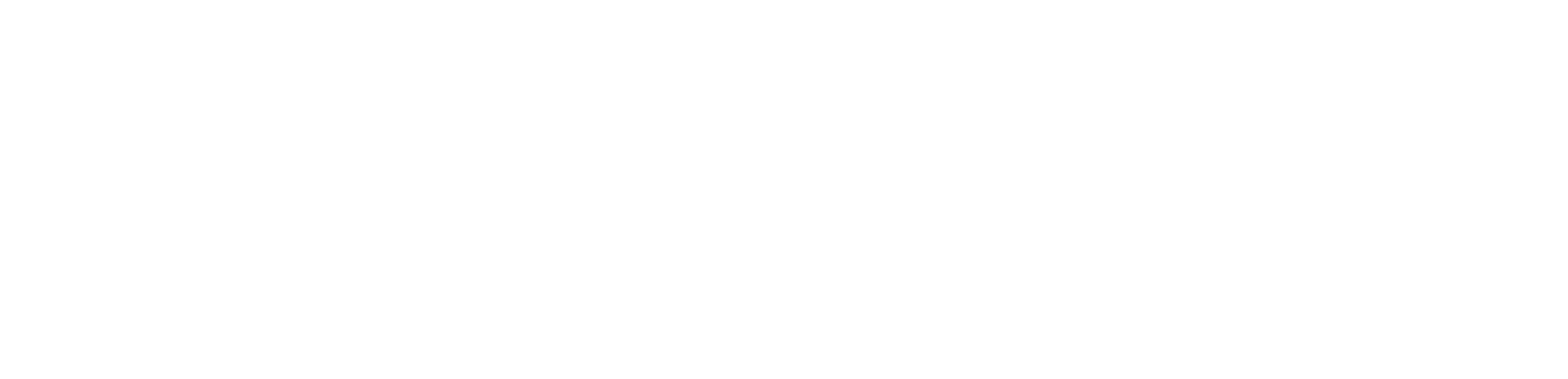
You have either reached a page that is unavailable for viewing or reached your viewing limit for this

@Seismicisolation



You have either reached a page that is unavailable for viewing or reached your viewing limit for this

@Seismicisolation



You have either reached a page that is unavailable for viewing or reached your viewing limit for this

@Seismicisolation



You have either reached a page that is unavailable for viewing or reached your viewing limit for this

@Seismicisolation



You have either reached a page that is unavailable for viewing or reached your viewing limit for this

@Seismicisolation



You have either reached a page that is unavailable for viewing or reached your viewing limit for this

@Seismicisolation

(i) $\omega_0 = \omega_r + \omega_s$, $r \neq s$. If $|\omega_r - \omega_s|$ and $|\omega_i \pm \omega_j|$, $i, j \neq r, s$, are not in the frequency band $\omega_0 - \frac{1}{2}\Delta\omega_0 < \omega < \omega_0 + \frac{1}{2}\Delta\omega_0$, then the elements of matrix \mathbf{A} are given by

$$\begin{aligned} A_{ii} &= -2\beta_{ii}, \quad A_{ij} = 0, \quad i, j \neq r, s, \\ A_{rr} + 2\beta_{rr} &= A_{ss} + 2\beta_{ss} = \frac{1}{4}k_{rs}k_{sr}S(\omega_r + \omega_s), \\ A_{rs} &= \frac{1}{4}k_{rs}^2S(\omega_r + \omega_s), \quad A_{sr} = \frac{1}{4}k_{sr}^2S(\omega_s + \omega_r). \end{aligned}$$

Matrix \mathbf{A} is of the form

$$\mathbf{A} = \begin{bmatrix} A_{11} & \cdots & & & & & \\ & \ddots & A_{rr} & 0 & \cdots & 0 & A_{rs} \\ & & 0 & \ddots & & & 0 \\ & & \vdots & & \ddots & & \vdots \\ & & 0 & & \ddots & & 0 \\ A_{sr} & 0 & \cdots & 0 & A_{ss} & \cdots & \\ & & & & & & A_{nn} \end{bmatrix}.$$

Since $A_{ii} < 0$, for all $i \neq r, s$, the stability of the moment $E[\|\mathbf{q}\|^2]$ is determined by the 2×2 submatrix

$$\mathbf{A}_{rs} = \begin{bmatrix} A_{rr} & A_{rs} \\ A_{sr} & A_{ss} \end{bmatrix}.$$

As in Case II, the eigenvalues of matrix \mathbf{A}_{rs} have negative real parts if

$$A_{rr} + A_{ss} < 0, \quad A_{rr}A_{ss} - A_{rs}A_{sr} > 0,$$

i.e.

$$\begin{aligned} -2(\beta_{rr} + \beta_{ss}) + \frac{1}{2}k_{rs}k_{sr}S(\omega_r + \omega_s) &< 0, \\ 4\beta_{rr}\beta_{ss} - \frac{1}{2}(\beta_{rr} + \beta_{ss})k_{rs}k_{sr}S(\omega_r + \omega_s) &> 0. \end{aligned} \tag{7.3.15}$$

It is seen that when $k_{rs}k_{sr} < 0$, conditions (7.3.15) are satisfied automatically; hence, there is no instability when $k_{rs}k_{sr} < 0$ and $\omega_0 = \omega_r + \omega_s$.

(ii) $\omega_0 = |\omega_r - \omega_s|$, $r \neq s$. If $\omega_r + \omega_s$ and $|\omega_i \pm \omega_j|$, $i, j \neq r, s$, are not in the frequency band $\omega_0 - \frac{1}{2}\Delta\omega_0 < \omega < \omega_0 + \frac{1}{2}\Delta\omega_0$, then the elements of matrix \mathbf{A} are given by

$$\begin{aligned} A_{ii} &= -2\beta_{ii}, \quad A_{ij} = 0, \quad i, j \neq r, s, \\ A_{rr} + 2\beta_{rr} &= A_{ss} + 2\beta_{ss} = -\frac{1}{4}k_{rs}k_{sr}S(\omega_r - \omega_s), \\ A_{rs} &= \frac{1}{4}k_{rs}^2S(\omega_r - \omega_s), \quad A_{sr} = \frac{1}{4}k_{sr}^2S(\omega_s - \omega_r). \end{aligned}$$

The stability conditions are given by

$$\begin{aligned} 2(\beta_{rr} + \beta_{ss}) + \frac{1}{2}k_{rs}k_{sr}S(\omega_r - \omega_s) &> 0, \\ 4\beta_{rr}\beta_{ss} + \frac{1}{2}(\beta_{rr} + \beta_{ss})k_{rs}k_{sr}S(\omega_r - \omega_s) &> 0. \end{aligned} \tag{7.3.16}$$

When $k_{rs}k_{sr} > 0$, conditions (7.3.16) are satisfied automatically; hence, there is no instability when $k_{rs}k_{sr} > 0$ and $\omega_0 = |\omega_r - \omega_s|$.



You have either reached a page that is unavailable for viewing or reached your viewing limit for this

@Seismicisolation



You have either reached a page that is unavailable for viewing or reached your viewing limit for this

@Seismicisolation



You have either reached a page that is unavailable for viewing or reached your viewing limit for this

@Seismicisolation



You have either reached a page that is unavailable for viewing or reached your viewing limit for this

@Seismicisolation



You have either reached a page that is unavailable for viewing or reached your viewing limit for this

@Seismicisolation



You have either reached a page that is unavailable for viewing or reached your viewing limit for this

@Seismicisolation



You have either reached a page that is unavailable for viewing or reached your viewing limit for this

@Seismicisolation



You have either reached a page that is unavailable for viewing or reached your viewing limit for this

@Seismicisolation



You have either reached a page that is unavailable for viewing or reached your viewing limit for this

@Seismicisolation



You have either reached a page that is unavailable for viewing or reached your viewing limit for this

@Seismicisolation

$$\begin{aligned}
&= \lim_{\substack{n \rightarrow \infty \\ \Delta \rightarrow 0 \\ n\Delta \rightarrow \infty}} \frac{1}{n\Delta} \sum_{j=0}^{n-1} \sum_{l=1}^d f^l(t_j) \Delta W_l(t_j), \quad \Delta W_l(t_j) = W_l(t_{j+1}) - W_l(t_j) \\
&= \lim_{\Delta \rightarrow 0} \frac{1}{\Delta} E \left[\sum_{l=1}^d f^l(t) \Delta W_l(t) \right], \quad \because E[X] = \lim_{n \rightarrow \infty} \frac{1}{n} \sum_{j=0}^{n-1} X(t_j).
\end{aligned}$$

Because $f^l(t)$ depends only on $W_k(s)$ for $0 \leq s \leq t$, $k=1, 2, \dots, d$, and $\Delta W_l(t)$ is independent of $W_k(s)$ for $0 \leq s \leq t$, $k=1, 2, \dots, d$, which leads to that $f^l(t)$ and $\Delta W_l(t)$ are independent, one has

$$\begin{aligned}
I &= \lim_{\Delta \rightarrow 0} \frac{1}{\Delta} \sum_{l=1}^d E[f^l(t)] E[\Delta W_l(t)] \\
&= \lim_{\Delta \rightarrow 0} \sum_{l=1}^d E[f^l(t)] E\left[\frac{\Delta W_l(t)}{\Delta}\right] = \sum_{l=1}^d E[f^l(t)] E[\xi_l(t)] = 0,
\end{aligned}$$

where $\xi_l(t)$ is a Gaussian white noise process of zero mean.

Equation (8.3.7) yields, when t goes to infinity,

$$\|\mathbf{x}(t)\| = \|\mathbf{x}_0\| \exp\{t \cdot E[Q(\mathbf{s})]\}, \quad \text{with probability 1.} \quad (8.3.8)$$

Hence $E[Q(\mathbf{s})]$ characterizes the rate of exponential growth or decay of the Euclidean norm of the response of system (8.3.1). The largest *Lyapunov exponent* of the linear Itô stochastic differential equation is then given by

$$\lambda = \lim_{t \rightarrow \infty} \frac{1}{t} \log \|\mathbf{x}\| = E[Q(\mathbf{s})] = \int Q(\mathbf{s}) v(d\mathbf{s}). \quad (8.3.9)$$

It is obvious that if $\lambda < 0$, the trivial solution $\mathbf{x}(t) = \mathbf{0}$ of system (8.3.1) is asymptotically stable with probability 1, i.e. $P\{\|\mathbf{x}\| \rightarrow 0, \text{ as } t \rightarrow \infty\} = 1$; while if $\lambda > 0$, then for $\mathbf{x}(0) \neq \mathbf{0}$, $P\{\|\mathbf{x}\| \rightarrow \infty, \text{ as } t \rightarrow \infty\} = 1$.

For first-order linear Itô equations, $E[Q(\mathbf{s})]$ can be evaluated directly. For second- and higher-order linear Itô equations, however, the knowledge of the invariant measure of the \mathbf{s} -process with respect to which the expectation is defined is required.

If the diffusion matrix $\tilde{\mathbf{b}}(\mathbf{x}) = [\tilde{b}_{ij}]$ is non-singular in the sense that, for any vector $\mathbf{v} = \{v_1, v_2, \dots, v_n\}^T$,

$$(\tilde{\mathbf{b}}(\mathbf{x}) \mathbf{v}, \mathbf{v}) \geq C \|\mathbf{x}\|^2 \|\mathbf{v}\|^2, \quad C > 0, \quad (8.3.10)$$

the \mathbf{s} -process is ergodic and there is a unique solution for the invariant measure of the \mathbf{s} -process on the unit hypersphere. However, if condition (8.3.10) is not satisfied, the singularities of the \mathbf{s} -process have to be determined and classified, since the Markov diffusion process $\mathbf{s}(t)$ may not be ergodic throughout the hypersphere. The invariant measure $v(d\mathbf{s})$ has to be studied separately for each ergodic component of the process $\mathbf{s}(t)$. A singularity of a Markov diffusion process is defined as a point at which the determinant of the diffusion matrix vanishes.



You have either reached a page that is unavailable for viewing or reached your viewing limit for this

@Seismicisolation



You have either reached a page that is unavailable for viewing or reached your viewing limit for this

@Seismicisolation



You have either reached a page that is unavailable for viewing or reached your viewing limit for this

@Seismicisolation



You have either reached a page that is unavailable for viewing or reached your viewing limit for this

@Seismicisolation



You have either reached a page that is unavailable for viewing or reached your viewing limit for this

@Seismicisolation



You have either reached a page that is unavailable for viewing or reached your viewing limit for this

@Seismicisolation



You have either reached a page that is unavailable for viewing or reached your viewing limit for this

@Seismicisolation



You have either reached a page that is unavailable for viewing or reached your viewing limit for this

@Seismicisolation



You have either reached a page that is unavailable for viewing or reached your viewing limit for this

@Seismicisolation



You have either reached a page that is unavailable for viewing or reached your viewing limit for this

@Seismicisolation



You have either reached a page that is unavailable for viewing or reached your viewing limit for this

@Seismicisolation



You have either reached a page that is unavailable for viewing or reached your viewing limit for this

@Seismicisolation



You have either reached a page that is unavailable for viewing or reached your viewing limit for this

@Seismicisolation



You have either reached a page that is unavailable for viewing or reached your viewing limit for this

@Seismicisolation



You have either reached a page that is unavailable for viewing or reached your viewing limit for this

@Seismicisolation



You have either reached a page that is unavailable for viewing or reached your viewing limit for this

@Seismicisolation



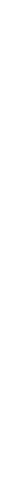
You have either reached a page that is unavailable for viewing or reached your viewing limit for this

@Seismicisolation



You have either reached a page that is unavailable for viewing or reached your viewing limit for this

@Seismicisolation



You have either reached a page that is unavailable for viewing or reached your viewing limit for this

@Seismicisolation



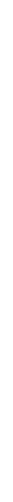
You have either reached a page that is unavailable for viewing or reached your viewing limit for this

@Seismicisolation



You have either reached a page that is unavailable for viewing or reached your viewing limit for this

@Seismicisolation



You have either reached a page that is unavailable for viewing or reached your viewing limit for this

@Seismicisolation



You have either reached a page that is unavailable for viewing or reached your viewing limit for this

@Seismicisolation



You have either reached a page that is unavailable for viewing or reached your viewing limit for this

@Seismicisolation



You have either reached a page that is unavailable for viewing or reached your viewing limit for this

@Seismicisolation



You have either reached a page that is unavailable for viewing or reached your viewing limit for this

@Seismicisolation



You have either reached a page that is unavailable for viewing or reached your viewing limit for this

@Seismicisolation



You have either reached a page that is unavailable for viewing or reached your viewing limit for this

@Seismicisolation



You have either reached a page that is unavailable for viewing or reached your viewing limit for this

@Seismicisolation

$$= \varepsilon \left[\frac{1}{2} (\hat{\lambda}_1 + \hat{\lambda}_2) \pm \frac{1}{8} k^2 S^- \right] + \int_0^{\frac{1}{2}\pi} [\Psi^2(\varphi) - \varepsilon c \cos 2\varphi] \mu(\varphi) d\varphi. \quad (8.6.12)$$

Substituting $\Psi^2(\varphi)$ in equations (8.6.4a) and $\mu(\varphi)$ in (8.6.10) into equation (8.6.12) and performing the indicated integration yield the following expression for the Lyapunov exponent:

$$\lambda = \varepsilon \left\{ \frac{1}{2} \left[(\hat{\lambda}_1 + \hat{\lambda}_2) + (\hat{\lambda}_1 - \hat{\lambda}_2) \coth \left(\frac{\hat{\lambda}_1 - \hat{\lambda}_2}{2\sqrt{\Delta}} \tanh^{-1} \frac{b}{\sqrt{\Delta}} \right) \right] \pm \frac{1}{8} k^2 S^- \right\}, \quad b > 0. \quad (8.6.13a)$$

Again, when $b < 0$, the corresponding trigonometric forms are substituted in the right side of equation (8.6.13a) to give

$$\lambda = \varepsilon \left\{ \frac{1}{2} \left[(\hat{\lambda}_1 + \hat{\lambda}_2) + (\hat{\lambda}_1 - \hat{\lambda}_2) \coth \left(-\frac{\hat{\lambda}_1 - \hat{\lambda}_2}{2\sqrt{-\Delta}} \tan^{-1} \frac{b}{\sqrt{-\Delta}} \right) \right] \pm \frac{1}{8} k^2 S^- \right\}, \quad b < 0. \quad (8.6.13b)$$

In the exceptional case when $b = 0$, the limiting form of (8.6.13a) is

$$\lambda = \varepsilon \left\{ \frac{1}{2} \left[(\hat{\lambda}_1 + \hat{\lambda}_2) + (\hat{\lambda}_1 - \hat{\lambda}_2) \coth \frac{4(\hat{\lambda}_1 - \hat{\lambda}_2)}{k^2 S^+} \right] \pm \frac{1}{8} k^2 S^- \right\}, \quad b = 0. \quad (8.6.13c)$$

Since

$$\begin{aligned} \Delta = b(a+b) &= \frac{1}{32^2} [k_{11}^2 S(2\omega_1) + k_{22}^2 S(2\omega_2) - 4k^2 S(\omega_1 \pm \omega_2)] \\ &\quad \times [k_{11}^2 S(2\omega_1) + k_{22}^2 S(2\omega_2) + 4k^2 S(\omega_1 \mp \omega_2)], \end{aligned}$$

it is easy to show that, for $b > 0$,

$$\sqrt{\Delta} = \frac{1}{32} \sqrt{K^2 - 4k^4 (S^+)^2},$$

where $K = k_{11}^2 S(2\omega_1) + k_{22}^2 S(2\omega_2) \mp 2k^2 S^-$. Let γ be defined by

$$\tanh \gamma = \frac{b}{\sqrt{\Delta}} = \sqrt{\frac{b}{a+b}}, \quad b > 0.$$

Since $0 < \sqrt{b/(a+b)} < 1$, $0 < \tanh \gamma < 1$, and hence $0 < \gamma < \infty$. Using an appropriate identity for hyperbolic functions, one obtains $\cosh 2\gamma = K/(2k^2 S^+)$. Hence the Lyapunov exponent (8.6.13a) can be written as

$$\lambda = \varepsilon \left\{ \frac{1}{2} \left[(\hat{\lambda}_1 + \hat{\lambda}_2) + (\hat{\lambda}_1 - \hat{\lambda}_2) \coth \left(\frac{\hat{\lambda}_1 - \hat{\lambda}_2}{\sqrt{\Delta_0}} \alpha \right) \right] \pm \frac{1}{8} k^2 S^- \right\}, \quad b > 0,$$

where

$$\alpha = 2\gamma = \cosh^{-1} \left(\frac{K}{2k^2 S^+} \right), \quad \Delta_0 = 16\Delta = \frac{1}{64} [K^2 - 4k^4 (S^+)^2].$$



You have either reached a page that is unavailable for viewing or reached your viewing limit for this

@Seismicisolation



You have either reached a page that is unavailable for viewing or reached your viewing limit for this

@Seismicisolation



You have either reached a page that is unavailable for viewing or reached your viewing limit for this

@Seismicisolation



You have either reached a page that is unavailable for viewing or reached your viewing limit for this

@Seismicisolation



You have either reached a page that is unavailable for viewing or reached your viewing limit for this

@Seismicisolation



You have either reached a page that is unavailable for viewing or reached your viewing limit for this

@Seismicisolation



You have either reached a page that is unavailable for viewing or reached your viewing limit for this

@Seismicisolation

To have a complete picture of the dynamic stability of system (9.1.10), it is important to study both the sample stability and the p th moment stability for all real values of p , and to determine both the top Lyapunov exponent and the p th moment Lyapunov exponent. The non-trivial zero δ of the moment stability $\Lambda(p)$, i.e. $\Lambda(\delta)=0$, is called the *stability index*.

The stability index characterizes the probability with which the response of an almost-surely system exceeds a threshold. It is shown in [21] that the probability of the solution exiting the sphere $\|\mathbf{x}(t)\| < r$ is of the order $\|\mathbf{x}\|^{\delta}$, for $\mathbf{x} \rightarrow 0$, for any $r > 0$ if system (9.1.10) is stable w.p.1. As shown in Figure 9.2, if the system is almost-surely unstable with $\lambda > 0$, then the p th moment is unstable for all $p > 0$. In this case, the stability index δ , which is negative, is not useful. On the other hand, if $\lambda < 0$, implying that system (9.1.10) is stable with probability 1, then $\Lambda(p) > 0$ when p is greater than the stability index δ , which implies that the p th moment is unstable.

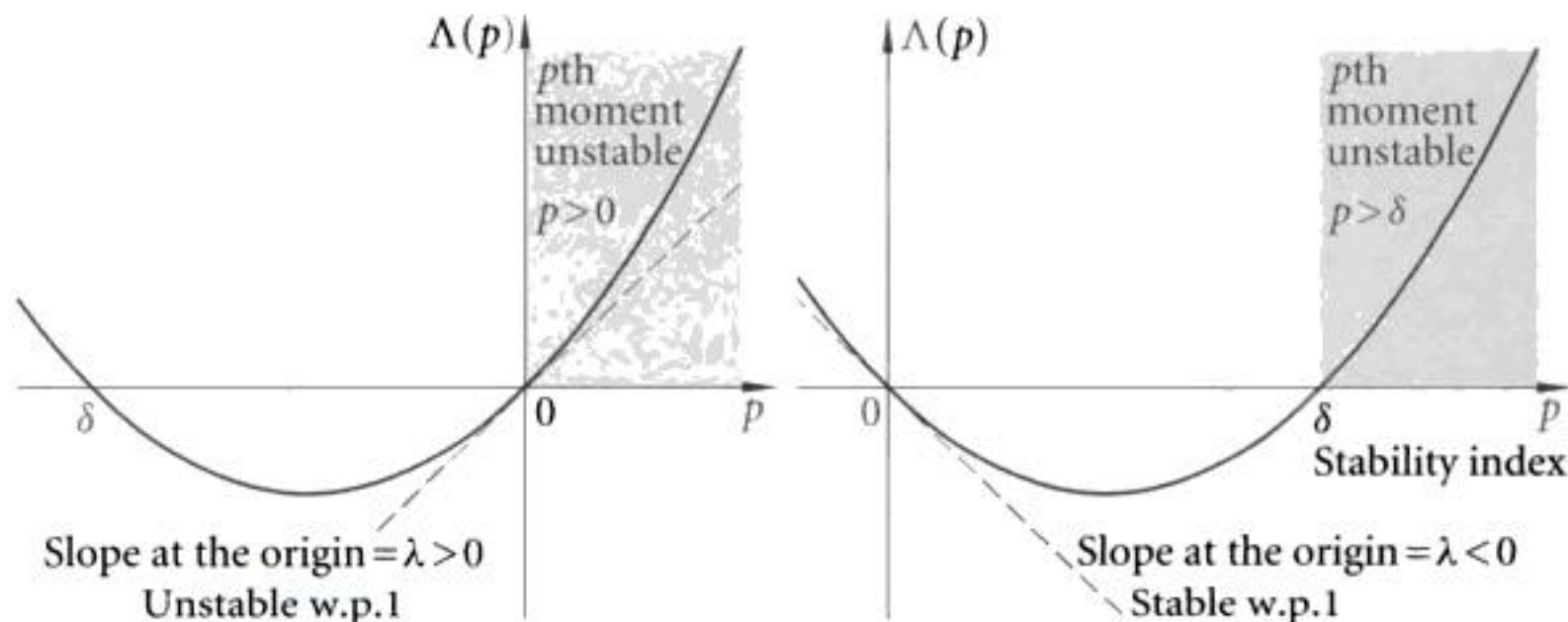


Figure 9.2 Sample stability and moment stability.

9.1.2 The Partial Differential Eigenvalue Problem for Moment Lyapunov Exponent

Suppose equation (9.1.10) can be rewritten as a system of linear Stratonovich stochastic differential equations

$$d^*\mathbf{x} = \mathbf{a}^*\mathbf{x} dt + \sum_{l=1}^d \sigma^l \mathbf{x} dW_l, \quad (9.1.14a)$$

where $\mathbf{x} = \{x_1, x_2, \dots, x_n\}^T$, and $W_1(t), W_2(t), \dots, W_d(t)$ are d mutually independent standard Wiener processes. The equivalent Itô equations are, using (5.13.6),

$$d\mathbf{x} = \mathbf{a}\mathbf{x} dt + \sum_{l=1}^d \sigma^l \mathbf{x} dW_l, \quad \mathbf{a} = \mathbf{a}^* + \frac{1}{2} \sum_{l=1}^d (\sigma^l)^2. \quad (9.1.14b)$$

Applying the Khasminskii transformation as presented in Section 8.3, one finds

$$\mathbf{s} = \frac{\mathbf{x}}{\|\mathbf{x}\|}, \quad \|\mathbf{x}\| = \sqrt{\mathbf{x}^T \mathbf{x}}, \quad \|\mathbf{s}\| = 1, \quad (9.1.15)$$



You have either reached a page that is unavailable for viewing or reached your viewing limit for this

@Seismicisolation



You have either reached a page that is unavailable for viewing or reached your viewing limit for this

@Seismicisolation



You have either reached a page that is unavailable for viewing or reached your viewing limit for this

@Seismicisolation



You have either reached a page that is unavailable for viewing or reached your viewing limit for this

@Seismicisolation



You have either reached a page that is unavailable for viewing or reached your viewing limit for this

@Seismicisolation



You have either reached a page that is unavailable for viewing or reached your viewing limit for this

@Seismicisolation



You have either reached a page that is unavailable for viewing or reached your viewing limit for this

@Seismicisolation



You have either reached a page that is unavailable for viewing or reached your viewing limit for this

@Seismicisolation



You have either reached a page that is unavailable for viewing or reached your viewing limit for this

@Seismicisolation

By means of a symbolic computation software, such as *Maple*, equations (9.3.18), (9.3.19), (9.3.21), and (9.3.23) can be easily manipulated. A *Maple* program and the results are shown in Appendix A.7.

The Lyapunov exponent $\lambda_{x(t)}$ versus σ_1 and σ_2 is shown in Figure 9.4. Typical results of the moment Lyapunov exponent $\Lambda_{x(t)}(p)$ with $\beta=0.2$ and $\varepsilon=0.1$ are shown in Figure 9.5 for the special case $\sigma_2=0$ and $\sigma_1=0$, respectively.

Note that when $\sigma_2=0$, equation (9.3.2) is similar to equation (8.5.5) with $\gamma_0=-1$. The Lyapunov exponent of system (8.5.5) obtained using asymptotic expansion of integrals is given by equation (8.5.25) with $\gamma=-\gamma_0-\beta^2\approx 1$, together with equation (8.5.8), which is the same as the ε -order term of equation (A.7.4b). On the other hand, when $\sigma_1=0$, equation (9.3.2) is of the form of equation (8.5.34). The Lyapunov exponent of system (8.5.34) obtained using asymptotic expansion of integrals and the method of stochastic averaging is given by equation (8.5.39), which is the same as the ε -order term of equation (A.7.5b).

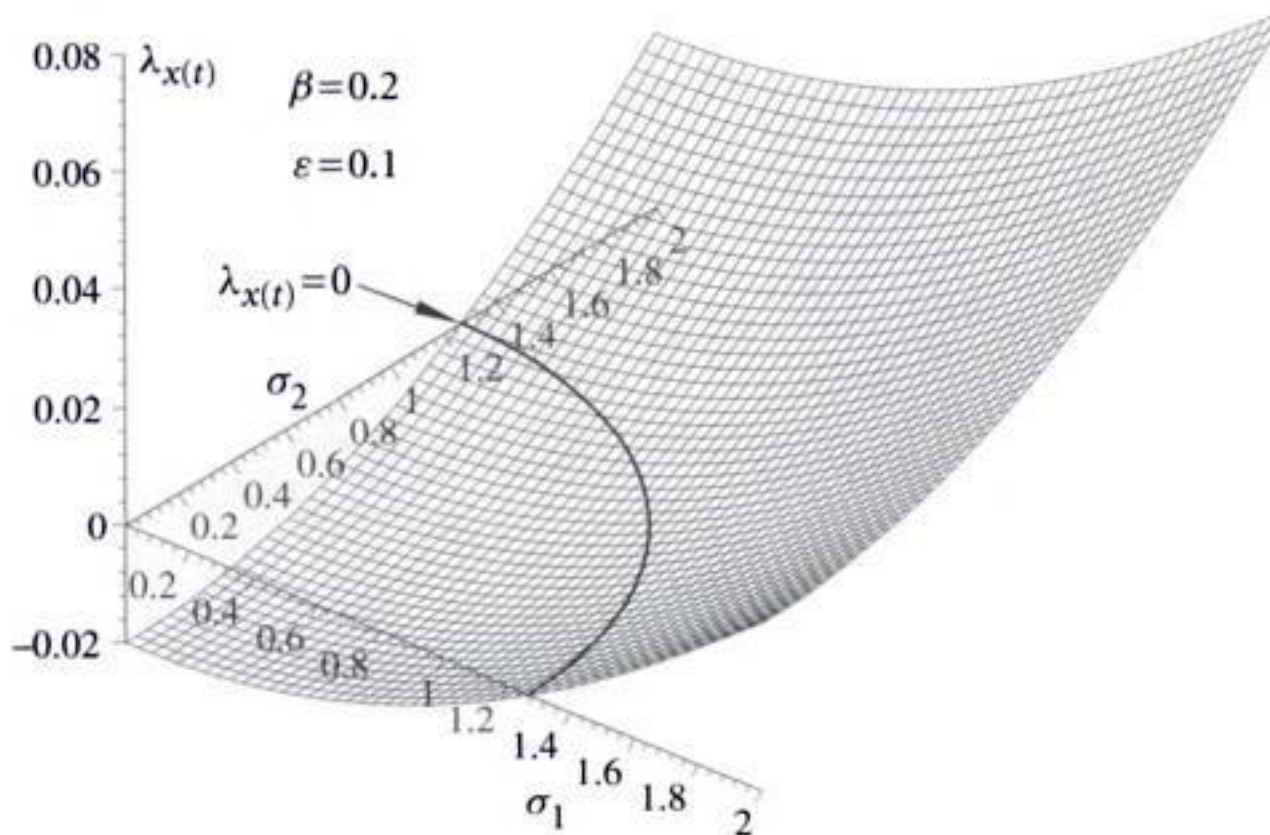


Figure 9.4 Lyapunov exponent.

具有版權的資料

9.4 Moment Lyapunov Exponents of a Two-Dimensional Near-Nilpotent System

9.4.1 Introduction

In Section 8.5.1, it is shown that investigations of the dynamic stability of elastic systems under randomly fluctuating axial loading frequently lead to the study of bifurcation behaviour of the solution of a nondimensional second-order differential equation of the form (8.5.4). In the absence of stochastic fluctuation, i.e. when $\sigma=0$, as the loading parameter γ_0 is increased from negative to positive values, the system undergoes a pitchfork bifurcation from the trivial equilibrium configuration into one of the two symmetric non-trivial equilibrium configurations.



You have either reached a page that is unavailable for viewing or reached your viewing limit for this

@Seismicisolation



You have either reached a page that is unavailable for viewing or reached your viewing limit for this

@Seismicisolation



You have either reached a page that is unavailable for viewing or reached your viewing limit for this

@Seismicisolation



You have either reached a page that is unavailable for viewing or reached your viewing limit for this

@Seismicisolation



You have either reached a page that is unavailable for viewing or reached your viewing limit for this

@Seismicisolation



You have either reached a page that is unavailable for viewing or reached your viewing limit for this

@Seismicisolation



You have either reached a page that is unavailable for viewing or reached your viewing limit for this

@Seismicisolation

The method of relaxation can be applied to solve the two-point boundary-value problem (9.4.18). The method of relaxation is advantageous when studying the variation of the moment Lyapunov exponent with the change of a parameter, since relaxation rewards a good initial guess with rapid convergence and the previous solution should be a good initial guess when the parameter is changed only slightly. Following the procedure as described in Section 9.4.4.1, discretize the domain of φ into M grid points $\varphi_m = -\frac{1}{2}\pi + (m-1)h$, $m=1, 2, \dots, M$, where $h=\pi/(M-1)$. Denoting

$$\bar{\varphi}_m = \frac{1}{2}(\varphi_m + \varphi_{m-1}), \quad \bar{y}_{i,m} = \frac{1}{2}(y_{i,m} + y_{i,m-1}), \quad i = 1, 2, 3,$$

at the grid points $\varphi_2, \varphi_3, \dots, \varphi_M$, one finds that the ordinary differential equations (9.4.18a) are replaced by the finite-difference equations

$$\begin{aligned} E_{1,m} &\equiv y_{1,m} - y_{1,m-1} - h\bar{y}_{2,m} = 0, \\ E_{2,m} &\equiv y_{2,m} - y_{2,m-1} - \frac{2h}{\cos^4 \bar{\varphi}_m} \left\{ [F_2(\bar{\varphi}_m) - p \sin \bar{\varphi}_m \cos^3 \bar{\varphi}_m] \bar{y}_{2,m} \right. \\ &\quad \left. - p F_1(\bar{\varphi}_m) \bar{y}_{1,m} + \bar{y}_{1,m} \bar{y}_{3,m} \right\} = 0, \\ E_{3,m} &\equiv y_{3,m} - y_{3,m-1} = 0. \end{aligned} \quad (9.4.19a)$$

At the first boundary point $\varphi = -\frac{1}{2}\pi$, there are two boundary conditions. From equations (9.4.18b),

$$E_{2,1} \equiv y_{2,1} + y_{1,1} y_{3,1} = 0, \quad E_{3,1} \equiv y_{1,1} - c = 0. \quad (9.4.19b)$$

At the second boundary point $\varphi = \frac{1}{2}\pi$, there are also two boundary conditions. From equations (9.4.18c),

$$E_{1,M+1} \equiv y_{2,M} + y_{1,M} y_{3,M} = 0, \quad E_{2,M+1} \equiv y_{1,M} - c = 0. \quad (9.4.19c)$$

The $3M$ corrections $\Delta y_{i,m}$, $i=1, 2, 3$, $m=1, 2, \dots, M$, and the undetermined constant c are given by the solution of the $3M+1$ linear algebraic equations (9.4.17) with $n_1=n_2=2$. For $m=2, 3, \dots, M$, there are $3(M-1)$ equations in (9.4.17a),

$$\begin{aligned} S_{1,1}^m &= -1, \quad S_{1,2}^m = S_{1,5}^m = -\frac{1}{2}h, \quad S_{1,3}^m = S_{1,6}^m = 0, \quad S_{1,4}^m = 1, \\ S_{2,1}^m &= -\frac{h}{\cos^4 \bar{\varphi}_m} [-p F_1(\bar{\varphi}_m) + \bar{y}_{3,m}] = S_{2,4}^m, \\ S_{2,2}^m &= -1 - \frac{h}{\cos^4 \bar{\varphi}_m} [F_2(\bar{\varphi}_m) - p \sin \bar{\varphi}_m \cos^3 \bar{\varphi}_m] = S_{2,5}^m - 2, \\ S_{2,3}^m &= -\frac{h}{\cos^4 \bar{\varphi}_m} \bar{y}_{1,m} = S_{2,6}^m, \\ S_{3,1}^m &= S_{3,2}^m = S_{3,4}^m = S_{3,5}^m = 0, \quad S_{3,3}^m = -1, \quad S_{3,6}^m = 1. \end{aligned} \quad (9.4.20a)$$

For the first boundary point, there are two equations in (9.4.17b),

$$S_{2,1}^1 = y_{3,1}, \quad S_{2,2}^1 = 1, \quad S_{2,3}^1 = y_{1,1}, \quad S_{3,1}^1 = 1, \quad S_{3,2}^1 = 0, \quad S_{3,3}^1 = 0, \quad (9.4.20b)$$



You have either reached a page that is unavailable for viewing or reached your viewing limit for this

@Seismicisolation



You have either reached a page that is unavailable for viewing or reached your viewing limit for this

@Seismicisolation



You have either reached a page that is unavailable for viewing or reached your viewing limit for this

@Seismicisolation



You have either reached a page that is unavailable for viewing or reached your viewing limit for this

@Seismicisolation



You have either reached a page that is unavailable for viewing or reached your viewing limit for this

@Seismicisolation



You have either reached a page that is unavailable for viewing or reached your viewing limit for this

@Seismicisolation



You have either reached a page that is unavailable for viewing or reached your viewing limit for this

@Seismicisolation



You have either reached a page that is unavailable for viewing or reached your viewing limit for this

@Seismicisolation



You have either reached a page that is unavailable for viewing or reached your viewing limit for this

@Seismicisolation



You have either reached a page that is unavailable for viewing or reached your viewing limit for this

@Seismicisolation



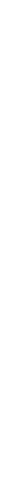
You have either reached a page that is unavailable for viewing or reached your viewing limit for this

@Seismicisolation



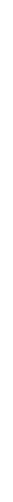
You have either reached a page that is unavailable for viewing or reached your viewing limit for this

@Seismicisolation



You have either reached a page that is unavailable for viewing or reached your viewing limit for this

@Seismicisolation



You have either reached a page that is unavailable for viewing or reached your viewing limit for this

@Seismicisolation



You have either reached a page that is unavailable for viewing or reached your viewing limit for this

@Seismicisolation



You have either reached a page that is unavailable for viewing or reached your viewing limit for this

@Seismicisolation



You have either reached a page that is unavailable for viewing or reached your viewing limit for this

@Seismicisolation



You have either reached a page that is unavailable for viewing or reached your viewing limit for this

@Seismicisolation



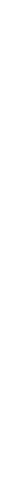
You have either reached a page that is unavailable for viewing or reached your viewing limit for this

@Seismicisolation



You have either reached a page that is unavailable for viewing or reached your viewing limit for this

@Seismicisolation



You have either reached a page that is unavailable for viewing or reached your viewing limit for this

@Seismicisolation



You have either reached a page that is unavailable for viewing or reached your viewing limit for this

@Seismicisolation



You have either reached a page that is unavailable for viewing or reached your viewing limit for this

@Seismicisolation



You have either reached a page that is unavailable for viewing or reached your viewing limit for this

@Seismicisolation



You have either reached a page that is unavailable for viewing or reached your viewing limit for this

@Seismicisolation



You have either reached a page that is unavailable for viewing or reached your viewing limit for this

@Seismicisolation



You have either reached a page that is unavailable for viewing or reached your viewing limit for this

@Seismicisolation



You have either reached a page that is unavailable for viewing or reached your viewing limit for this

@Seismicisolation



You have either reached a page that is unavailable for viewing or reached your viewing limit for this

@Seismicisolation

This book presents a systematic introduction to the theory of parametric stability of structures under both deterministic and stochastic loadings. A comprehensive range of theories are presented and various application problems are formulated and solved, often using more than one approach. Investigation of an elastic system's dynamic stability frequently leads to the study of dynamic behavior of the solutions of parametrically excited systems. Parametric instability or resonance is more dangerous than ordinary resonance as it is characterized by exponential growth of the response amplitudes even in the presence of damping. The emphasis in this book is on the applications and various analytical and numerical methods for solving engineering problems. The materials presented are as self-contained as possible, with all of the important steps of analysis provided in order to make the book suitable as a graduate-level textbook and especially for self-study.

WEI-CHAU XIE is a Professor in the Department of Civil Engineering at the University of Waterloo. He is the author of numerous articles on dynamic stability of structures, non-linear dynamics, and stochastic mechanics. He is the recipient of the Teaching Excellence Award in recognition of his exemplary record as a teacher.

Cover design by Alice Soloway

CAMBRIDGE
UNIVERSITY PRESS
www.cambridge.org

ISBN 0-521-85266-8



9 780521 852661 >

@Seismicisolation